



MASTERARBEIT

STUDIES TOWARDS TUNGSTEN- ACETYLENE COMPLEXES

Structural Mimics for the Active Site of
Acetylene Hydratase

Lydia Maria Christina Peschel, BSc

Betreuerin: Univ.- Prof. Dr. Nadia C. Mösch-Zanetti
Anorganische Chemie, Karl-Franzens Universität Graz

Vorgelegt am 17. August 2012 an der Technischen Universität Graz, im Rahmen des Kooperationsprojekts NAWI Graz zur Erlangung des akademischen Grades „Master of Science“

*Dedicated to my late grandmother.
I miss you.*

ACKNOWLEDGEMENT

First I would like to thank my supervisor Dr. Nadia Mösch-Zanetti for giving me the opportunity to work in her research group, for the provision of exceptional working conditions and for the fruitful meetings.

I am deeply indebted to my adviser Dr. Jörg Schachner. Thank you for sharing your knowledge and experience with me. Thank you for the countless hours you've spent with me in front of the computer, trying to make sense of yet another not so clear result.

I would also like to thank our crystallographer Dr. Ferdinand Belaj for his patience with me and my enthusiasm as a newbie in the mysterious art of crystal growing. Thank you for giving all these disordered twin crystals a try.

I would also like to thank Dr. Doris Kühnelt and Mag. Natascha Stock for the ESI measurements and Ing. Bernd Werner for the NMR measurements. I am truly grateful to our excellent lab technicians Doris Eibinger and Alexandra Renzhammer for finding yet another Schlenk flask and for forgiving me all those broken NMR-Vials. I would also like to thank Mag. Martina Judmaier for helping me find my way around glove box techniques and glove box maintenance.

Furthermore I would like to express my gratitude to our students Marcello Entner and Sebastian Grimm for supporting me in the lab.

Moreover I would like to thank my partner for his patience and understanding.

I am also much obliged to my friends, fellow master students and flat mates for lending me their ears, encouraging me to go on and for sometimes cheering me up over a glass of wine.

Least but not last, I would like to say thank you to my family, especially to my mother. Without her continuous support and trust in my talents I wouldn't have been able to make it this far.

TABLE OF CONTENTS

Abbreviations	iv
I. ABSTRACT	1
II. INTRODUCTION	3
1. Bioinorganic Chemistry	3
Active Site Modeling	3
Structural Modeling	4
Functional Modeling	4
Structural-Functional Modeling	4
Tungsten vs. Molybdenum	5
2. Bioinorganic Chemistry of Tungsten	7
Tungstoenzymes	7
Classes of Tungstoenzymes	8
Biomimetic Ligand Systems	9
3. Acetylene Hydratase	10
Pelobacter Acetylenicus- The Host Organism	10
Acetylene- The Substrate	11
Enzyme Characteristics	11
Molecular Structure of Acetylene Hydratase	12
Mechanistic Proposals for Acetylene Hydration	13
Mechanism A	14
Mechanism B	14
Mechanism C	15
Mechanism D	16
Summing up...	16
Relevant Modeling Chemistry	17
Structural Modeling Chemistry	17
Structural-Functional Modeling Chemistry	18
Mechanistic Studies on the Structural-Functional Model	18
4. Objectives	20

III. RESULTS AND DISCUSSION	22
Ligand Synthesis and Ligand Properties	22
Precursor Synthesis	24
[W(CO) ₃ (PPh ₃) ₂ Cl ₂] vs. [Ph ₃ PCl] ₂ [WCl ₆]	24
[W(CO) ₄ Cl ₂] and [W(CO) ₂ (NCMe) ₂ Cl ₂]	28
[W(CO) ₄ Br ₂] vs. [W ₂ (CO) ₇ Br ₄]	30
Coordination Compounds	32
Influence of Heteroatoms in the Dithiocarbamate-System	32
Precursor Versatility	34
Reactions with Acetylene	36
Oxygen Atom Transfer Reactions	38
The Choice of Oxygen Atom Transfer Reagent	38
Oxidation of Carbonyl-Acetylene Compounds	39
Oxidation of Dicarbonyl Compounds	40
IV. CONCLUSION	42
V. EXPERIMENTAL	43
1. General Methods	43
2. Ligands	44
3. Precursors	46
4. Coordination Compounds	49
Carbonyl Compounds	49
Carbonyl-Acetylene- Compounds	52
Oxo-Tungsten(IV)-Acetylene Complexes	53
VI. REFERENCES	55
VII. APPENDIX	59
Crystal Data Refinement	59

ABBREVIATIONS

aa	Amino acid residues
ACN	Acetonitrile
ADP	Adenosine diphosphate
AH	Acetylene hydratase
AK	Acetate kinase
Ala	Alanine
ALDH	Aldehyde dehydrogenase
AOR	Aldehyde ferredoxin oxidoreductase
Asp	Aspartic acid
ATP	Adenosine triphosphate
b.p.	Boiling point
bdt	1,2-Benzenedithiolate
cdt	4H-[1,3]Dithiolo[4,5-c]chromen-2-one
C _q	Quaternary carbon atom
Cys	Cysteine
detc	Diethyldithiocarbamate
DFT	Density functional theory
DMSO	Dimethyl sulfoxide
dtc	Dithiocarbamate
dtp	Diethyl dithiophosphate
E ⁰	Standard reduction potential
edt	Ethylene-1,2-dithiolate
equiv.	Equivalents
Et	Ethyl group
Fd	Ferredoxin
FDH	Formate dehydrogenase
FeMoco	Iron-molybdenum cofactor
FMDH	N-formylmethanofuran dehydrogenase
FOR	Formaldehyde ferredoxin oxidoreductase
GAPOR	Glyceraldehyde-3-phosphate ferredoxin oxidoreductase
h	Hours
IR	Infrared (Spectroscopy)

L	Ligand
LOD	Limit of detection
mCPBA	<i>meta</i> -Chloroperoxybenzoic acid
Me ₃ N	Trimethylamine
Me ₃ NO	Trimethylamine <i>N</i> -oxide
MFR	N-Formylmethanofuran
MGD	Molybdopterin guanine dinucleotide cofactor
mnt	1,2-Dicyanoethylenedithiolate (malonitrile)
NADPH	Nicotinamide adenine dinucleotide phosphate
<i>n</i> -Bu	Butyl group (normal butyl-group)
OAT	Oxygen atom transfer
pdt	2,3-Dihydro-2H-pyran-4,5-dithiolate
ppbv	Parts per billion (volume)
PTA	Phosphate acetyltransferase
Py	Pyridine
PyNO	Pyridine <i>N</i> -oxide
QM/MM	Hybrid quantum mechanics/ molecular modeling
QM-only	Quantum mechanics-only
RT	Room temperature
S,N-oxa	2-(4,4-dimethyl-4,5-dihydrooxazol-2-yl)benzenethiol
S ₂ C ₂ Me ₂	1,2-Dimethyl-1,2-ethylenedithiolate
S ₂ C ₂ Ph ₂	1,2-Diphenyl-1,2-ethylenedithiolate
<i>t</i> -Bu	Tertiary butyl group
THF	Tetrahydrofurane
TMS	Tetramethylsilane
ΔG	Gibbs free energy

I. ABSTRACT

Enzymes are responsible for the catalysis of all chemical reactions in the metabolism of all organisms. Roughly a third of these enzymes are metalloenzymes meaning that their functionality depends on metal ions. Of all the thousands of known enzymes roughly a dozen depends on tungsten, the heaviest metal in biology. Acetylene hydratase (AH) is unique among its already small family of redox-active Mo and W DMSO reductases. It may share the structural features of a redox enzyme, but nonetheless AH catalyzes the net-hydration reaction of acetylene to acetaldehyde.

Enzymes are characterized by structural complexity. Due to this fact modeling chemistry has been developed to help in the understanding of their structural and mechanistic features. The modeling chemistry of AH is still at the beginning, only one example of a structural, yet functional model has been described.

This piece of work presents first steps towards the development of new structural models for acetylene hydratase. On the way promising tungsten(II) precursors of the general form $[W^{II}(\text{CO})_n\text{X}_2]$ ($n = 2, 3, 4, \text{X} = \text{Cl}, \text{Br}$) were investigated. $[\text{W}_2(\text{CO})_7\text{Br}_4]$ (**9**) could be identified as a reliable precursor for W(II) tricarbonyl compounds, which is obtainable by a straightforward oxidation reaction of $[\text{W}(\text{CO})_6]$ with Br_2 .

It was found that the synthesis of the known precursors $[\text{W}(\text{CO})_3(\text{PPh}_3)_2\text{Cl}_2]$ (**7**), $[\text{W}(\text{CO})_4\text{Cl}_2]$ (**8a**) is not as straightforward as described in literature. The problems with over-oxidation are elucidated. Modified procedures for the synthesis of **7** and **8a** from $[\text{W}(\text{CO})_6]$ and Cl_2 , and PPh_3 for **7**, are presented. The new compounds $[\text{W}(\text{CO})_2(\text{NCMe})_2\text{Cl}_2]$ (**8b**), obtainable by adduct-formation of **8a** with acetonitrile is shown to be a new possible precursor for W(II) carbonyl compounds.

$[\text{PPh}_3\text{Cl}]_2[\text{WCl}_6]$ (**6**) the product of over-oxidation of **7** could be identified and characterized. Preliminary results suggest sulfur transfer activity from dithiocarbamates to **6**. Its interesting, new reactivity is currently being investigated.

The known compounds $[\text{W}(\text{CO})_3(\text{S}_2\text{CR})_2]$ ($\text{R} = \text{NEt}_2, \text{NC}_4\text{H}_8$) were reproduced and the novel compounds $[\text{W}(\text{CO})_3(\text{S}_2\text{CR})_2]$ ($\text{R} = \text{OEt}, \text{O}i\text{-Bu}, \text{S}t\text{-Bu}$) could be added to the family of W(II) tricarbonyl dithiocarbamates. A novel synthesis strategy using salt metathesis of **9** with the respective ligands is presented.

The novel W(II) and W(VI) acetylene complexes $[W(C_2H_2)(CO)(S_2CNC_4H_8)_2]$ (**15b**) $[OW(C_2H_2)(S_2CNC_4H_8)_2]$ (**16b**) could be synthesized from the corresponding tricarbonyl compounds and acetylene. Trimethyl *N*-oxide is shown to be a powerful oxygen atom transfer (OAT) reagent, capable of replacing the literature method with $[Mo_2O_3(S_2P(OEt)_2)_4]$ (**10**).

All results on the dithiocarbamate system imply that the nitrogen atom in the ligand is of central electronic importance for the coordination of acetylene to the tungsten center.

The molecular structures of $[W(CO)_2(PPh_3)_2Cl_2]$ (**7'**), $[W_2(CO)_7Br_4]$ (**9**) and $[PPh_3Cl]_2[WCl_6]$ (**6**) could be solved by X-ray diffraction analysis. Furthermore $W(CO)_2(S,N-oxa)_2$ (**14**) was synthesized and characterized as the first W(II) dicarbonyl thiooxazolin compound.

II. INTRODUCTION

1. BIOINORGANIC CHEMISTRY

Bioinorganic chemistry is a discipline right at the interface of chemistry and biology. Even though biology is generally associated with organic chemistry, inorganic elements are essential to life. Enzymes are the largest and most diverse sub-group of proteins, being responsible for the catalysis of all chemical reactions in the metabolism of all organisms. Virtually all biochemical reactions are catalyzed by an enzyme.^[1] They play a vital role in the regulation of the metabolism within the cells, as drug targets, and in a wide range of biotechnological applications.^[2] Compared to chemical catalysts enzymes display high substrate specificity and large structural complexity.^[1,3]

Metal cations are commonly found as natural constituents in proteins. Roughly a third of all enzymes are metalloproteins. Clearly nature has learned to benefit from the special properties of metal ions enabling it to perform a wide variety of otherwise impossible tasks. Many crucial biological processes require the presence of metal ions including respiration, nitrogen fixation, photosynthesis, nerve transmission, muscle contraction and signal deduction. Metals mainly function as electron carriers, centers for binding and activating substrates and as atom or group transfer agents. Furthermore non-essential metals have found their way into human medicine as diagnostic probes and drugs.^[4]

ACTIVE SITE MODELING

In most cases the reactivity and the selectivity of metalloenzymes are not only controlled by the immediate coordination sphere, but are also influenced by the entire protein structure.^[5] Due the structural complexity of enzymes synthetic modeling chemistry has been developed to help in the understanding of the spectroscopic, structural and mechanistic data of enzymes. In most cases the protein crystal structures are either unknown or not resolved well enough to determine the exact metal coordination sphere, i.e. how the cofactor is bound and which additional ligands are present. Small

functionalities like =O, -OH, -OH₂, =S or -SH are often hard to identify in close proximity to the heavy scattering metal sites. The synthesis of coordination compounds that mimic the reactivity and/or coordination geometry of enzymes has become an important and efficient strategy to shed light on these properties.^[3,6] Such studies can help to define the reactivity parameters of the protein, even if the full reproduction of the biological function(s) is not entirely achieved.^[5]

Structural Modeling

Structural modeling chemistry, also called biomimetic modeling chemistry, focuses on the replication of the metal's coordination sphere in the native metalloprotein. The ligand systems around the metal are constructed as close as possible to the coordinating environment and the active site structure found in the respective enzyme. Thus the synthesized complexes should have the most similar donor atom environments feasible.^[7]

Functional Modeling

Functional modeling chemistry, also called bio-inspired modeling chemistry, focuses on the duplication of the enzymatic function under ambient conditions, irrespective of the nature of the employed ligands. The synthesized model complexes ought to react with the biological substrate or at least a proxy substrate in a fashion similar to the native enzyme. Functional models may not exhibit the exactly identical activity of the metal center present in the enzyme, i.e. not follow Michaelis-Menten saturation kineticsⁱ. Functional modeling chemistry is essentially solution chemistry, as the vital role of water as an omnipresent reactant in enzymatic reactions is to be borne in mind. Hence functional models in non-aqueous media are a good start, but still have a long way to go to mimicking the native enzymatic function.^[7]

Structural-Functional Modeling

Structural-functional modeling chemistry, the coalescence of structural and functional modeling aspects is undoubtedly the highest art in active site modeling. The ultimate aim is the synthesis of complexes with biomimetic coordination spheres that react with the

ⁱ One of the simplest and best known models for enzymatic reactions. It relates the reaction rate to the concentration of the substrate.

respective enzyme's biological substrate in aqueous media, obeying Michaelis-Menten saturation kinetics.^[7]

TUNGSTEN VS. MOLYBDENUM

Tungsten and molybdenum are the only elements of the second and third row of transition metals that occur in native enzymes.^[8] Tungstate $[\text{WO}_4]^{2-}$ and molybdate $[\text{MoO}_4]^{2-}$ show unusually high bioavailabilities and unique versatilities.^[9] Their pronounced chemical and physical similarities are based on virtually equal atomic and ionic radii, caused by the lanthanide contraction, similar electronegativities, valence electron configurationsⁱⁱ and coordination characteristics (cp. Table 1).^[8,10] Tungsten's greater electron affinity and higher ionization energy reveal its general tendency to be easier oxidized than molybdenum.^[8] These similarities were long used to explain why tungsten is an antagonist for many molybdoenzymes. However W and Mo are sufficiently different so that biology has found ways to distinguish them.^[11,12]

Table 1: Comparative properties of octahedral species of molybdenum and tungsten^[8]

Property	Mo	W
Atomic number	42	74
Atomic weight	95.94 g/mol	183.84 g/mol
Abundance in Earth's crust	1000 µg/kg	1000 µg/kg
1 st Ionization energy	7.0995 eV	7.980 eV
Electron affinity	0.746 eV	0.815 eV
Standard potential $[\text{MO}_4]^{2-} / \text{M}^0$ ⁱⁱⁱ	-0.913 V	-1.074 V
Ground state configuration	$[\text{Kr}]4d^55s^1$	$[\text{Xe}]4f^{14}6s^25d^4$
Atomic radius	1.36 Å	1.37 Å
Ionic radii M(IV)-M(VI) ^[13]	0.79- 0.73 Å	0.80- 0.74 Å
Possible oxidation states ^[14]	-II, -I, 0, +I, +II, +III, +IV, +V, +VI	-II, -I, 0, +I, +II, +III, +IV, +V, +VI
Biological oxidation states	+IV, +V, +VI	+IV, +V, +VI
Possible coordination numbers ^[14]	4, 5, 6, 7,8 (and higher)	4, 5, 6, 7,8 (and higher)

ⁱⁱ In all oxidation states of nearly all relevant compounds.

ⁱⁱⁱ Basic or neutral solution.

Molybdenum and, to a minor extent, tungsten can be found in a wide array of enzymes, almost all of which catalyze oxygen atom transfers to, or from the substrate or oxidative hydroxylations, with the metal changing its oxidation state between +IV and +VI.^[15,16] The central role of molybdenum in biological systems has been known for many decades, whereas the biological function of tungsten has been elucidated more recently. Molybdoenzymes are ubiquitous in the aerobic world and are found in archaea, bacteria, eukarya, flora, fauna and humans.^[7,17] Prominent members include oxidases, reductases, dehydrogenases and nitrogenases. They are not only important in the metabolism and energy generation of their host organisms, but also in the global nitrogen, sulfur, carbon and arsenic cycles.^[7,18] More than fifty Mo-containing enzymes have been identified to date.^[10]

The few known species, that do not require Mo for growth, namely hyperthermophiles like *Pyrococcus furiosus*, use W instead.^[9,11,19] The use of tungsten allows for enhanced thermal stability and bond strength, due to stronger π -interactions.^[17] As a result W-complexes are generally kinetically slower in oxygen atom transfer reactions than their Mo-counterparts.^[11] In addition the lower redox potentials for W-compounds make them better suited to catalyze low potential redox processes like the conversion of acids to aldehydes, which display the lowest reduction potentials in biochemistry. It seems that tungstoenzymes require higher temperatures to achieve conversion rates that are comparable to those of molybdoenzymes at milder conditions.^[11,17]

On the contrary to other transition metals, which are often directly coordinated to histidine, cysteine, serine or tyrosine residues Mo and W are, in their biologically active form, coordinated by variants of the molybdopterin cofactor (cp. Figure 2). It is present in all relevant enzymes, except nitrogenase, where the molybdenum is coordinated to a large iron-sulfur cluster, MoFe_7S_9 (FeMoco).^[20] All tungstoenzymes are located in the cytoplasm and are oxygen-sensitive, whereas many molybdoenzymes are membrane-bound and usually insensitive towards oxygen.^[17]

2. BIOINORGANIC CHEMISTRY OF TUNGSTEN



Figure 1: Metallic tungsten^{[21] iv}

Tungsten has long been valued for its high melting point, great strength and good conductivity.^[17] Today it is widely known as filament in light bulbs, anode material in x-ray tubes, component of high-quality steel or as material for rocket nozzles and heat shields.^[10,14] In addition tungsten is, with its

atomic number of 74, also the heaviest element in biology. In general, biological systems do not incorporate elements with atomic numbers greater than 35 (bromine). Molybdenum (42), iodine (53) and tungsten (74) being the exceptions.^[17]

Tungsten is relatively scarce in nature (< 0.5 nM), but special habitats like marine hydrothermal vents, alkaline brine lakes, hot spring waters or sulfide-enriched waters hold significantly higher concentrations (> 50 nM).^[10,11,17] The natural abundance and speciation in aqueous solution are central for the bioavailability and incorporation of an element into natural products.^[8] The only biologically relevant form of tungsten is believed to be tungstate $[\text{WO}_4]^{2-}$ resulting from leaching of tungsten ores like wolframite ($[\text{Fe/Mn}]\text{WO}_4$), scheelite (CaWO_4) and less frequently tungstenite (WS_2).^[6,17] The octahedral oxoanion $[\text{WO}_4]^{2-}$ is stable, redox indifferent and highly soluble. It is transported into the cytoplasm, where it enters the biosynthetic machinery.^[6,22]

For decades tungstate was thought to have solely negative or, at best, neutral influence in biology. Especially its role as an antagonist of molybdoenzymes was used to identify the latter.^[10]

TUNGSTOENZYMES

It was not until 1983 that the first tungsten enzyme, a NADP-dependent formate dehydrogenase, was purified and characterized by Ljungdahl and coworkers.^[23] *Clostridium thermoaceticum*^v uses the tungsten-selenium-iron protein for the first step in the reduction of CO_2 to formate.^[10]

To date, more than a dozen tungsten-dependent enzymes have been identified.^[11] Except acetylene hydratase, all of them have been found in thermophilic or extremely thermophilic microorganisms that grow at temperatures close to or even greater than 100°C .^[9,17] All tungstoenzymes have been isolated from strictly anaerobic archaea or

^{iv} Licensed for non-commercial use by <http://periodicnetwork2011tag.pbworks.com>.

^v Also known as *Moorella thermoacetica*.

bacteria.^[6,17] W-dependent enzymes usually contain iron-sulfur cofactors that are utilized together with the W atom to catalyze redox reactions of a low reduction potential ($E_0 < -400$ mV).^[24] The W-atom is always coordinated by the dithiolene groups of two molybdopterin guanine dinucleotide (MGD) cofactors and has oxidation numbers ranging from +IV to +VI (cp. Figure 2, Figure 3).^[6,11,13,25,26] It seems that the bis(dithiolene) coordination of the W-centers via the two molybdopterin cofactors is essential for tungstoenzymes to maintain the redox potentials $[W^{IV}/W^{VI}]$ required for redox activity under physiological conditions.^[17]

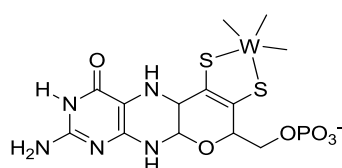


Figure 2: The pterin cofactor^[9]

It has been suggested that tungstoenzymes are more ancient than Mo-utilizing enzymes.^[10] W is thought to be an evolutionary “old” element, which is being replaced by the “modern” Mo, coinciding with the significant correlation between archael life and W-biochemistry.^[6] Given the fact that the majority of tungstoenzymes was isolated from thermophilic or hyperthermophilic, anaerobic archaea and the hot, anoxic conditions under which life probably arose, W might have been essential once upon a time.^[6,13,27] The deep sea hydrothermal vents, where most tungsten-dependent microorganisms are found, are believed to mirror the conditions on the primitive Earth.^[28,29]

Classes of Tungstoenzymes

All known tungsten-containing enzymes can be classified into three functional families, aldehyde ferredoxin oxidoreductases (AORs), formate dehydrogenases (F(M)DHs) and acetylene hydratase (AH). From an evolutionary perspective these families appear to be unrelated.^[17]

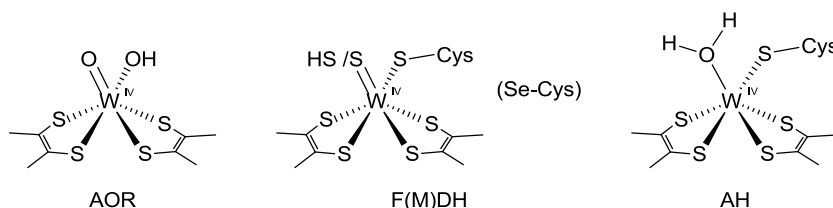
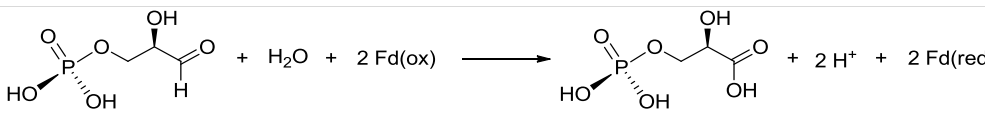


Figure 3: Proposed active site structures of the three tungsten containing enzyme families; the molybdopterin cofactors are represented by 1,2-dimethylethylenedithiolate ligands^[9,30]

Most known tungstoenzymes, e.g. aldehyde ferredoxin oxidoreductase (AOR), formaldehyde ferredoxin oxidoreductase (FOR) and glyceraldehyde-3-phosphate ferredoxin oxidoreductase (GAPOR) belong to the AOR family which catalyzes the oxidation of various aldehydes to the corresponding carboxylic acids, and uses a [4Fe:4S] ferredoxin as electron acceptor.^[9] The F(M)DH family has two members, both of which accept carbon dioxide as substrate, namely formate dehydrogenase (FDH) and formylmethanofuran dehydrogenases (FMDH). FDH catalyzes the first step in the conversion of CO₂ to formate which is further metabolized to yield acetate, while FMDH facilitates the first step in the conversion of CO₂ to methane.^[11] The third class of tungstoenzymes is made up by acetylene hydratase alone. It is unique among tungsten and molybdenum-dependent enzymes as it does not catalyze a redox reaction, but a hydration reaction. Neither its W atom nor the [4Fe:4S] cluster change their oxidation states during catalysis.^[16]

Table 2: Selected reactions catalyzed by tungstoenzymes^[17]

Enzyme	Reaction catalyzed
AOR	$\text{R}-\overset{\text{O}}{\parallel}{\text{C}}-\text{H} + \text{H}_2\text{O} + 2 \text{Fd(ox)} \longrightarrow \text{R}-\overset{\text{O}}{\parallel}{\text{C}}-\text{OH} + 2 \text{H}^+ + 2 \text{Fd(red)}$ <p>R= H, C1-C4, Ar</p>
FOR	$\text{R}-\overset{\text{O}}{\parallel}{\text{C}}-\text{H} + \text{H}_2\text{O} + 2 \text{Fd(ox)} \longrightarrow \text{R}-\overset{\text{O}}{\parallel}{\text{C}}-\text{OH} + 2 \text{H}^+ + 2 \text{Fd(red)}$ <p>R= H, C1-C3, C4-C6 di-semialdehydes</p>
GAPOR	
FDH	$\text{CO}_2 + \text{NADPH} + \text{H}^+ \longrightarrow \text{H}-\overset{\text{O}}{\parallel}{\text{C}}-\text{OH} + \text{NADP}^+$
FMDH	$\text{CO}_2 + \text{MFR} + 2 \text{H}^+ \longrightarrow \text{H}-\overset{\text{O}}{\parallel}{\text{C}}-\text{MFR} + \text{H}_2\text{O}$
AH	$\text{H}-\text{C}\equiv\text{C}-\text{H} + \text{H}-\text{O}-\text{H} \xrightarrow{\text{AH}} \text{H}-\overset{\text{O}}{\parallel}{\text{C}}-\text{CH}_3$

Biomimetic Ligand Systems

All tungstoenzymes contain molybdopterin cofactors coordinated through the dithiolene moiety. Therefore complexes with two dithiolene ligands around the W-center are popular motifs in the respective modeling chemistry.^[6,13,30–32] Dithiolenes have been shown to be non-innocent ligands. They influence the electronic structure of the model compounds, but do not affect the metal coordination geometry significantly, which is largely determined by the metal ion itself.^[31]

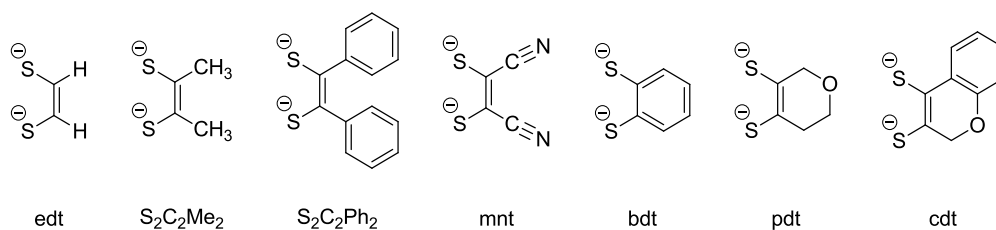


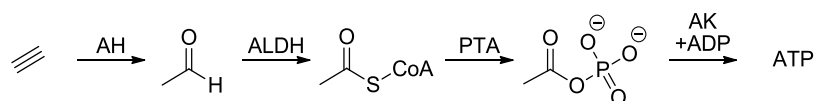
Figure 4: Selected dithiolene ligands

Malonitrile (mnt) has been most frequently used as it is the easiest to synthesize, handle and coordinate to the metal. Despite its simple structure mnt was shown to be a surprisingly good functional model for a number of enzymes, including sulfite oxidase, aldehyde oxidoreductase and formate dehydrogenase.^[7,30]

3. ACETYLENE HYDRATASE

PELOBACTER ACETYLENICUS- THE HOST ORGANISM

Pelobacter acetylenicus, a strictly anaerobic, mesophilic, fermenting bacterium, isolated from marine and freshwater sediments, can live of acetylene as sole source of carbon and energy.^[33] First it uses acetylene hydratase to hydrate acetylene to acetaldehyde, which is then used by aldehyde dehydrogenase (ALDH) to generate acetyl-coenzyme A. This is in turn converted to acetyl phosphate by phosphate acetyltransferase (PTA). Finally the acetyl phosphate is attached to ADP by acetate kinase to yield ATP.^[34] Optimum conditions are a temperature of 50 to 55°C and a pH value between 6.0 and 6.5.^[35]



Scheme 1: Metabolization of acetylene

ACETYLENE- THE SUBSTRATE

Today acetylene is only a minor trace gas on Earth. Mixing levels in the atmosphere vary according to the collection site, ranging from below LOD to 10 ppbv.^[36] It is thought to be entirely of anthropogenic origin, most notably combustion of gasoline and diesel fuels, biomass burning and industrial pollution.^[37] However reports of abiotic and biogenic sources of acetylene have surfaced. For example iron ores like pyrite and magnetite have been reported to transform tetrachloroethylene to acetylene and several methanogenic organisms were found to produce acetylene when exposed to 1,2-dibromoethylene.^[38] To date no biogenic oceanic source could be identified to explain the unexpectedly large amounts of acetylene in open oceanic atmospheres.^[39]

Acetylene is a well-known inhibitor and interference factor for numerous microbial processes including nitrogen fixation, nitrous oxide reduction, ammonium, methane and ethylene oxidation as well as anaerobic methane oxidation.^[36,39,40] Nevertheless it may act as sole source of carbon and energy for the aerobic bacteria strains *Nocardia rhodochrous*,^[41] *Rhodococcus A1*,^[42] *Rhodococcus rhodochrous*,^[43] a *Bacillus* species^[44] and the anaerobic *Pelobacter acetylenicus*.^[33]

The solubility of acetylene in water, of more than 45 mM, is unexpectedly high compared to other apolar gasses like H₂, N₂ or O₂ which have approximate solubilities of 1 mM, therefore bacteria can easily live of the dissolved amounts of acetylene, if an adequate source is available.^[29,45] It has been speculated, that the metabolization of acetylene might represent an early form of life, as the hydration of acetylene depends on W.^[9,10] Photochemical processes in the upper atmosphere and volcanic eruptions may have provided early forms of life with an easily accessible source of carbon and energy.^[39]

ENZYME CHARACTERISTICS

Acetylene Hydratase (AH^{vi}) is a tungsten-iron-sulfur enzyme belonging to the group of hydro-lyases.^[24] Sequence comparisons assigned it to be a member of the dimethyl sulfoxide (DMSO) reductase family of molybdenum and tungsten enzymes, whereas among tungstoenzymes AH represents its own family. Members of the DMSO reductase family include: trimethylamine-*N*-oxide reductase, dimethyl sulfoxide reductase and biotin sulfoxide reductase.^[46] AH activity stands out from other tungsten and molybdenum enzymes as it uses two redox active metal sites in order to perform a non-redox

^{vi} Protein Data Bank [PDB] Code: 2E7Z; EC number: 4.2.1.112, CAS Registry Number: 75788-81-7.

reaction.^[27] However several iron-sulfur proteins that catalyze hydration reactions instead of redox reactions have been described.^[27]

AH is the only enzyme known to accept acetylene as substrate, apart from nitrogenase, which reduces it to ethylene.^[47] AH demonstrates high substrate specificity. Up to date no further substrates could be identified. Attempts to hydrate propyne, ethylene, nitriles, including acetonitrile, isonitriles and carbon monoxide have failed.^[27,47-49] Cyanide and nitric oxide were found to be inhibitors of AH activity.^[27]

MOLECULAR STRUCTURE OF ACETYLENE HYDRATASE

Acetylene hydratase is a monomer of 730 aa residues weighing 83 kDa. It contains two molybdopterin guanine dinucleotide (MGD) cofactors, a cubane-type [4Fe:4S] cluster and a tungsten center, meaning that it shares the general structural features of members of the DMSO reductase family. However the active site of AH is rearranged providing access to a completely different part of the metal's coordination sphere.^[16]

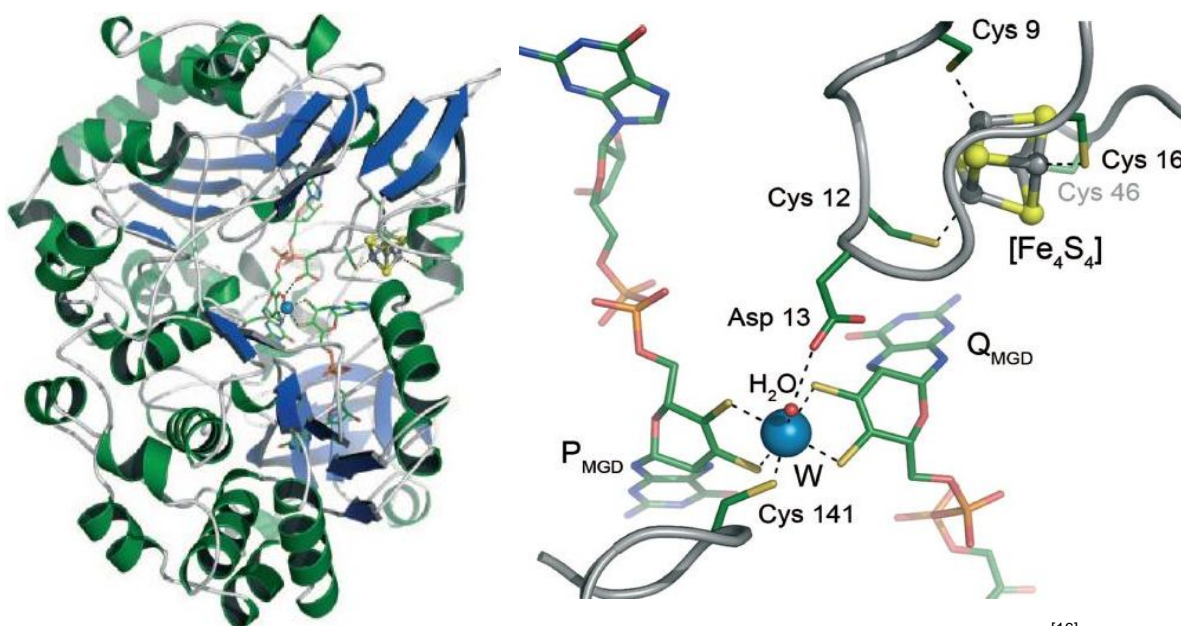


Figure 5: Overall structure of AH from *P. acetylenicus*, viewing down the substrate channel onto the active site.^[16]

Figure 6: Cofactors and active site of AH.^[16]

The tungsten(IV) center is coordinated by the two, respectively four, sulfur atoms of the dithiolene moieties of the two MGD cofactors, a cysteine residue (Cys-141) and a sixth oxygen ligand at 2.04 Å. Acetylene may access the active site through a hydrophobic channel (17x 6-8 Å) terminating in a binding pocket which would place the acetylene's

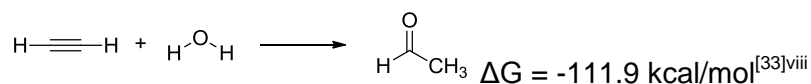
carbon atoms right above the tungsten-bound oxygen ligand. The nature of the oxygen ligand plays a key part in the clarification of the catalytic mechanism. At a resolution of 1.26 Å Seiffert et al.^[16] found a W-O distance of 2.04 Å which may result from a loosely bound hydroxo ligand (1.9- 2.1 Å) or from a tightly coordinated water molecule (2.0- 2.3 Å)^{vii}. These two possibilities lead to various mechanistic scenarios as the hydroxo ligand would act as a strong nucleophile and the coordinated water would act as an electrophile. The exact tungsten-oxygen distance is challenging to derive from the X-ray experiment as tungsten is a heavy scatterer and thus Fourier series termination effects may distort the crystal structure. This being taken into account the corrected W-O bond length is 2.25 Å which is in good agreement with the sixth ligand being a water molecule.^[16]

MECHANISTIC PROPOSALS FOR ACETYLENE HYDRATION

Up to date the actual catalytic mechanism of the acetylene hydration has not been agreed upon. Theoretical calculations employing the quantum-mechanical method (QM-only) density functional theory (DFT) or a combined hybrid quantum mechanics/ molecular modeling (QM/MM) approach have been carried out. Four suggestions have been put forward since the crystal structure's solution. These are in order of their publication:

Table 3: Proposed mechanisms for acetylene hydration

Mechanism	Description	ΔG^\ddagger [kcal/mol]	Approach
A	Electrophilic attack of water on acetylene ^[16]	43.9 ^[15]	QM-only
B	Nucleophilic attack of water on acetylene ^[50]	41.0 ^[15]	QM-only
C	Electrophilic attack of Asp13 on acetylene ^[15]	34.0 ^[15]	QM-only
D	Formation of a tungsten-acetylene adduct ^[25]	16.7 ^[48]	QM/MM

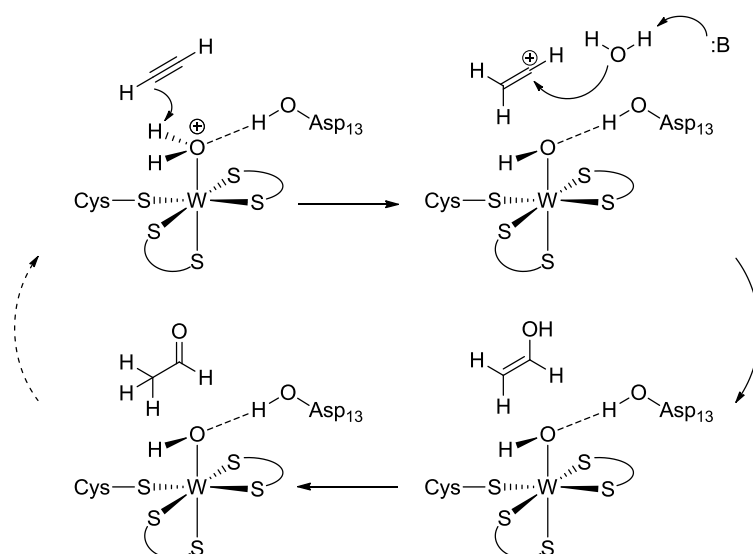


Scheme 2: Reaction catalyzed by AH

^{vii} Expected Values.

^{viii} Uncatalyzed. Thermodynamically favored, but inhibited kinetically.

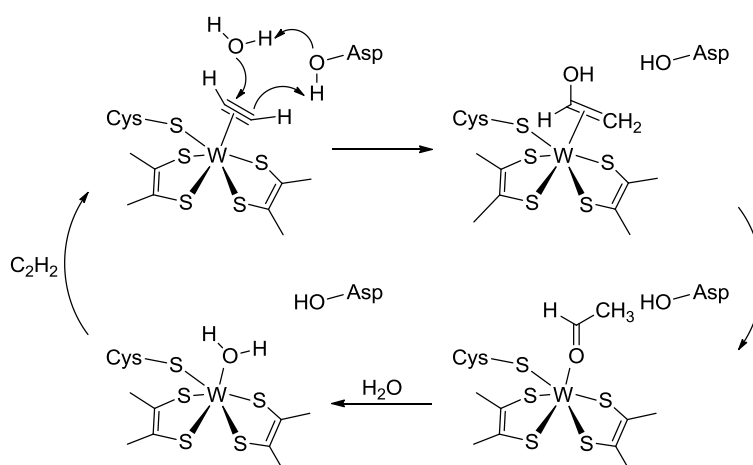
Mechanism A



Scheme 3: Mechanism A- the electrophilic attack of a tungsten bound water molecule on acetylene, drawn according to Antony et al.^[50]

Seiffert et al.^[16] favor a mechanism where the protonated Asp13 residue forms a short hydrogen bond to the coordinated water molecule resulting in a positive charge on the oxygen atom. It can then act as an electrophile and attack the acetylene's triple bond directly. The resulting vinyl cation intermediate is then attacked by a hydroxyl, which results from deprotonation of another water molecule. The so formed ethenol tautomerizes spontaneously to yield acetaldehyde.

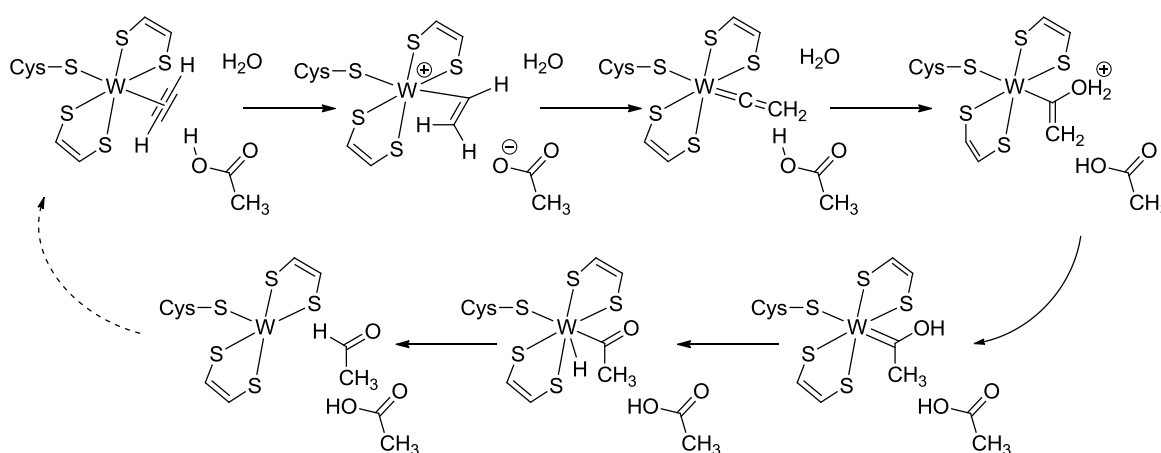
Mechanism B



Scheme 4: Mechanism B- the nucleophilic attack of water on acetylene assisted by the neutral Asp13 residue^[50]

Based on DFT calculations on dithiocarbamate (dtc) and dithiolate model complexes Anthony et al. propose that catalysis occurs through nucleophilic attack of water on coordinated acetylene. Reasoning that acetylene coordination is favored over water coordination by 12 kcal/mol, which in turn is endergonic by 7 kcal/mol (ΔG). As a consequence the suggested stages of the catalytic cycle are: nucleophilic attack of water on an η^2 -acetylene combined with the Asp13 residue acting as proton shuttle, followed by formation of ethenol, tautomerization to acetaldehyde and its replacement by water, which in turn is replaced by acetylene to re-enter the catalytic cycle.

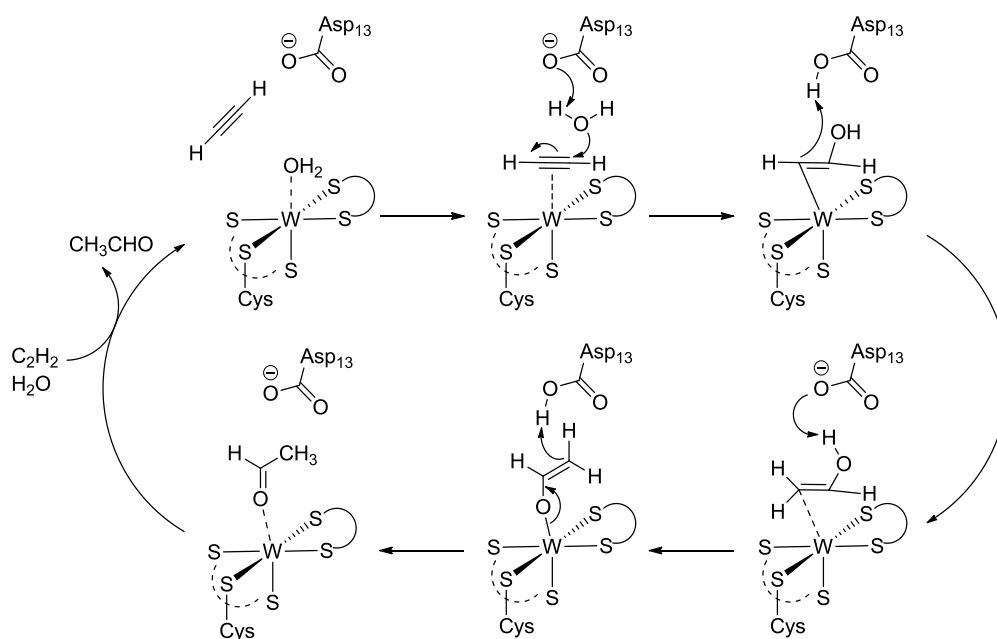
Mechanism C



Scheme 5: Mechanism C- the electrophilic attack of the neutral Asp13 on acetylene to form a vinylidene intermediate^[15]

Based on their own set of DFT calculations Vincent et al.^[15] propose yet another mechanism. In accordance to Anthony et al.^[50] η^2 -bound acetylene is found to be lower in energy than water coordinated to tungsten. The catalytic cycle starts with a proton shuttling mechanism between Asp13 and the acetylene to yield a stable vinylidene complex, whose central carbon atom is then attacked by a water molecule. The proton transfer from water to the substrate's terminal carbon atom to form a stable carbene intermediate is again achieved via a proton shuttling mechanism involving Asp13. Free acetaldehyde is formed through hydrogen transfer from oxygen to carbon via a tungsten hydride intermediate.

Mechanism D



Scheme 6: Mechanism D- the displacement of water by acetylene to form a tungsten-acetylene adduct^[25]

Based on extensive DFT calculations Liao et al.^[25] proposed a fourth mechanism. On the contrary to the previous pathways this one demands a deprotonated Asp13 residue. The acetylene substrate displaces the water molecule, as its coordination is favored. It is then attacked nucleophilically by the liberated water supported by concomitant proton transfer to Asp13. The resulting vinyl anion is then protonated by Asp13 to yield a vinyl alcohol intermediate. Its tautomerization to acetaldehyde might occur outside the active site or again through a proton shuttle mechanism involving Asp13.

Recently Liao and Thiel^[48] published QM/MM calculations on an even bigger model (157 vs. 116 atoms) lowering the energetic barrier of mechanism D to 16.7 kcal/mol.

Summing up...

All proposed mechanisms identify Asp13 as a key player in the hydration of acetylene. This is strongly supported by site-directed mutagenesis experiments, where AH activity is reduced to almost zero if Asp13 is replaced by an alanine residue.^[47] Whereas the importance assigned to tungsten ranges from minor to relevant. Especially the Mechanisms A and B assign little weight to the metal coordination. Mechanism C involves activated η^2 -acetylene and two tungsten complexes as stable intermediates. This reflects the fact that the inhibition of AH by $C\equiv O$ and $N\equiv O$ indicates π -interactions between metal and substrate.^[51] Yet mechanism D is the first to assign significant influences to tungsten. In addition to binding and activating acetylene tungsten provides electrostatic stabilization

to the transition states and intermediates. This is in good agreement with the experimental finding that the specific activity of AH is lowered by 60% if molybdenum is incorporated into the MGD cofactor instead of tungsten.^[35] However attempts to crystalize the enzyme with acetylene in the active site have failed thus far.^[16]

RELEVANT MODELING CHEMISTRY

Modeling chemistry of acetylene hydratase is scarce.^[7] Most structurally relevant compounds were synthesized years before the discovery of AH, with nitrogenase modeling chemistry in mind.^[52-55] Other complexes were synthesized to provide structural evidence for acetylene as four-electron donor.^[52,56,57] One of the problems in the synthesis of mononuclear oxo-molybdenum and oxo-tungsten complexes is the usually irreversible formation of a dimeric μ -oxo species, i.e. $M^{IV}O$ and M^VO_2 react to yield $M_2^VO_3$. This undesired side-reaction may be prevented by sterically demanding ligands.^[6]

Structural Modeling Chemistry

A number of Mo(II) and W(II)-acetylene carbonyl complexes of the form $[M(CO)(R^1C\equiv CR^2)(S_2CNR^3_2)_2]$ ($R^1 = R^2 = H, Me, Et, Ph$; $R^3 = i-Pr, Et_2, Me_2$) have been described.^[52,53,56,57] However +II is a biologically irrelevant oxidation state. A series of $[MoO(R^1C\equiv CR^2)(S_2CNR^3_2)_2]$ ($R^1 = R^2 = H, Me, Et, Ph$; $CO_2Me, COC_6H_5Me, CO_2Me$; $R^3 = Et_2, Me_2$) compounds have been described where the carbonyl was substituted by an oxo-group and the Mo can thus be regarded as Mo(IV). Yet the especially interesting $[MoO(HC\equiv CH)(S_2CNEt_2)_2]$ could only be detected in solution as the formed adduct is labile and dissociates upon solvent removal.^[54,55,58] These complexes were of particular interest as only a handful mononuclear acetylene complexes were known at the time.^[55] The synthesis of the first oxo-tungsten(IV)-acetylene complex $[WO(HC\equiv CH)(S_2CNR^3_2)_2]$ ($R^3 = Et_2, Me_2$) was accomplished by Newton and coworkers through controlled oxidation of the corresponding carbonyl complex with the oxygen atom transfer reagent $[Mo_2O_3(S_2P(OEt)_2)_4]$.^[59] On the contrary to its Mo-counterpart the W-species is stable towards alkyne dissociation. The crystal structure of $[WO(HC\equiv CH)(S_2CNEt_2)_2]$ was the first mononuclear Mo(IV)/ W(IV) acetylene structure to be resolved.^[59]

Structural-Functional Modeling Chemistry

To date only one compound has been proven to fulfill the criteria to structurally and functionally mimic acetylene hydratase. $[\text{Et}_4\text{N}]_2[\text{W}^{\text{IV}}\text{O}(\text{mnt})_2]$ was originally designed as a mimic for aldehyde ferredoxin oxidoreductase and actually responded to metal exchange reactions with $[\text{MoO}_4]^{2-}$ and displayed sulfur reductase activity^{ix}.^[60]

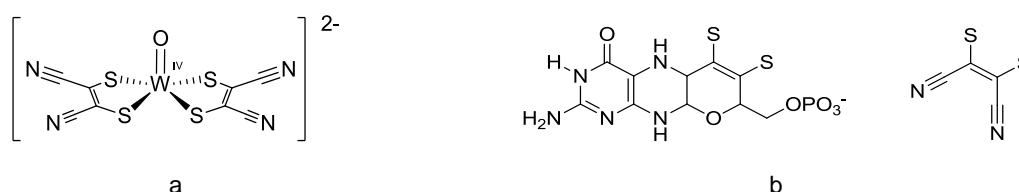


Figure 7: a) $[\text{Et}_4\text{N}]_2[\text{W}^{\text{IV}}\text{O}(\text{mnt})_2]$; b) Comparison between the natural pterin cofactor and the biomimetic 1,2-dicyanoethylenedithiolate(mnt)

Additionally $[\text{Et}_4\text{N}]_2[\text{W}^{\text{IV}}\text{O}(\text{mnt})_2]$ was found to be able to catalytically hydrate acetylene.^[51] In a rather complicated assay, due to the low boiling point of acetaldehyde (20.4°C ^[61]), Sarkar and coworkers could show that it is capable of performing approximately nine turnovers. Ten years prior to the solution of AH's crystal structure^[16] $[\text{Et}_4\text{N}]_2[\text{W}^{\text{IV}}\text{O}(\text{mnt})_2]$ hinted at the participation of a reduced tungsten species (W^{IV}) in catalysis, as the corresponding oxidized species did not show catalytic activity.^[7,51] Although no η^2 -acetylene adduct could be observed the adduct formation with dimethyl acetylenedicarboxylate ($\text{H}_3\text{COC}(\text{O})\text{C}\equiv\text{C}(\text{O})\text{OCH}_3$) suggests an activation of acetylene via electron donor-acceptor complexation and the existence of a short-lived η^2 -adduct.^[7,51]

Mechanistic Studies on the Structural-Functional Model

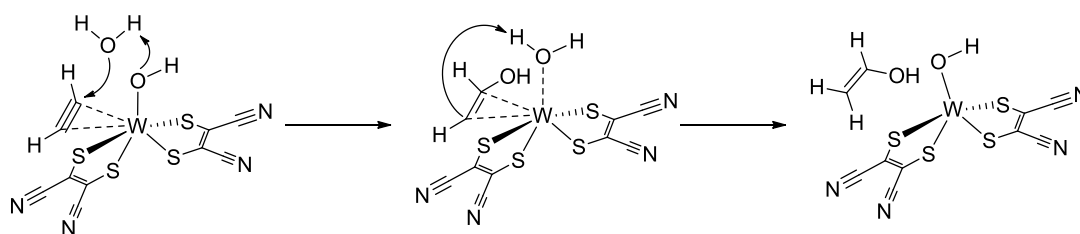
It is still not fully clarified how $[\text{Et}_4\text{N}]_2[\text{W}^{\text{IV}}\text{O}(\text{mnt})_2]$ catalyzes the hydration of acetylene, but Liu et al.^[3] investigated possible mechanisms using DFT-calculations. Three different first-shell models, in which a hydroxo (A), an aquo (B) or an oxo (C) species coordinates to tungsten were calculated (cp. Table 4).

The calculations clearly favor model A and a mechanism where tungsten first coordinates acetylene in a η^2 -fashion. The tungsten-bound hydroxide activates a water molecule which then carries out a nucleophilic attack on acetylene. The so formed vinyl anion abstracts a proton from the newly formed W-coordinated water resulting in the formation of ethenol. The final isomerization to acetaldehyde can then occur in solution assisted by water molecules (cp. Scheme 7).^[3]

^{ix} $\text{Ph}_3\text{P} + \text{S} \rightarrow \text{Ph}_3\text{PS}$ and $\text{H}_2 + \text{S} \rightarrow \text{H}_2\text{S}$

Table 4: Possible mechanisms for the $[\text{Et}_4\text{N}]_2[\text{W}^{\text{IV}}\text{O}_2(\text{mnt})_2]$ catalyzed hydration of acetylene^[3]

Model	Oxygen-species	Description	ΔG^\ddagger [kcal/mol]
A	Hydroxo	Activation of water by hydroxide, nucleophilic attack on η^2 -acetylene	20.8
B	Aquo	Electrophilic attack of water on one of the acetylene carbons by delivering a proton	30.4
B'	Aquo	Proton transfer to thiolate ligand to generate a hydroxide, nucleophilic attack by OH	38.4
C	Oxo	W=O functions as a base to activate a water molecule, nucleophilic attack on acetylene	> 43.8
Uncatalyzed	-	-	57.4



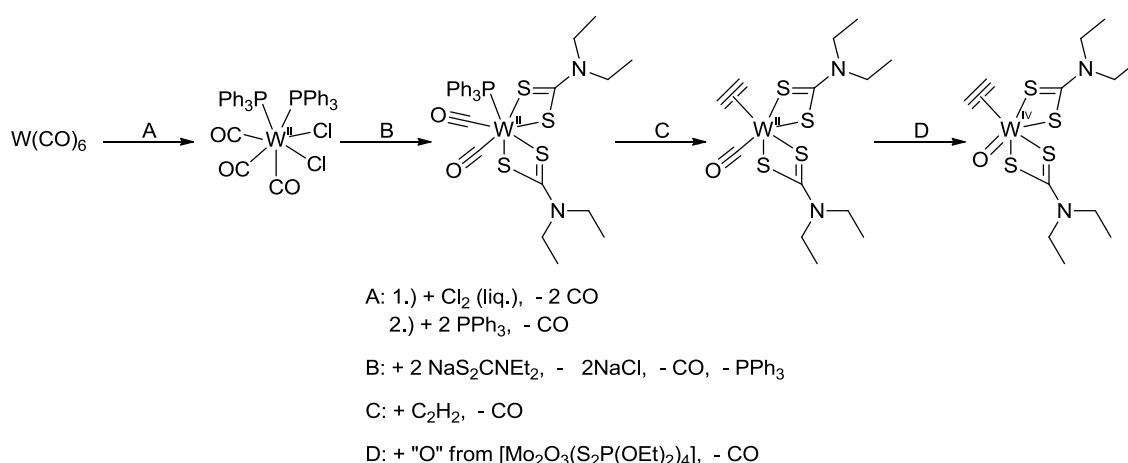
Scheme 7: Model A- the favored mechanism for the hydration of acetylene catalyzed by $[\text{Et}_4\text{N}]_2[\text{W}^{\text{IV}}\text{O}_2(\text{mnt})_2]$ ^[3]

It is suggested that the hydroxide residue assumes the central role that Asp13 fulfills in the native enzyme.^[34] This mechanism directly involves tungsten in the reaction as it is used to coordinate and activate acetylene. Furthermore W provides electrostatic stabilization to the intermediates. In this respect the proposed mechanism for the model-compound is similar to the above described mechanism D^[25] for the enzymatic equivalent acetylene hydratase (cp. Scheme 6).

4. OBJECTIVES

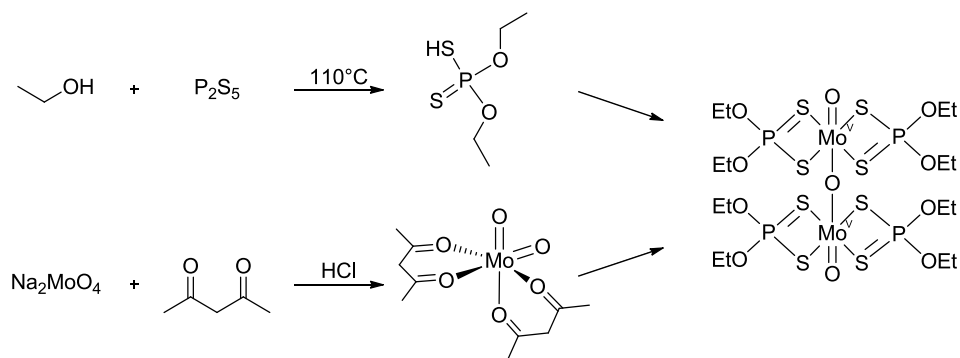
More than twenty years ago Sarkar and coworkers had shown that a tungsten(IV)-oxo compound may be able to mimic the reactivity and immediate coordination sphere of acetylene hydratase.^[51] The characteristics of their structural-functional model being the W(IV)-oxo center and a sulfur-rich ligand system. Ever since no further, improved models have been published. Hence the central idea of this master's thesis was to combine the characteristics of the model complex with a ligand system that is capable of stabilizing adducts with unsubstituted acetylene. The W(II) and W(IV)-dithiocarbamate systems are the only reported systems that are able to stabilize monomeric adducts with free acetylene.^[52,53,56,57,59] The only example of an oxygen atom transfer reaction was carried out using the dimeric Mo(V)-species $[\text{Mo}_2\text{O}_3(\text{S}_2\text{P}(\text{OEt})_2)_4]$ as oxygen atom transfer reagent.^[59] Thus the replication of this established synthesis route (cp. Scheme 8) was chosen as entry point into the tungsten(IV)-oxo chemistry.

Thereby the removal of the last carbonyl substituent and the concomitant oxidation of W(II) to the biologically relevant W(IV) state is of central interest. $[\text{Mo}_2\text{O}_3(\text{S}_2\text{P}(\text{OEt})_2)_4]$ may be a potent oxygen atom transfer reagent, but it requires a three-step synthesis (cp. Scheme 9) and exhibits a fairly bad atom economy^x,^[62] e.g. 35% for $[\text{WO}(\text{HC}\equiv\text{CH})(\text{S}_2\text{CNEt}_2)_2]$. Therefore novel oxygen atom transfer agents, powerful enough to substitute the remaining carbonyl and preferably commercially available were to be investigated. The established reactivity of the dtc-system was chosen as a "control-group". The lessons learned from this system were to be applied in the synthesis and application of new ligand systems.



Scheme 8: Literature method towards W(IV)-oxo compounds^[56,59,63]

^x Atom economy [%] = [(molecular weight of desired product) ÷ (molecular weight of all reactants) × 100]



Scheme 9: Synthesis of the oxygen atom transfer reagent $\text{Mo}_2\text{O}_3[\text{S}_2\text{P}(\text{OEt})_2]_4$ ^[64–66]

All of the published dtc-acetylene systems use nitrogen as heteroatom in the ligand.^[52,53,56,57,59] Thus a broadening of the ligand system to oxygen and sulfur as heteroatoms was to be attempted. Their influence on the electron donor and acceptor qualities of the ligand and the subsequent consequences for the coordination of acetylene were to be studied.

A reliable precursor synthesis, preferably with high yields, is of central relevance in the development of new synthesis routes. Thus the identification of such a precursor and the optimization of its synthesis are another important objective of this thesis.

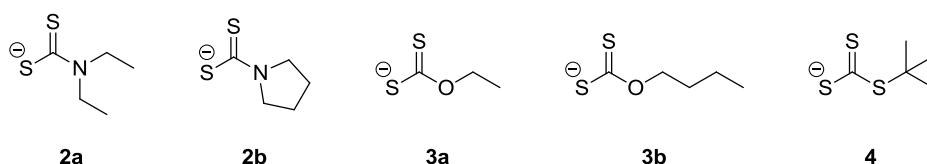
III. RESULTS AND DISCUSSION

LIGAND SYNTHESIS AND LIGAND PROPERTIES

In preparation for the oxidation of the W(II) coordination compounds $\text{HS}_2\text{P}(\text{OEt})_2$ (**1**), the ligand for the oxygen atom transfer reagent $[\text{Mo}_2\text{O}_3(\text{S}_2\text{P}(\text{OEt})_2)_4]$ (**10**) was prepared by a modified literature procedure (cp. page 44).^[64]

The ligands $\text{M}[\text{S}_2\text{CYR}]$ ($\text{M} = \text{K}, \text{Ag}, \text{NH}_4$; $\text{YR} = \text{NEt}_2, \text{NC}_4\text{H}_8, \text{OEt}, \text{O}n\text{-Bu}, \text{S}t\text{-Bu}$) studied were designed with variations of the heteroatom and the aliphatic R-group to modify the donor and acceptor abilities of the ligand. $[\text{S}_2\text{CNEt}_2]$ (**2a**), the ligand used in the structural model, is referred to as reference point. The silver salt of **2a** and the ammonium salt of **2b** were used as they are commercially available.

$\text{K}[\text{S}_2\text{COEt}]$ (**3a**) was expected to increase the acidity on the quaternary carbon (C_q) due to the higher electronegativity of O compared to N and the comparatively weak +I-effect of the ethyl substituent. $\text{K}[\text{S}_2\text{CS}t\text{-Bu}]$ (**4**) on the other hand was expected to yield a comparatively electron-rich C_q , because of the strong +I-effect of the *t*-butyl group and the similar electronegativities of C and S.



Scheme 10: Studied ligands

To the best of our knowledge this is the first report on the actual synthesis of $\text{K}[\text{S}_2\text{CS}t\text{-Bu}]$ (**4**), including full experimental details. The ligand and salt metathesis reactions have been described previously, but no experimental detail was given.^[67] Synthesis of **4** followed a published procedure for secondary amines.^[68] 2-Methylpropan-2-thiol was added to KOH suspended in THF and small quantities of water (< 5%), after stirring for 15 min CS_2 was added at 0°C . Reduction of the volume in vacuo and layering with ether caused the product to precipitate. $\text{Na}[\text{S}_2\text{CS}t\text{-Bu}]$ has been prepared similarly.^[69]

K[S₂COEt] (**3a**) and K[S₂CO*n*-Bu] (**3b**) were prepared by dissolving KOH in the respective alcohol and addition of CS₂ at 0°C. The work-up was carried out according to the procedure for secondary amines.^[68]

Care has to be taken to ensure acid-free systems, as the ligands are labile towards acid-catalyzed breakdown, resulting in the elimination of the CS₂ unit.^[70] The ligands should be stored under an atmosphere of nitrogen, or at least at low temperatures as O₂ has been shown to cause disulfide formation.^[71]

Table 5: Overview- quaternary carbons S₂CY (Y = N, O, S) of the ligands

	Compound	¹³ C NMR (DMSO) δ
2a	Ag[S ₂ CNEt ₂]	202.97 ^{xi}
2b	NH ₄ [S ₂ CNC ₄ H ₈]	208.30
3a	K[S ₂ COEt]	229.86
3b	K[S ₂ CO <i>n</i> -Bu]	230.12
4	K[S ₂ CS <i>t</i> -Bu]	241.42

The ¹³C NMR data for **2a**^[72], **2b**^[73] and **3a**^[71] have been reported previously. Surprisingly ¹³C NMR spectra reveal that **4** has the most acidic carbon of all used ligands at δ = 241 ppm (cp. Table 5). The trend is continued in the dicarbonyl compounds where the ligand appears to withdraw electron density from the W-center (vide infra, page 33). On the causes for this observations can only be speculated.

^{xi} CD₂Cl₂. Solubility in DMSO not high enough to obtain ¹³C-spectra.

PRECURSOR SYNTHESIS

A reliable precursor is central in every effective synthesis strategy. Good precursors should meet as many of the following (selected) criteria as possible:

- Reproducibility of the synthesis
- High yields
- Reasonable stability
- Reasonable shelf-life
- Upscaling potential
- Few side reactions
- Easy purification procedure
- Full characterization available
- Versatile reactivity
- Solubility in organic solvents

As expected, bearing all these ideals in mind, identifying such a species turned out to be a tough challenge. The published routes to W(II)-dihalide precursors may look straightforward on paper, but their experimental realization poses a number of difficulties. Synthesis usually starts with $[W(CO)_6]$, which is commercially available and reasonably priced. As tungsten(0) hexacarbonyl is a relatively unreactive species rather harsh conditions are needed to oxidize it to W(II). However W(IV) and W(VI) are stable species too, hence they are easily accessible, thermodynamically, as well as kinetically. Therefore the conditions have to be chosen carefully. Clearly the applied stoichiometry and the reaction rate are key factors in this pursuit.

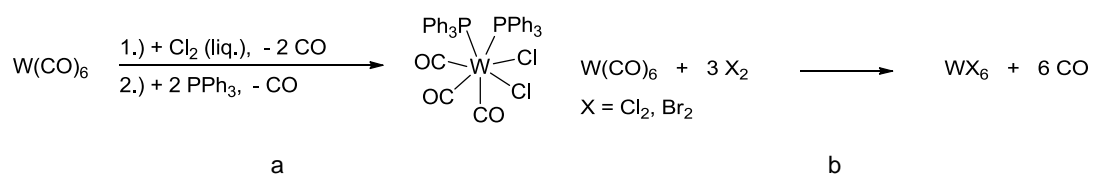
Central point of interest were tungsten(II) precursors of the general form $[W^{II}(CO)_nX_2]$ ($n = 2, 3, 4$, $X = Cl, Br, I$). In literature there are two of these systems which have been described to react with dithiocarbamate salts $M[S_2CYR]$ ($M = Na, K$; $Y = O, N, S$; $R = \text{alkyl, aryl}$). The phosphine-stabilized, 18-electron species $[W(CO)_3(PPh_3)_2X_2]$ ^[63,74] which are described as being more stable and the phosphine-free 16-electron species $[W(CO)_4X_2]$ ^[75-78]. The stability criterion however is outweighed by considerations about time, effort and safety precautions needed to realize the species. Another vital criterion is how well the stoichiometry may be adjusted, e.g. the amount of gaseous or condensed chlorine is harder to control, than the amount of bromine added via a syringe.

$[W(CO)_3(PPh_3)_2Cl_2]$ vs. $[Ph_3PCI]_2[WCl_6]$

The synthesis of $[W(CO)_3(PPh_3)_2Cl_2]$ (**7**) turned out to be associated with unexpected problems, that were not described in literature.^[63] According to Chen et al. condensation of chlorine onto hexacarbonyl, stirring for 40 min, evaporation of the chlorine and dropwise addition of triphenylphosphine in dichloromethane, keeping the reaction vessel at $-78^\circ C$ the entire time, should yield the desired product in acceptable yields.

However it was found that the reaction between $[W(CO)_6]$ and Cl_2 starts immediately upon contact as evidenced by a color change of the hexacarbonyl from white to dark brown and

the evolution of carbon monoxide gas. The brown color is thought to originate from a mixture of $[\text{W}(\text{CO})_4\text{Cl}_2]$ (yellow)^[75] and undesired $[\text{WCl}_6]$ (black)^{xii}.^[79]



Scheme 11: a) Intended precursor synthesis^[63]; b) Side-reaction^[79]

The over-oxidation to W(VI) represents a serious problem in this synthetic approach, as the stoichiometry of the reagents is hard to control and as the reaction does not stop before the last trace amount of chlorine is removed. Alternatively the stoichiometric, dropwise addition of liquid chlorine to a solution of $[\text{W}(\text{CO})_6]$ has been described.^[80] However this method was rejected due to safety issues.

Subsequently after following the protocol by Chen et al.^[63] an orange precipitate formed instead of a yellow one. A first analysis by IR spectroscopy revealed that the microcrystalline product did not show any carbonyl stretching frequencies at all. Complete loss of the CO and concomitant over-oxidation had apparently occurred. Crystals of the unknown compound, which was obtained in large quantities, could be grown from a supersaturated dichloromethane solution at -35°C . The product could be identified as bis(chlorotriphenylphosphonium) hexachloro-tungsten(IV) **6** by single crystal X-ray diffraction analysis. The octahedral $[\text{WCl}_6]^{2-}$ anion [$\text{W1}-\text{Cl1}$ 2.3824(3) Å] has a site symmetry of $\bar{3}$ (= C_{3i} symmetry), the cations [$\text{P1}-\text{Cl2}$ 1.9993(7) Å; $\text{P}(1)-\text{C}(1)$ 1.7807(11)] are situated on a three-fold rotation axis (cp. Figure 8). The newly identified compound is similar to the previously published structures for $[\text{Ph}_3\text{PCl}]_2[\text{MCl}_6]$ (M = Mo, Sn, Te).^[81,82]

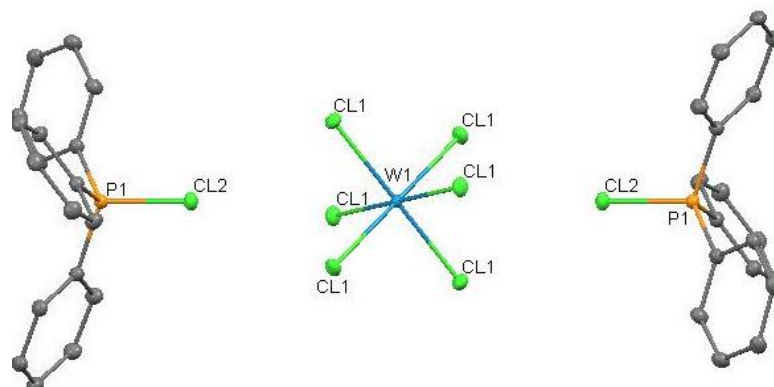
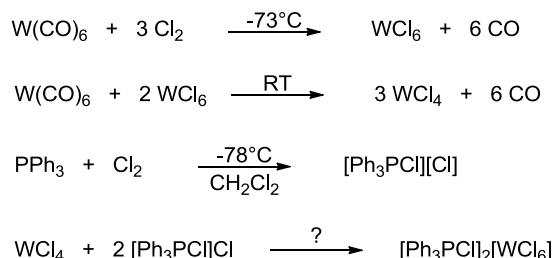


Figure 8: Mercury plot of **6** showing the atomic numbering scheme. The probability ellipsoids are drawn at 50% probability level. For a full list of bond lengths and angles see Appendix.

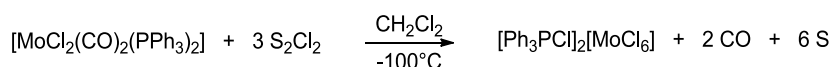
^{xii} The intermediate species $\text{W}(\text{CO})_2\text{Cl}_4$ has not been described yet.

It has not been fully elucidated how the formation of $[\text{Ph}_3\text{PCI}]_2[\text{WCl}_6]$ (**6**) happened, but residual Cl_2 is believed to have been a key player. The following known reactivities may give hints at the actual events (cp. Scheme 12). A combination of over-chlorination, disproportionation of $\text{W}(0)$ and $\text{W}(\text{VI})$ to $\text{W}(\text{IV})$ and oxidation of triphenylphosphine might have been responsible for the formation of the $\text{W}(\text{IV})$ salt in 88% yield.



Scheme 12: Suggested reaction cascade to $[\text{Ph}_3\text{PCI}]_2[\text{WCl}_6]$ (**6**)^[79,83]

The unwanted oxidation of **7** to **6** could have occurred in a fashion similar to the described oxidative addition of two equivalents “Cl” to $[\text{Mo}(\text{CO})_2(\text{PPh}_3)_2\text{Cl}_2]$ to yield $[\text{Ph}_3\text{PCI}]_2[\text{MoCl}_6]$.^[81] Instead of disulfur dichloride residual Cl_2 could have been responsible for the oxidation of $\text{W}(\text{II})$ to $\text{W}(\text{IV})$.



Scheme 13: Chlorination of $[\text{Mo}(\text{CO})_3(\text{PPh}_3)_2\text{Cl}_2]$ ^[81]

The reactivity of $[\text{Ph}_3\text{PCI}]_2[\text{WCl}_6]$ (**6**) is currently being investigated. There are no accounts on the reactivity of its structural analogues (Mo, Sn, Te) so this is an especially exciting new compound. Preliminary experiments showed that **6** reacts with $\text{Ag}[\text{S}_2\text{CNET}_2]$ (**2a**) under sulfur atom transfer to yield triphenylphosphine sulfide. The fate of the tungsten-species is yet to be clarified. Furthermore $[\text{WCl}_6]^{2-}$ is a $\text{W}(\text{IV})$ dianionic species, which despite structurally different, may share some electronic features of $[\text{W}^{\text{IV}}\text{O}(\text{mnt})_2]^{2-}$. We have thus speculated, whether **6** might be able to display sulfur reductase activity^{xiii} in analogy to Sarkar’s system.^[60]

After identifying the problem of over-chlorination, further attempts were carried out to synthesize $[\text{W}(\text{CO})_3(\text{PPh}_3)_2\text{Cl}_2]$ (**7**) (cp. Scheme 11). The reduction of the amount of chlorine to half, a shortened exposure time, extremely careful evaporation of the chlorine and smaller batch sizes finally afforded **7** in poor yields. Understandably all these extra

^{xiii} $\text{Ph}_3\text{P} + \text{S} \rightarrow \text{Ph}_3\text{PS}$ and $\text{H}_2 + \text{S} \rightarrow \text{H}_2\text{S}$

efforts to prevent over-chlorination lead to under-chlorination and the problem of how to remove residual $[\text{W}(\text{CO})_6]$. Both species turned out to be sparingly soluble in polar, as well as apolar solvents. $[\text{W}(\text{CO})_3(\text{PPh}_3)_2\text{Cl}_2]$ (**7**) co-crystallized with tungsten hexacarbonyl as dicarbonyl-dichloro-bis(triphenylphosphine)-tungsten(II) dichloromethane solvate (1:2) $[\text{W}(\text{CO})_2(\text{PPh}_3)_2\text{Cl}_2]$ (**7'**) from a super-saturated solution of dichloromethane at -35°C . The complex is situated on a two-fold rotation axis and shows an unusual trigonal-prismatic surrounding of the W atom.

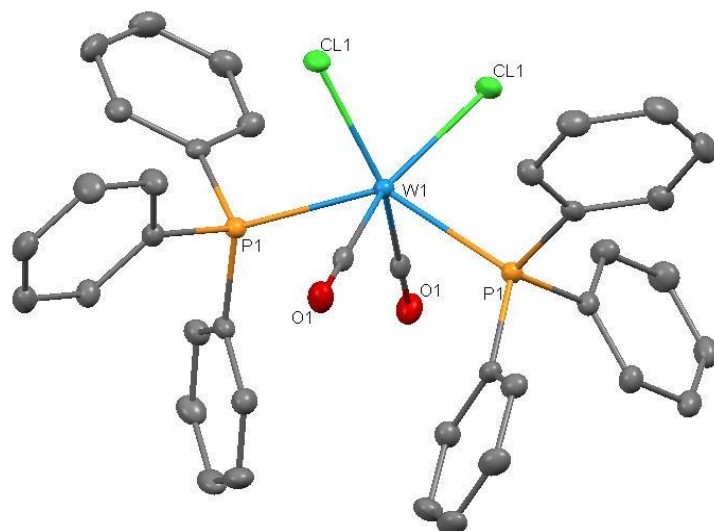
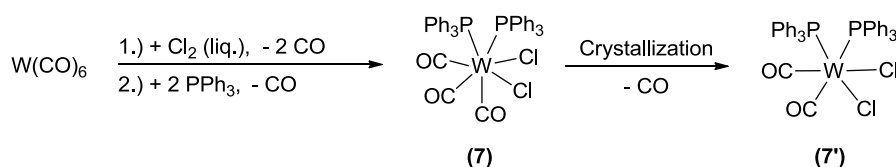


Table 6: Selected bond lengths [Å]

W1-C	1.9622)
W1-C1	2.4140(6)
W1-P1	2.4816(7)
C1-O1	1.159(3)
P1-C11	1.826(3)
P1-C21	1.837(2)
P1-C31	1.827(3)

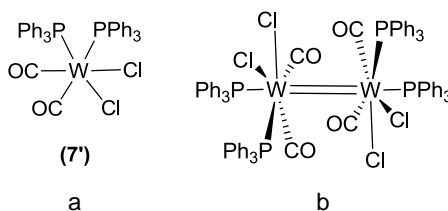
Figure 9: Mercury plot of (**7'**) showing the atomic numbering scheme. The probability ellipsoids are drawn at 50% probability level. For a full list of bond lengths and angles see Appendix.



Scheme 14: Synthesis and crystallization of $[\text{W}(\text{CO})_3(\text{PPh}_3)_2\text{Cl}_2]$ (**7**).

Surprisingly the crystallized compound is has lost one $\text{C}\equiv\text{O}$ -ligand. The microcrystalline yellow powder (**7**) showed, in good agreement with the literature, displaying three carbonyl stretching frequencies [IR (cm^{-1}): $\nu(\text{CO}) = 2011$ (s), 1929 (s), 1887 (s)].^[63,80,84] The crystals of (**7'**) on the other hand display lower frequency CO-stretches [IR (cm^{-1}): $\nu(\text{CO}) = 1954$ (w), 1930 (w), 1864 (s)], demonstrating a higher double-bond character of the two remaining $\text{C}\equiv\text{O}$ -ligands. This indicates that the 16-electron species stabilizes itself through stronger π -backbonding, compared to the 18-electron species, which coordinates the carbonyls less tightly. $[\text{W}(\text{CO})_2(\text{PPh}_3)_2\text{Cl}_2]$ (**7'**) has been previously suggested to be one subunit of the dimeric product of thermal decomposition of **7** accessible through

refluxing in CH_2Cl_2 for four days (cp. Scheme 15).^[80] The authors reasoned that the compound has to be a dimer, in order to explain its diamagnetic behavior. However later it was known that distorted geometries can cause new orbital arrangements and a loss of degenerate energy levels. Consequently 16 electron species can be diamagnetic. Tomkins and coworkers described their product as light blue solid, the crystals of **7'** on the other hand were dark red. The IR stretches of **7'** and the proposed dimeric species are very similar, so it remains unclear if both species, or just **7'** exist.



Scheme 15: a) Solved molecular structure for $[\text{W}(\text{CO})_2(\text{PPh}_3)_2\text{Cl}_2]$; b) suggested dimeric structure $[\text{W}(\text{CO})_2(\text{PPh}_3)_2\text{Cl}_2]_2$ ^[80]

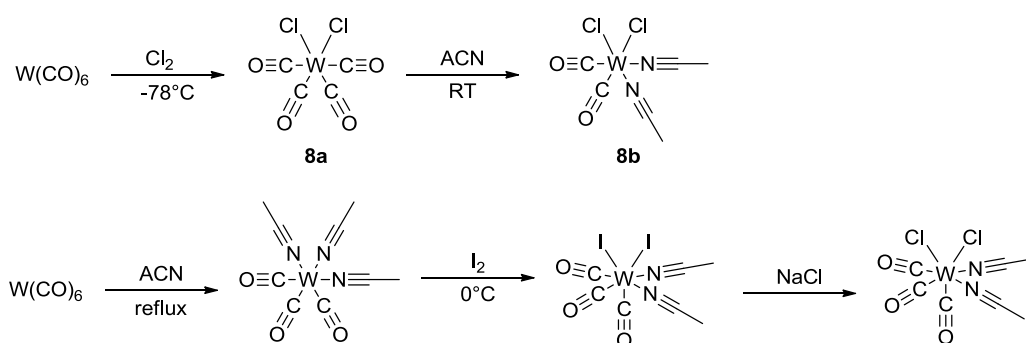
$[\text{W}(\text{CO})_3(\text{PPh}_3)_2\text{Cl}_2]$ (**7**) might be a relatively air-stable precursor with a long shelf life, but its synthesis poses too many risks to make it suitable for large scale routine synthesis. Additionally the desired acetylene-adduct complexes are phosphine-free (cp. Scheme 8, page 20). Thus it seemed somewhat redundant to add two equivalents of PPh_3 in the first step and then remove them successively in the second and third step, just for the sake of higher precursor stability. Triphenylphosphine is highly soluble in most organic solvents, so are $\text{W}(\text{II})$ -trithiocarbamate compounds **11-13**, as will be seen later (cp. page 32). In order to ensure a more efficient, straightforward synthesis route, alternative, less stable precursors were sought after.

$[\text{W}(\text{CO})_4\text{Cl}_2]$ and $[\text{W}(\text{CO})_2(\text{NCMe})_2\text{Cl}_2]$

The obvious choice as ideal precursor complex would be $[\text{W}(\text{CO})_4\text{Cl}_2]$ (**8a**) the first product of the oxidative addition on the way to the phosphine-stabilized species $[\text{W}(\text{CO})_3(\text{PPh}_3)_2\text{Cl}_2]$ (**7**). Despite previous speculations about thermal instability,^[63] **8a** had been isolated and characterized.^[75,76] Understandably the preparation from $[\text{W}(\text{CO})_6]$ and Cl_2 posed the same risk of over-oxidation, as we again refrained from the stoichiometric, dropwise addition of liquid Cl_2 . Residual chlorine turned out to be the major problem. Even after vacuum drying the crude $[\text{W}(\text{CO})_4\text{Cl}_2]$ (**8a**) for hours Cl_2/HCl fumes leaving the Schlenk flask were observed when purged with nitrogen. Further evaporation finally let the Cl_2/HCl fumes cease, but even then upon stepwise removing the acetone/dry ice bath

under vacuum a spontaneous boiling of residual chlorine and concomitant discoloration from yellow to brown could not always be prevented.

All batches of **8a** contained variable amounts of unreacted $[W(CO)_6]$, identified by its four characteristic IR stretches at (cm^{-1}): $\nu = 1057$ (w), 1000 (w), 940 (w) and 882 (w). Purification could be achieved by extraction of **8a** under adduct formation with acetonitrile and extraction of $[W(CO)_6]$ with pentane. The acetonitrile adduct of **8a** could be identified as the previously unknown species bis(acetonitrile)dicarbonyldichloro- tungsten(II) (**8b**). The W(II)-acetonitrile adducts $[W(CO)_3(NCMe)_2X_2]$ ($X = Cl^{xiv}$, Br, I) have been reported previously. The synthesis strategy to the published adducts, however is reversed. The adduct is formed first, succeeded by oxidation (cp. Scheme 16).^[85-87]



Scheme 16: Synthesis of W(II)-acetonitrile adducts^[85-87]

The seven-coordinate species and derivatives thereof have been shown to be active catalysts in homogenous catalysis, such as metathesis polymerization of norbornadiene, emulsion polymerization of styrene and trimerization and polymerization of alkynes.^[86]

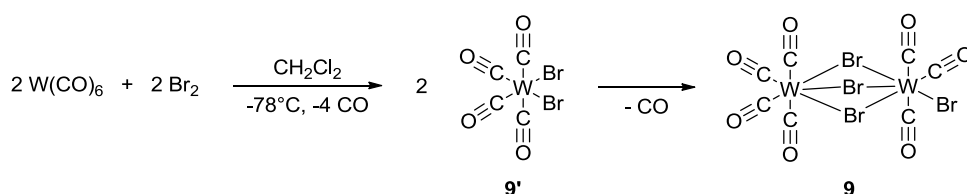
The new six-coordinate species $[W(CO)_2(NCMe)_2Cl_2]$ (**8b**) reacts analogously to $[W(CO)_4Cl_2]$ (**8a**) with $Ag[S_2CNEt_2]$ (**2a**) to $[W(CO)_2(S_2CNEt_2)_2]$ (**11b'**). Therefore it may be seen as an improved, more stable alternative to **8a**, even though its synthesis adds an additional step. On the plus side, however analytically pure samples, free of $[W(CO)_6]$, can be obtained in acceptable yields. Furthermore it needs to be mentioned that the yields for **8b** solely depend on the ratio of $[W(CO)_6]$ to **8a** and not on the adduct formation which can be seen as virtually quantitative. Yields of 40-50% **8b** could be achieved. However the expenditure of time needed to obtain analytically pure **8b** is disproportionately high. Therefore yet again alternative precursors had to be sought after.

^{xiv} Generated in-situ from $X = I$

$[\text{W}(\text{CO})_4\text{Br}_2]$ vs. $[\text{W}_2(\text{CO})_7\text{Br}_4]$

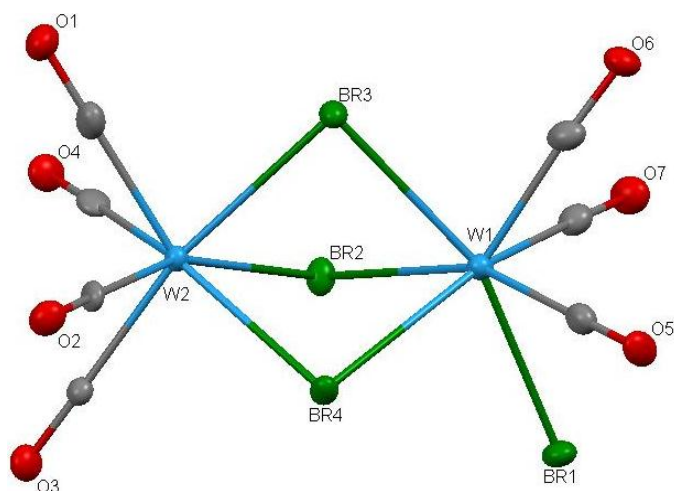
Tungsten is a comparatively soft cation and chlorine is a rather hard anion, thus the orbital overlap between the metal center and the halogen should be improved by the use of bromine or iodine, resulting in higher stability. Both species $[\text{W}(\text{CO})_4\text{Br}_2]$ (**9'**)^[75,77] and $[\text{W}(\text{CO})_4\text{I}_2]$ ^[78] have been described previously. The oxidative addition reaction of iodine to $[\text{W}(\text{CO})_6]$ seemed most promising at first, as it does not proceed spontaneously at RT, but needs to be initiated photochemically. However it had to be ruled out, due to the lack of a photochemical reaction vessel. The oxidative addition of bromine on the other hand proceeds willingly at -78°C , but less vigorously than the corresponding reaction with chlorine.

All attempts to synthesize the monomeric species $[\text{W}(\text{CO})_4\text{Br}_2]$ (**9'**) according to published literature methods^[75,77] did not result in the formation of a, presumably, orange compound with four defined carbonyl stretches [IR (CHCl_3) (cm^{-1}): $\nu = (\text{CO})$ 100 (w), 2020 (m), 1980 (s), 1935 (m)],^[75] but rather yielded a dark brown microcrystalline powder which exhibited at least six CO-stretches, nine if the shoulders are assigned to be individual CO-stretches. The solution IR spectrum (CH_2Cl_2) finally gave the vital hint to the dimeric species $[\text{W}_2(\text{CO})_7\text{Br}_4]$ (**9**).^[88]



Scheme 17: Bromination of $[\text{W}(\text{CO})_6]$

The identity of **9** could be confirmed by X-ray crystallography of crystals grown from a saturated dichloromethane solution at -35°C . On the contrary to the published structure, **9** crystallized in a new monoclinic modification, instead of the published orthorhombic one.^[88] In the orthorhombic modification the molecules lie on mirror planes, whereas in the monoclinic modification all atoms lie on general positions, showing roughly C_s symmetry (cp. Figure 10). The two modifications have almost identical intra-molecular geometry parameters but quite different packing arrangements.

Table 7: Selected bond lengths [\AA]

W1-C5	1.990(11)
W1-C6	1.972(11)
W1-C7	2.006(10)
W1-Br1	2.6234(10)
W1-Br2	2.6905(11)
W1-Br3	2.6715(10)
W1-Br4	2.6961(10)

Figure 10: Mercury plot of **9** showing the atomic numbering scheme. The probability ellipsoids are drawn at 50% probability level. For a full list of bond lengths and angles see Appendix

By raising the reaction temperature from -78°C ^[75,77] or -60°C ^[88] respectively, to -20°C the yield could be improved significantly. Constant conversion rates of greater than 95% could be ensured. Furthermore **9** proved itself a valuable precursor for compounds of the general form $[\text{W}^{\text{II}}(\text{CO})_n\text{L}_2]$ ($n = 2, 3$). The dimeric species **9** was found to be a lot more stable than the monomeric species $[\text{W}(\text{CO})_4\text{Cl}_2]$ (**8a**). The μ -bromo-bridging seems to be strong enough to stabilize the species, but weak enough to be broken up through adduct formation with coordinating solvents such as acetonitrile or THF, as indicated by CO evolution and NMR-experiments., in order to allow for further reactions.

Table 8: ^{13}C NMR shifts and IR stretches [cm^{-1}] of the $\text{C}\equiv\text{O}$ ligands of $[\text{W}_2(\text{CO})_7\text{Br}_4]$ (**9**), in dependence of the solvent

Solvent	W(II)-Species	$\delta \text{C}\equiv\text{O}$	$\nu (\text{C}\equiv\text{O})$
CD_2Cl_2	$[\text{W}_2(\text{CO})_7\text{Br}_4]$ (9)	206.60, 193.67	2107, 2022, 2008, 1974, 1966, 1949, 1936
THF-d8	$[\text{W}(\text{CO})_3(\text{THF})_2\text{Br}_2]$	206.34, 202.78, 199.75	2098, 2085, 2015, 1920, 1900,
CD_3CN	$[\text{W}(\text{CO})_3(\text{NCMe})_2\text{Br}_2]$	226.37, 223.54, 205.90	2091, 2022, 2014, 1907

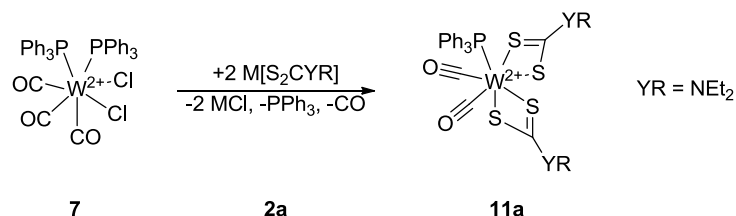
The ^{13}C NMR shifts indicate that THF and acetonitrile both form seven-coordinate, 18 electron species with **9** displacing one CO. THF seems to be better suited to coordinate to the tungsten center as indicated by NMR shifts showing less acidic carbons. Stronger σ -donation by the oxygen lone-pair of THF, compared to the nitrogen lone-pair of acetonitrile, causes higher electron density on the W-center. This may be used for stronger π -backdonation into the $\pi^*_{\text{C}\equiv\text{O}}$ of the carbonyls resulting in less acidic carbons.

COORDINATION COMPOUNDS

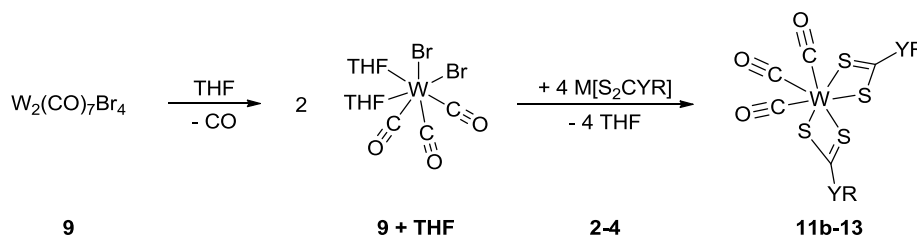
In preparation for the oxidation of the W(II) coordination compounds the oxygen atom transfer reagent $[\text{Mo}_2\text{O}_3(\text{S}_2\text{P}(\text{OEt})_2)_4]$ (**10**) was prepared by a modified literature procedure (cp. Page 49).^[66]

Influence of Heteroatoms in the Dithiocarbamate-System

$[\text{W}(\text{CO})_2(\text{PPh}_3)(\text{S}_2\text{CNEt}_2)_2]$ (**11a**) was prepared according to literature from $[\text{W}(\text{CO})_3(\text{PPh}_3)_2\text{Cl}_2]$ (**7**). The work-up procedure turned out to be lengthy due to residual $[\text{W}(\text{CO})_6]$ and the removal of the PPh_3 . A synthesis starting with the phosphine-free precursor **9** on the other hand turned out to be straight-forward.



Scheme 18: Synthesis of $[\text{W}(\text{CO})_2(\text{PPh}_3)\text{L}_2]$ (**11a**)



Scheme 19: Synthesis of $[\text{W}(\text{CO})_3\text{L}_2]$ (**11b-13**)

The salt metathesis reactions of $[\text{W}_2(\text{CO})_7\text{Br}_4]$ (**9**) with the ligands **2-4** were carried out in THF or acetonitrile, in order to break up the dimer before the addition of the ligand's salt. $[\text{W}(\text{CO})_2(\text{THF})_2\text{Br}_2]$ and $[\text{W}(\text{CO})_3(\text{NCMe})_2\text{Br}_2]$ yield species that display the same ^1H and ^{13}C NMR-spectra and solution IR spectra.

Extensive studies on tungsten carbonyl complexes with dithiocarbamate ligands, including $[\text{W}(\text{CO})_3(\text{S}_2\text{CNEt}_2)_2]$ (**11b**), have been carried out by Broomhead and Young.^[89] Among their findings was that the 18-electron species **11b** shows only one carbonyl and one dithiocarbamate ^{13}C NMR resonance, even at low temperatures, however the authors failed mention the actual CO shift. The findings were explained by fluxionality of the CO-groups in solution.

A literature search revealed that, so far only the ^1H -shifts of **11b** and **11c** had been published.^[89,90] The data presented below (cp. Table 10) provides new insight into the field. It is to be noted, that the quaternary S_2CY (Y = N, O, S) C-atom shows resonances in the carbonyl region. Hence the signals could not be distinguished for sure.

Table 9: Comparison of ^{13}C NMR spectra (CD_2Cl_2);

Compound	δC_q : $\text{C}\equiv\text{O}$ and CS_2CY
11a [W(CO) ₂ (PPh ₃)(S ₂ CNEt ₂) ₂]	obscured
11b [W(CO) ₃ (S ₂ CNEt ₂) ₂]	234.07, 207.74
11c [W(CO) ₃ (S ₂ CNC ₄ H ₈) ₂]	234.27, 203.77
12a [W(CO) ₃ (S ₂ COEt) ₂]	230.15, 229.33
12b [W(CO) ₃ (S ₂ CO <i>n</i> -Bu) ₂]	230.17, 229.41
13 [W(CO) ₃ (S ₂ CS <i>t</i> -Bu) ₂]	246.78, 231.01

Five IR stretches for the three CO-groups have been described for [W(CO)₃(S₂CNEt₂)₂] (**11b**) in CsI pellets and three in CH₂Cl₂ solution.^[89] According to the authors this is due to local site symmetry effects, solid state interactions and the presence of isomers. The main ligand arrangement was identified as having a *cis*-configuration of the COs. Similar effects seem to account for the different number of CO stretches of **11-13** in the solid and liquid state.

Table 10: Overview- IR (cm⁻¹): ν (CO), synthesis in THF

Compound	solid	CH ₂ Cl ₂
11a [W(CO) ₂ (PPh ₃)(S ₂ CNEt ₂) ₂]	2008, 1911, 1823.	2015, 1976, 1923
11b [W(CO) ₃ (S ₂ CNEt ₂) ₂]	2009, 1931, 1911, 1878, 1868	2016, 1975, 1924
11c [W(CO) ₃ (S ₂ CNC ₄ H ₈) ₂]	2007, 1929, 1905, 1867	2017, 1976, 1924
12a [W(CO) ₃ (S ₂ COEt) ₂]	2023, 1929, 1909	2030, 1976, 1943
12b [W(CO) ₃ (S ₂ CO <i>n</i> -Bu) ₂]	2022, 1933, 1910	2031, 1975, 1943
13 [W(CO) ₃ (S ₂ CS <i>t</i> -Bu) ₂]	2023, 1930, 1900	2028, 1944, 1927

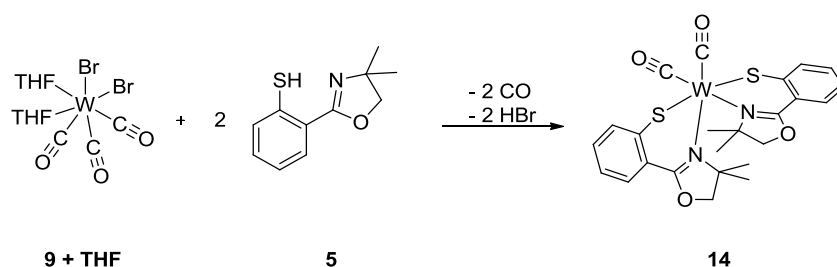
A comparison of the highest IR stretching frequencies of the 18-electron species **11-13** indicates that ligands with Y = O, S (**3a**, **3b**, **4**) coordinate stronger to the tungsten center than aliphatic ligands with Y = N. The σ -bonding ability of the ligands **3-4** is supposed to be weaker and thus more of the electron-density on W is needed for the stabilization of the coordinated dithiocarbamate. This in turn reduces the ability of W for π -backbonding into the $\pi^*_{\text{C}\equiv\text{O}}$. The W-C bond is weakened and the C \equiv O bond is strengthened compared to the N-containing ligands. As a consequence the carbonyls are coordinated less tightly.

Hence their removal should be easier. However the desired substitution of $C\equiv O$ by $H-C\equiv C-H$ could turn out to be less favored, if the ability of W for π -backdonation into the $\pi^*_{C\equiv C}$ is not sufficient.

Precursor Versatility

Further studies will be needed to explore the synthetic scope of the identified precursor $[W_2(CO)_7Br_4]$ (**9**) beyond reactions with dithiocarbamate salts. The reaction with 2-(4,4-dimethyl-2-oxazolin-2-yl)phenylthiol (S,N-oxa) (**5**) is a promising start. The thiooxazolin may still be a monoanionic bidentate ligand, but it demands the formation of a 6-membered ring, instead of a 4-membered ring, resulting in a wider bite angle. Furthermore the electron donation is via an anionic S and a N lone-pair, instead of a conjugated S_2C -system.

The reaction between **9** and **5** was carried out at RT in THF, work-up included extraction with toluene, trituration with heptane and crystallization. The relatively air-stable product $[W(CO)_2(S,N-oxa)_2]$ (**14**) is obtained in moderate yields as yellow to orange microcrystalline solid. Upon formation of **14**, one set of signals is observed for both ligands in the 1H , due to the overall C_2 symmetry of the complex. Furthermore coordination of the oxazolin ligand leads to two distinct sets of methyl and methylene groups, caused by the N atom to W (cp. Page 51). The precursor THF-adduct and the free S,N-oxa react without the addition of a base or the need to make the salt first. **14** may also be prepared in a similar reaction starting with $[W(CO)_3(PPh_3)_2Cl_2]$ (**7**).



Scheme 20. Synthesis of $W(CO)_2(S,N-oxa)_2$ (**14**)

Crystals suitable for structural analysis by X-ray crystallography were obtained from a saturated solution in toluene at $-35^\circ C$. The structure (cp. Figure 11) showed the tungsten center to be in a distorted octahedral arrangement. W is surrounded by two sulfur atoms in *trans* positions, two carbonyl ligands and two nitrogen atoms in *cis* positions each. As expected, the weaker coordinating N takes the positions *trans* to the COs. There are only two other dicarbonyl compounds with two S and two N atoms coordinated to tungsten.

One shows octahedral coordination as well and the other structure shows an unusual trigonal prismatic coordination.^[91,92]

In **14** both carbonyl ligands are at an equal distance of $W(1)-C(1) = 1.9718(15)$ Å. Trans to the COs the N donor atoms of the oxazolin moiety are located at a distance of $W(1)-N(13) = 2.2190(12)$ Å. The sulfur atoms in the axial positions *cis* to the CO ligands are located at $W(1)-S(1) = 2.3636(4)$ Å. This is in the expected range of the other two published systems.^[91,92] The deviation from ideal octahedral geometry is reflected e.g. by the angle of the two *cis* oriented carbonyl ligands, which is $C(1)^b-W(1)-C(1) = 77.46(8)^\circ$. Finally the CO's bond length of $C(1)-O(1) = 1.1589(19)$ Å displays reduced triple bond character and significant π -backbonding from W, which is also indicated by the IR stretching frequencies of 1917 and 1807 cm^{-1} .

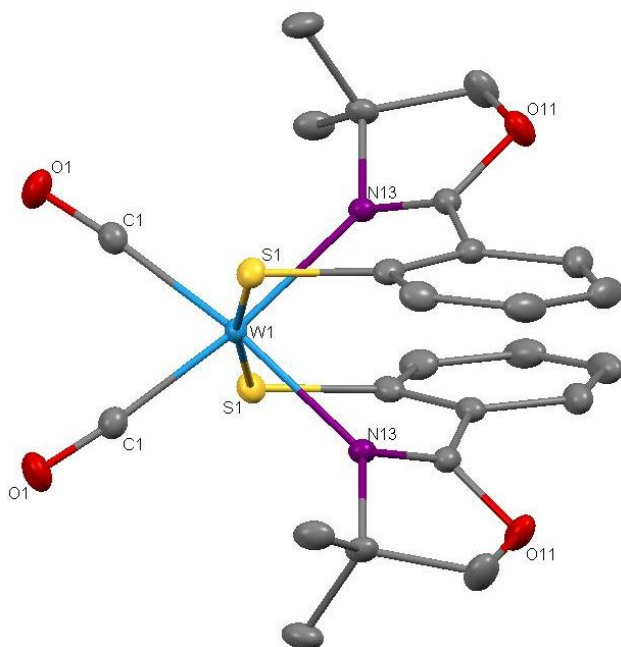


Table 11.: Selected bond lengths [Å]

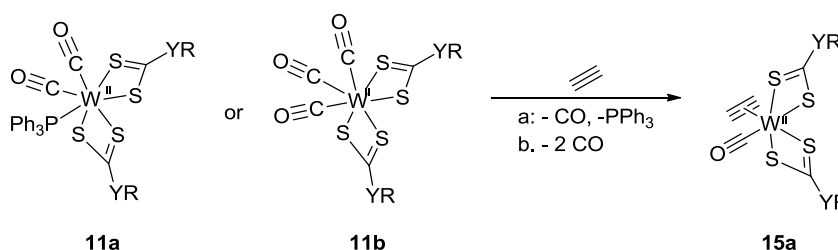
W1-C1	1.9718(15)
W1-N1	2.2190(12)
W1-S1	2.3636(4)
C1-O1	1.1589(19)
O11-C12	1.3496(17)
C12-N13	1.2893(18)
N13-C14	1.5197(18)
C14-C15	1.524(2)
O11-C15	1.4531(19)
S1-C21	1.7658(14)

Figure 11: Mercury plot of **14** showing the atomic numbering scheme. The probability ellipsoids are drawn at 50% probability level. For a full list of bond lengths and angles see Appendix.

$[W(CO)_2(S,N\text{-oxa})_2]$ (**14**) shows two IR stretches in the carbonyl region at 1917 and 1807 cm^{-1} . Compared to the stretching frequencies of the least tightly bound CO in the dtc systems studied **11-13**, this indicates that it coordinates its two carbonyls more tightly. A replacement of a CO by acetylene could therefore turn out to be difficult under the applied reaction conditions. From a steric point of view the substitution should be possible, as the W-center is rather open.

REACTIONS WITH ACETYLENE

The substitution of a coordinated carbonyl by acetylene was to be the second last step on the way to W(IV) acetylene-oxo complexes. So far only few examples of W(II) acetylene compounds have been described. All are of the general form $W(CO)(HC\equiv CH)(S_2CNR^1)_2$ ($R = i\text{-Pr}, Et_2, Me_2$).^[56,57] There are no examples of dithiocarbamate systems with heteroatoms other than nitrogen. $[W(CO)(HC\equiv CH)(S_2CNEt_2)_2]$ (**15a**) is indeed easily prepared according to literature from the corresponding dicarbonyl species **11a**.^[56] It was found that the phosphine-free species **11b** can be used alternatively (cp Scheme 21). This was observed to be preferential as the work-up procedure is reduced to a single trituration. The simple method of stirring a solution of the educt under an acetylene rich atmosphere or bubbling acetylene through the solution works very smoothly in systems with nitrogen containing ligands. The new pyrrolidine compound $[W(CO)(HC\equiv CH)(S_2CNC_4H_8)_2]$ (**15b**) could be obtained analogously.



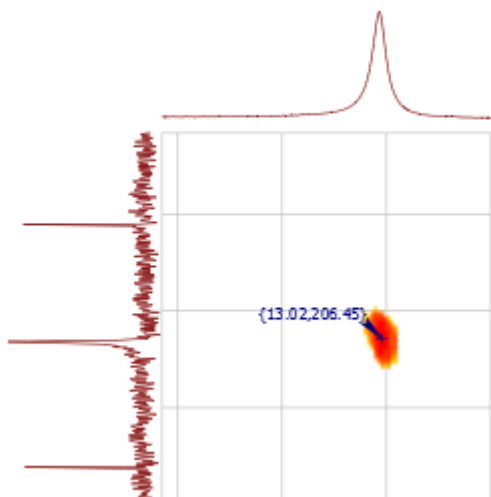
Scheme 21: Scheme 22: Substitution of CO by acetylene; YR = NEt₂

Acetylene has been postulated to act as a neutral four-electron donor to the tungsten center, through a delocalized, 2- π -aromatic system, which would be the product of the interaction of both $C\equiv C$ π -bonds with the appropriate empty W-atom orbitals.^[52,56,57] The hypothesis is in good agreement with the extreme downfield shifts observed in the 1H NMR spectra for the coordinated acetylene protons (cp. Figure 12) and literature data for **15a**.^[56]

Ricard and Weiss could obtain a crystal structure of **15a** which shows the acetylenic carbons (C1 and C2) to be inequivalent. C1 and C2 are sp^2 - hybridized and orientated parallel to the $C\equiv O$ ligand. The singlet signal in the NMR spectra is most likely due to fluxionality and rotation of the coordinated acetylene around the $W-C\equiv C$ bond.

Table 12: Comparison- ^1H and ^{13}C NMR (CD_2Cl_2) and IR (cm^{-1}) data for W(II)- acetylene complexes; see also Figure 13

Compound	^1H NMR δ	^{13}C NMR δ	$\nu(\text{C}\equiv\text{O})$
15a $[\text{W}(\text{CO})(\text{HC}\equiv\text{CH})(\text{S}_2\text{CNEt}_2)]$	13.03 (s, 2H).	206.59	1904
15b $[\text{W}(\text{CO})(\text{HC}\equiv\text{CH})(\text{S}_2\text{CNC}_4\text{H}_8)_2]$	13.09 (s, 2H).	207.55	1903
$\text{HC}\equiv\text{CH}$	~ 2.3 (s, 2H).		-

Figure 12 HSQC-spectra; a) $[\text{W}(\text{CO})(\text{HC}\equiv\text{CH})(\text{S}_2\text{CNEt}_2)]$ (**15a**)

Under the same reaction conditions as for **11b** $[\text{W}(\text{CO})_3(\text{S}_2\text{CS}t\text{-Bu})_2]$ (**13**) was reacted with acetylene. No apparent color change was observed, as the reaction mixture remained dark red. The solvent was evaporated to dryness and the crude product was analyzed by ^1H , IR and ESI. In the IR spectrum no characteristic bands for carbonyl ligands could be detected. ^1H NMR displayed a new singlet at 1.41 ppm, which is neither starting material nor free ligand. However no signals for coordinated acetylene could be detected. Finally in the ESI spectrum (c.p Figure 14, Appendix) the expected mass peak could be observed, tentatively hinting at the presence of the intended product $[\text{W}(\text{CO})(\text{HC}\equiv\text{CH})(\text{S}_2\text{CS}t\text{-Bu})_2]$ (found: 567.0 m/z calculated: 566.9 for $\text{C}_{13}\text{H}_{19}\text{OS}_6\text{W}$ m/z). Nevertheless several peaks with higher masses were also present in the ESI spectrum, indicating the formation of higher molecular weight dimeric species. For example the observed mass peak at 1024.8 was cautiously assigned to the dinuclear species $\text{L}_2\text{W}=\text{WL}_2$ (found: 1024.8 m/z calculated: 1026.8 for $\text{C}_{20}\text{H}_{35}\text{S}_{12}\text{W}_2$ m/z), which would be consistent with the calculated isotopic pattern, IR and NMR.

OXYGEN ATOM TRANSFER REACTIONS

The first and only oxo-tungsten(IV)-acetylene complexes $[\text{WO}(\text{HC}\equiv\text{CH})(\text{S}_2\text{CNR}^1_2)_2]$ ($\text{R}^1 = \text{Et}_2, \text{Me}_2$) were prepared through controlled oxidation of the corresponding carbonyl complex with the oxygen atom transfer (OAT) reagent $[\text{Mo}_2\text{O}_3(\text{S}_2\text{P}(\text{OEt})_2)_4]$ (**10**).^[59] In solution the Mo(V) complex dissociates into a $\text{Mo}^{\text{IV}}\text{O}$ and a $\text{Mo}^{\text{VI}}\text{O}_2$ species. The latter was postulated as a source of kinetically activated oxygen and thus being the actual OAT agent.^[59,93]

Tertiary amine oxides have been shown to transfer their oxygen atom quickly and relatively cleanly to metal centers.^[94] Pyridine *N*-oxide (PyNO) has been used to oxidize W(II) to W(IV) with concomitant oxygen transfer.^[95] Trimethyl *N*-oxide (Me_3NO) has also been reported to transfer its oxygen atom fast and in high yields to W(IV).^[94] Further compounds that have been shown to transfer oxygen include Me_2SO , Ph_3PO , Ph_3AsO , Ph_2SeO , $\text{PhN}\equiv\text{N}(\text{O})\text{Ph}$ and most recently mCPBA.^[94,96] It is to note that amine oxides are rather reactive donors, while phosphine oxides are near the bottom of the reactivity scale.^[94] Pyridine *N*-oxide and trimethylamine *N*-oxide were selected for comparison with $\text{Mo}_2\text{O}_3[\text{S}_2\text{P}(\text{OEt})_2]_4$ (**10**).

The Choice of Oxygen Atom Transfer Reagent

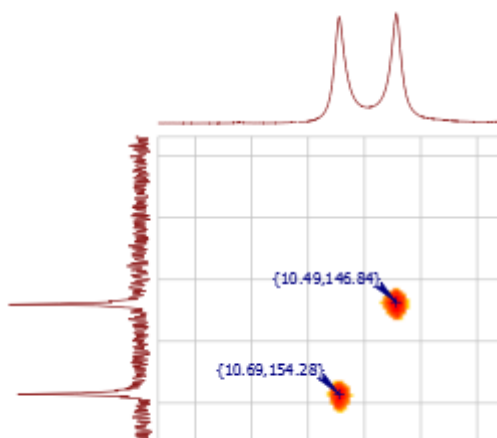
$[\text{W}(\text{C}_2\text{H}_2)(\text{CO})(\text{S}_2\text{CNEt}_2)_2]$ (**15a**) was chosen as model substrate. All OAT reactions were carried out at RT in dichloromethane using 1.2 equivalents of the oxidant. The dissolved OAT reagent was slowly added to a solution of **15a** in dichloromethane. Reaction control was performed by solution IR spectroscopy, by monitoring the disappearing of the $\text{C}\equiv\text{O}$ stretch at 1904 cm^{-1} . **10** was found to be the fastest oxygen atom transfer agent, taking less than 10 min for complete conversion. Me_3NO reached completion after 3 to 5 h PyNO after stirring overnight. After evaporating the reaction mixtures to dryness their purity was assessed by ^1H NMR spectroscopy. The crude products obtained by using the *N*-oxides were of comparable purity. Neither coordinated pyridine nor coordinated trimethylamine could be observed. The crude reaction mixture with the Mo OAT agent **10** contained large amounts of the reduced Mo(IV) species. Templeton and Ward speculated it to be present as $\text{OMo}[\text{S}_2\text{P}(\text{OEt})_2]_2$.^[59] **10** is thought to offer a selectivity comparable to the *N*-oxides, however the purity is hard to assess as the product signals are partially covered under the signals of oxidized Mo species, requiring a comparably lengthy work-up procedure of trituration and filtration, whereas Py and Me_3N can be removed simply by evaporation under reduced pressure.

Table 13: Comparison of oxygen atom transfer agents

OAT Agent	Conversion	Time	Atom Economy for 15a
$\text{Mo}_2\text{O}_3[\text{S}_2\text{P}(\text{OEt})_2]_4$	> 98%	< 10 min	35%
Pyridine <i>N</i> -oxide	> 98%	16 h	83%
Trimethylamine <i>N</i> -oxide	> 98%	3-5 h	86%

$[\text{Mo}_2\text{O}_3[\text{S}_2\text{P}(\text{OEt})_2]_4]$ **10** clearly is a powerful OAT agent, but the time and reagents needed to synthesize it are in no relation to the commercially available *N*-oxides. Furthermore the *N*-oxides offer increased atom economy.^[62] Additionally it was observed that **10** decomposes in solution, if the mixture is stirred overnight or longer. Despite being more costly trimethyl *N*-oxide was selected as OAT agent of choice as it is more active and easier to handle than PyNO.

Oxidation of Carbonyl-Acetylene Compounds

Figure 13: HSQC-spectra; $[\text{OW}(\text{HC}\equiv\text{CH})(\text{S}_2\text{CNEt}_2)]$ (**16a**)Table 14: Comparison- ^1H and ^{13}C NMR (CD_2Cl_2) and IR (cm^{-1}) data for W(II)- acetylene complexes

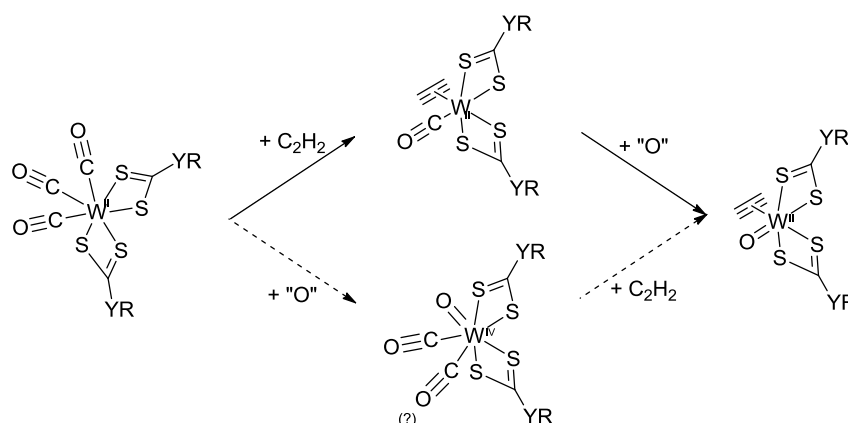
Compound	^1H NMR δ	^{13}C NMR δ	$\nu(\text{W}=\text{O})$
16a $[\text{OW}(\text{HC}\equiv\text{CH})(\text{S}_2\text{CNEt}_2)]$	10.69 (s, 1H),	154.28,	937
	10.49 (s, 1H).	146.84	
16b $[\text{OW}(\text{HC}\equiv\text{CH})(\text{S}_2\text{CNC}_4\text{H}_8)_2]$	10.69 (s, 1H),	154.27,	938
	10.49 (s, 1H).	147.67	

NMR data for **16a** were described previously by Newton et al.^[59] The authors could show by variable temperature ^1H NMR experiments, that the acetylenic protons display stereochemical nonrigidity on the NMR time scale at RT. The onset of fluxional behavior is observed upon heating the sample.

The presented data is in good agreement with their findings. Contrarily to the expected trend ^1H and ^{13}C NMR spectra of the oxo-tungsten compounds **16a** and **16b** indicate significantly increased electron density on the acetylene's nuclei compared to the W(II) species **15a** and **15b**. The reduced electron density of W(IV) compared to W(II) was expected to cause more electron deficient species.

However the extreme downfield shifts of **15a** and **15b** are thought to originate from a delocalized 2- π -aromatic system.^[52,56,57] The oxidation and concomitant lowering of the electron density on W could lead to a loss of aromaticity. Furthermore it has been speculated that one oxygen lone-pair of the oxo-group could be available for π -donation into the appropriate metal d^* -orbitals. π -donation from the oxo group and the perpendicular filled $\pi_{\text{C}=\text{C}}$ is thought to occur concomitantly with retrodonative metal to ligand donation from the metal center bonding into the $\pi^*_{\text{C}=\text{C}}$.^[59]

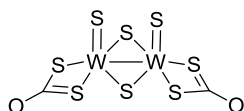
Oxidation of Dicarbonyl Compounds



Scheme 23: Could it be possible to reverse the order of coordination of acetylene and the oxidation?

Attempts to oxidize $[\text{W}(\text{CO})_3(\text{S}_2\text{COEt})_2]$ (**12a**) at RT in dichloromethane with 1.2 equiv. Me_3NO to $[\text{OW}(\text{CO})_2(\text{S}_2\text{COEt})_2]$ or $[\text{OW}(\text{CO})(\text{S}_2\text{COEt})_2]$ did not yield either one of the desired products. IR spectra indicated incomplete conversion to a carbonyl-free species. Addition of another 1.2 equiv. resulted in the formation of a carbonyl-free species, which was identified as $\text{W}_2\text{S}_4(\text{S}_2\text{CNEt}_2)_2$ by ESI measurements (found: 776.0 m/z, calculated: 777.8 m/z for $\text{C}_9\text{H}_{18}\text{OS}_8\text{W}_2$). The data found are in good agreement with literature.^[97,98]

Attempts to oxidize $[\text{W}(\text{CO})_3(\text{S}_2\text{COEt})_2]$ (**13a**) with an excess of Me_3NO to $[\text{OW}(\text{CO})_2(\text{S}_2\text{COEt})_2]$ or $[\text{OW}(\text{CO})(\text{S}_2\text{COEt})_2]$ did not yield either of the desired products again, but a dimeric W(VI) species of the form $\text{W}_2\text{S}_4\text{L}_2$ (cp. Scheme 24). Crystal data refinement is under progress. The first coordination sphere of W can nonetheless be seen as assured. A similar structure has been found for $[\text{W}_2\text{S}_4(\text{S}_2\text{CNEt}_2)_2]$.^[98]



Scheme 24: Connectivity of the product of over-oxidation of $[\text{W}(\text{CO})_3(\text{S}_2\text{COEt})_2]$ (**12a**); Refinement of structural data was still under progress during the writing of this thesis

It seems that the $\text{W}(\text{II})$ tricarbonyl compounds (**11-13**) are too labile to be oxidized directly by the means of Me_3NO . The compounds with coordinated acetylene (**15a**, **15b**) appear to have just the right stability to be oxidized in a controlled manner. Further studies with milder, less powerful OAT reagents will be needed to see whether the mono-oxidation of the tricarbonyl compounds is feasible or not.

IV. CONCLUSION

The synthesis of novel W(II) dithiocarbamate compounds was straightforward after $[W_2(CO)_7Br_4]$ (**9**) had been identified as an effective precursor for this system. The development of this reliable precursor synthesis turned out to be a challenging and laborious obstacle. Furthermore an improved synthesis strategy for the dtc ligands **3a**, **3b** and **4** has been developed. It was found that the coordination of acetylene to the W(II) dtc system seems to be strongly correlated to the use of nitrogen as heteroatom in the dithiocarbamate ligand backbone.

Further studies will be needed to investigate the conditions for coordination of acetylene to dtc systems with non-nitrogen ligands. The studied ligands were shown to cause W-centers to be too electron deficient, which are no longer able to provide for a stable acetylene coordination. Thus novel ligands with electron-donating properties will have to be developed to favor acetylene coordination.

Trimethylamine *N*-oxide was shown to be a more straightforward, alternative OAT agent, compared to the published route with $[Mo_2O_3(S_2P(OEt)_2)_4]$ (**10**). Attempts to oxidize the W(II) dtc system prior to coordination of acetylene turned out to yield dimeric W(V) species instead of monomeric W(VI) carbonyl species. Trimethylamine *N*-oxide was shown to be a potent, sometimes even too powerful oxygen atom transfer agent.

The novel compound $[W(CO)_2(S,N-oxa)_2]$ (**14**) could be isolated and fully characterized. Studies are underway to verify if the thiooxazolin system can coordinate acetylene and if it can be oxidized, with or without bound acetylene.

Studies are underway to test the catalytic activity of the synthesized W(VI) compounds $[OW(C_2H_2)(S_2CNEt_2)_2]$ (**16a**) and $[OW(C_2H_2)(S_2CNC_4H_8)_2]$ (**16b**). In analogy to Sarkar's system^[51] the formation of acetaldehyde will be assessed with (2,4-dinitrophenyl)hydrazine as scavenger and subsequent detection of the acetaldehyde (*E*)-(2,4-dinitro-phenyl)-hydrazone.

V. EXPERIMENTAL

1. GENERAL METHODS

All tungsten-compounds were prepared under an atmosphere of pure N₂ employing standard Schlenk and glovebox techniques. Ligand synthesis, except **5**, was performed under ambient conditions. Chlorine 2.8 was dried with P₄O₁₀ and H₂SO₄. Acetylene 2.6 was dried with CaCl₂ and H₂SO₄. Chemicals were purchased from commercial sources and were used without further purification. Solvents were purified via a Pure Solv Solvent Purification System. All NMR spectra were measured on a Bruker Avance III 300 MHz spectrometer. ¹H and ¹³C NMR spectroscopy chemical shifts are given in ppm and are referenced to residual protons in the solvent. Spectra were obtained at 25°C. IR spectra were directly measured on a Bruker ALPHA-P Diamant ATR-FTIR spectrometer at a resolution of 2 cm⁻¹. Solution IR spectra were measured using a Bruker ALPHA-T probe head at a resolution of 2 cm⁻¹. Signal intensities are assigned according to their relative intensities as strong (s), medium (m), weak (w) or very weak (vw). All IR-bands are listed in cm⁻¹. Mass spectra were recorded with an Agilent 5973 MSD – Direct Probe using the EI ionization technique. Elemental analyses were carried out using a Heraeus Vario Elementar automatic analyzer. X-ray data collection was performed with a Bruker AXS SMART APEX 2 CCD diffractometer by using graphite-monochromated Mo-K_α radiation (0.71073 Å) from a fine-focus sealed tube at 100 K. SHELXS-97^[99]

was used as structure solution and structure refinement program. Full-matrix least-squares on F² was employed as refinement method.

HS₂P(OEt)₂ (**1**)^[64] and 2-(4,4-dimethyl-2-oxazolin-2-yl)phenylthiol (**5**)^[100] were prepared according to modified literature procedures. The synthesis of the dithiocarbamate ligands (**3a**, **3b**, **4**) was designed on the basis of a published procedure for secondary amines.^[68]

[W(CO)₃(PPh₃)₂Cl₂] (**7**) was prepared by variations of the published literature procedure.^[63]

[W(CO)₄Cl₂] (**8a**) and [W₂(CO)₇Br₄] (**9**) were prepared by modified literature procedures.^[75,77,88] [MoO₂(acac)₂] was prepared according to literature.^[65]

[Mo₂O₃(S₂P(OEt)₂)₄] (**10**) was prepared according to a modified literature procedure without the use of an inert atmosphere.^[66] [W(CO)₂(PPh₃)₂(S₂CNEt₂)₂] (**11a**) was prepared according to literature.^[63]

2. LIGANDS

HS₂P(OEt)₂ (1)

Ethanol (26.8 mL, 460 mmol, 5.1 equiv.) was added dropwise to a well stirred suspension of P₂S₅ (20.070 g, 90.1 mmol, 1.0 equiv.) in 200 mL toluene. H₂S liberation commenced immediately. It was removed from the workspace via an exhaust tube and the fume hood ventilation. The mixture was heated to reflux for 3.5 h until the gas evolution had stopped. The solvent was thoroughly removed in vacuo to yield crude **1** as yellow oil, which was further purified by distillation with a vigreux column (b.p.: 30-46°C at 1.0-1.1 mbar) to yield **1** as colorless oil. Yield: 12.397 g (67 mmol, 40%)

¹H NMR (300 MHz, CDCl₃) δ 4.23 (dq, *J* = 10.1, 7.1 Hz, 1H), 1.38 (td, *J* = 7.1, 0.8 Hz, 2H).

³¹P NMR (121 MHz, CDCl₃) δ 85.05.

Ag[S₂CNEt₂] (2a)

Commercially available, used without further purification- data listed for comparison purposes only.

¹H NMR (300 MHz, CD₂Cl₂) δ 4.02 (q, *J* = 7.0 Hz, 4H), 1.34 (t, *J* = 7.0 Hz, 6H).

¹H NMR (300 MHz, DMSO) δ 4.01 (d, *J* = 6.6 Hz, 4H), 1.28 (t, *J* = 7.0 Hz, 6H).

¹³C NMR (75 MHz, CD₂Cl₂) δ 202.97, 52.46, 12.61.

IR (cm⁻¹): ν = 2969 (w), 2928 (vw) 2866 (w), 1488 (s), 1458 (vw), 1449 (w), 1422 (m), 1376 (w), 1351 (m), 1294 (w), 1264 (s), 1199 (s), 1138 (m), 1093 (w), 1074 (vw), 1063 (m), 974 (m), 901 (s), 838 (m), 776 (w), 558 (m), 428 (m)

NH₄[S₂CNC₄H₈] (2b)

Commercially available, used without further purification- data listed for comparison purposes only.

¹H NMR (300 MHz, DMSO-d₆) δ 7.38 (q, *J* = 9.5, 6.6 Hz, 4H), 3.63 (q, *J* = 8.5, 6.8 Hz, 4H), 1.81 (q, *J* = 9.7, 6.6 Hz, 4H).

¹³C NMR (75 MHz, DMSO) δ 208.30, 52.93, 25.77.

IR (cm⁻¹): ν = 2945 (vw), 2857 (w), 2744 (m), 1453 (vw), 1409 (w), 1373 (s), 1324 (w), 1241 (w), 1213 (w), 1173 (w), 1154 (m), 1095 (w), 1037 (w), 989 (s), 934 (s), 908 (w), 857 (vw), 821 (w), 696 (w), 586 (vw), 443 (m), 418 (m)

K[S₂COEt] (3a)

KOH (0.561 g, 10 mmol, 1 equiv.) dissolved in 100 mL ethanol was stirred for 30 min. Afterwards CS₂ (0.6 mL, 10 mmol, 1 equiv.) was slowly added at 0°C. The resulting yellow solution was stirred at RT for 2 h. After reduction of the volume in vacuo and layering with

ether the product precipitated as white solid, which was isolated by filtration and washed with cold ether. Yield. 0.763 g (0.48 mmol, 47%)

^1H NMR (300 MHz, DMSO- d_6) δ 4.22 (q, J = 7.1 Hz, 2H), 1.17 (t, J = 7.1 Hz, 3H).

^{13}C NMR (75 MHz, DMSO) δ 229.86, 66.00, 14.50.

IR (cm^{-1}): ν = 2981 (vw), 2969 (w), 1463 (m), 1440 (w), 1380 (w), 1137 (s), 1117 (w), 1096 (s), 1047 (m), 1007 (w), 864 (vw), 815 (w), 701 (vw), 666 (w), 446 (s)

CHN: calculated: C: 22.48%, H: 3.14; found: C: 22.11%, H: 2.98%

K[S₂C(On-Bu)] (3b)

KOH (0.560 g, 10 mmol, 1 equiv.) dissolved in 50 mL 2-butanole was stirred for 30 min. Afterwards CS₂ (0.6 mL, 10 mmol, 1 equiv.) was slowly added at 0°C. The resulting yellowish solution was stirred at RT for 2 h. After reduction of the volume in vacuo and layering with ether the product precipitated as off-white solid, which was isolated by filtration and washed with cold ether. Yield: 1.422 g (0.75 mmol, 76%)

^1H NMR (300 MHz, DMSO- d_6) δ 4.17 (t, J = 6.7 Hz, 2H), 1.55 (p, J = 7.0 Hz, 2H), 1.30 (dq, J = 14.3, 7.3 Hz, 2H), 0.87 (t, J = 7.4 Hz, 3H).

^{13}C NMR (75 MHz, DMSO) δ 230.12, 70.36, 30.66, 18.97, 13.82.

IR (cm^{-1}): ν = 2958 (m), 2943 (vw), 2870 (w), 1460 (m), 1452 (vw), 1445 (vw), 1375 (vw), 1303 (vw), 1261 (w), 1228 (w), 1173 (w), 1150 (m), 1135 (w), 1102 (m), 1062 (s), 1014 (vw), 959 (w), 923 (w), 839 (w), 747 (w), 669 (w), 503 (m), 435 (m)

CHN: calculated: C: 31.88%, H: 4.82%; found: C: 31.71%, H: 4.72%

K[S₂C(St-Bu)] (4a)

KOH (0.563 g, 10 mmol, 1 equiv.) suspended in 100 mL THF was stirred for 30 min, before the addition of 2-methylpropan-2-thiol (1.1 mL, 10 mmol, 1 equiv.) and 2.5 mL water. After 15 min CS₂ (0.6 mL, 11 mmol, 1.1 equiv.) was slowly added at 0°C. The resulting orange solution was stirred at RT for 2 h. After reduction of the volume in vacuo and layering with ether the product precipitated as yellow solid, which was isolated by filtration and washed with cold ether. Yield: 1.465 g (0.81 mmol, 88%)

^1H NMR (300 MHz, DMSO- d_6) δ 1.43 (s, 9H).

^{13}C NMR (75 MHz, DMSO) δ 241.42, 50.14, 28.73.

IR (cm^{-1}): ν = 2989 (vw), 2958 (m), 2920 (vw), 2897 (vw), 2860 (vw), 1476 (w), 1444 (w), 1393 (w), 1360 (s), 1218 (w), 1160 (m), 1028 (s), 999 (s), 829 (s), 491 (m)

CHN: calculated: C: 29.38%, H: 4.44; found: 28.32%, 4.25%

2-(4,4-dimethyl-2-oxazolin-2-yl)phenylthiol (5)

A solution of n-BuLi in hexanes (1.6 M, 6.8 mL, 11 mmol, 1.1 equiv.) was slowly added to 4,4-Dimethyl-2-phenyloxazolin (1.75 mL, 10 mmol, 1 equiv.) dissolved in 50 mL heptane. After stirring at RT for 2.5 h the white precipitate was isolated, washed with heptane and dried in vacuo. The residue was suspended in 30 mL ether and sulfur (0.322 g, 10 mmol, 1 equiv.) was added at 0°C. After stirring at RT for 16 h a yellow precipitate had formed. 30 mL deaerated water were added. The organic layer was washed with deaerated water (3 x 15 mL), dried with MgSO₄ and evaporated to dryness to yield **5** as yellow solid. Yield: 0.314 g (1.5 mmol, 15%)

¹H NMR (300 MHz, CD₂Cl₂) δ 7.72 (dd, *J* = 7.3, 1.9 Hz, 1H), 7.35 – 7.29 (m, 1H), 7.27 (dd, *J* = 7.1, 5.3 Hz, 1H), 7.22 (dd, *J* = 7.4, 1.8 Hz, 1H), 3.97 (s, 2H), 1.28 (s, 6H).

¹³C NMR (75 MHz, CD₂Cl₂) δ 161.55, 137.69, 133.04, 131.21, 130.82, 130.40, 127.07, 79.39, 68.74, 28.53.

IR (cm⁻¹): ν = 3059 (vw), 2969 (m), 2927 (w), 2888 (w), 1662 (w), 1642 (s), 1584 (w), 1560 (w), 1468 (s), 1468 (s), 1432 (m), 1384 (w), 1366 (w), 1348 (s), 1308 (s), 1275 (w), 1258 (s), 1212 (w), 1185 (m), 1137 (m), 1088 (m), 1045 (w), 1026 (s), 988 (vw), 965 (w), 955 (m), 918 (m), 867 (m), 799 (m), 768 (s), 733 (s), 717 (w), 708 (w), 680 (m), 657 (w), 616 (m), 554 (w), 533 (m), 508 (w), 472 (vw)

3. PRECURSORS

[W(CO)₆]

Commercially available, used without further purification- data listed for comparison purposes only.

¹³C NMR (75 MHz, CD₂Cl₂) δ 191.97 (t, *J*_{C-W} = 63.2 Hz).

¹³C NMR (75 MHz, THF) δ 192.29 (t, *J*_{C-W} = 63.3 Hz).

¹³C NMR (75 MHz, CD₃CN) δ 192.06.

[PPh₃Cl]₂[WCl₆] (6)

Chlorine (approx. 120 mL) was condensed (acetone/ dry ice) into a Schlenk flask containing [W(CO)₆] (15.438 g, 43.9 mmol, 1 equiv.). The resulting dark red solution was stirred for 1 hr. at -78°C. Keeping the reaction vessel at -78°C, the chlorine was evaporated in vacuo into a trap cooled to -196°C. PPh₃ (23.312 g, 88.9 mmol, 2.03 equiv.), dissolved in 80 mL CH₂Cl₂, was added dropwise over an hour to the dark red residue. After stirring at -78°C for 30 min, the reaction mixture was allowed to warm to

room temperature. Gas evolution re-commenced and an orange solid started to precipitate, which was isolated by filtration and washed with ether (3 x 50 mL) to yield **6** as a bright orange microcrystalline solid. Crystals of **6** suitable for structure determination by X-ray crystallography were obtained by slow evaporation of CH₂Cl₂ at RT. Yield: 38.360 g (39 mmol, 88%)

¹H NMR (300 MHz, CD₂Cl₂) δ 7.98 – 7.74 (m, 30H).

¹³C NMR (75 MHz, CD₂Cl₂) δ 148.65 , 139.25 (d, *J* = 3.1 Hz), 137.71 (d, *J* = 13.2 Hz), 136.39 , 134.64 (d, *J* = 14.8 Hz), 131.79 , 119.23 (d, *J* = 93.4 Hz).

³¹P NMR (121 MHz, CD₂Cl₂) δ 72.55.

IR (cm⁻¹): ν = 3093 (vw), 3073 (w), 3056 (vw), 1580 (w), 1477 (w), 1436 (s), 1312 (w), 1183 (w), 1165 (w), 1107 (s), 995 (m), 859 (w), 756 (s), 727 (s), 684 (s), 614 (w), 575 (s), 510 (s), 469 (w), 449 (m)

CHN: calculated: C: 43.59, H 3.05; found. C: 43.50, H: 2.72

[W(CO)₃(PPh₃)₂Cl₂] (**7**)

[W(CO)₆] (2.512 g, 7.1 mmol, 1 equiv.) was added to a Schlenk flask containing roughly 10 mL condensed chlorine (acetone/ dry ice). The yellow slurry was stirred for 20 min. at -78°C. Keeping the reaction vessel at -78°C, the chlorine was evaporated in vacuo into a trap cooled to -196°C. PPh₃ (3.755 g, 14.3 mmol, 2.02 equiv.), dissolved in 50 mL CH₂Cl₂, was added dropwise over 90 min to the bright yellow residue. After stirring at -78°C for 15 min, the reaction mixture was allowed to warm to room temperature, whereupon a bright yellow solid precipitated. Removal of the solvent in vacuo yielded crude **7** as bright yellow microcrystalline solid. IR spectra showed the crude product contain unreacted [W(CO)₆]. Crystals of **7** and [W(CO)₆] suitable for structure determination by X-ray crystallography were obtained from a supersaturated CH₂Cl₂ solution at -35°C. Yield: 2.838 g (3.3 mmol, 46%)

¹H NMR (300 MHz, CD₂Cl₂) δ 7.68 – 7.27 (m, 30H).

¹³C NMR (75 MHz, CD₂Cl₂) δ C_q obscured, 136.06 – 125.89.

³¹P NMR (121 MHz, CD₂Cl₂) δ 14.81, 9.13.

IR (cm⁻¹): ν (CO) 2011, 1929, 1887

IR (cm⁻¹): CH₂Cl₂: ν (CO) 2015, 1976, 1923

[W(CO)₄Cl₂] (**8a**)

[W(CO)₆] (2.503 g, 7.1 mmol, 1 equiv.) was added to a Schlenk flask containing roughly 15 mL condensed chlorine (acetone/ dry ice). The smooth reaction (approx. 1 CO-bubble/sec.) was allowed to stir at -78°C for 40 min to yield a bright yellow precipitate and a bright red solution. Keeping the reaction vessel at -78°C, the chlorine was evaporated in vacuo

into a trap cooled to -196°C . After drying thoroughly and repeatedly scratching the residue from the flask's inside the cooling bath was removed stepwise over 20 min to yield crude **8a**. Yield: 2.333 g, (6.4 mmol, 89%)

^{13}C NMR (75 MHz, CD_2Cl_2) δ 208.53.

IR (cm^{-1}): ν (CO) 2099, 1983, 1962, 1931

[W(CO)₂(NCMe)₂Cl₂] (8b)

Crude $\text{W}(\text{CO})_4\text{Cl}_2$ **8a** (7.823 g, 21.3 mmol, 1 equiv.) containing 40-50% of unreacted $[\text{W}(\text{CO})_6]$ was repeatedly extracted with acetonitrile under gas evolution. The combined acetonitrile extracts (approx. 80 mL) were washed with pentane (3 x 80 mL) and evaporated to dryness to yield **8b** as black solid. Yield: 3.670 g (9.3 mmol, 44%).

^1H NMR (300 MHz, CD_2Cl_2) δ 2.06 (s, 6H).

^{13}C NMR (75 MHz, CD_2Cl_2) δ 210.94, 117.04, 2.33.

IR (cm^{-1}): ν (CO) 2040, 1939, 1913

ESI: 351.2 H- $[\text{W}(\text{CO})_2(\text{NMe}_3)\text{Cl}_2]$, 394. 0 H- $[\text{W}(\text{CO})_2(\text{NMe}_3)_2\text{Cl}_2]$

CHN: calculated: C:18.34, H: 1.54, N:7.13; found: C:17.55, H: 1.58, N:7.54

[W₂(CO)₇Br₄] (9)

At -20°C (ice/ NaCl) Br_2 (0.5 mL, 9.8 mmol, 1.1 equiv.) was added dropwise to a suspension of $[\text{W}(\text{CO})_6]$ (3.130 g, 8.9 mmol, 1 equiv.) in ca.50 mL CH_2Cl_2 . The smooth reaction (approx. 1 CO-bubble/ sec.) was stirred at -20°C for 2 h After which the gas evolution had stopped. The dark brown slurry was allowed to warm to RT. Removal of the solvent in vacuo yielded crude **9**, which was used without further purification. Crystals of **9** suitable for structure determination by X-ray crystallography were obtained from a saturated solution in CH_2Cl_2 at -35°C . The compound forms a $\text{W}(\text{CO})_3(\text{NCMe}_3)_2\text{Br}_2$ adduct with acetonitrile and a $\text{W}(\text{CO})_3(\text{THF})_2\text{Br}_2$ adduct with THF. Yield: 3.885 g, (4.4 mmol, 99%)

^{13}C NMR (75 MHz, CD_2Cl_2) δ 206.60, 193.67^{xv}.

^{13}C NMR (75 MHz, CD_3CN) δ 226.37, 223.54, 205.90, 131.73, 128.04, 4.47.

^{13}C NMR (75 MHz, THF) δ 206.34, 202.78, 199.75, 70.30, 70.03, 26.44.

IR (cm^{-1}): solid: ν (CO) 2107, 2022, 2008, 1974, 1966, 1949, 1936

IR (cm^{-1}): CH_2Cl_2 : ν (CO) 2113, 2089, 2051, 2021, 1992, 1971, 1945

^{xv} Broad, weak signals, detectable only in an overnight experiment.

4. COORDINATION COMPOUNDS

[Mo₂O₃(S₂P(OEt)₂)₄] (10)

HS₂P(OEt)₂ (**1**) (2.636 g, 14.2 mmol, 3.6 equiv.) diluted with 3 mL methanol was added to a suspension of MoO₂(acac)₂ (1.270 g, 3.98 mmol, 1 equiv.) in 20 mL methanol. The solution's color changed within minutes from yellow to purple and a dark purple precipitate started to form. After stirring for 1.5 h at RT, reduction of the volume in vacuo and crystallization at 0°C the product was isolated by filtration, washed with cold ether and dried in vacuo. Yield: 1.887 g (1.9 mmol, 99%)

¹H NMR (300 MHz, CDCl₂) δ 4.24 (dt, *J* = 15.9, 6.7 Hz, 16H), 1.36 (t, *J* = 7.1 Hz, 24H).

¹³C NMR (75 MHz, CD₂Cl₂) δ 65.43, 16.35, 16.25.

³¹P NMR (121 MHz, CDCl₂) δ 96.64.

IR (cm⁻¹): ν (Mo=O) 950

Carbonyl Compounds

[W(CO)₂(PPh₃)(S₂CNEt₂)₂] (11a)

Ag[S₂CNEt₂] (**2a**) (0.455 g, 1.8 mmol, 2.2 equiv.) suspended in 35 mL CH₂Cl₂ was slowly added to a Schlenk flask containing crude [W(CO)₃(PPh₃)₂Cl₂] (**7**) (0.701 g, 0.81 mmol, 1 equiv.) dissolved in 35 mL CH₂Cl₂, to yield a red solution and an off-white precipitate. After reduction of the volume to half and filtration the solution was evaporated to dryness to yield crude **11a** as red solid.

Yield: 0.244 g (0.31 mmol, 58%)

¹H NMR (300 MHz, CDCl₃) δ 7.37 (ddt, *J* = 9.2, 7.0, 1.8 Hz, 15H), 3.68 (dq, *J* = 21.2, 7.1 Hz, 8H), 1.30 (td, *J* = 7.1, 2.2 Hz, 12H).

¹H NMR (300 MHz, CD₂Cl₂) δ 7.44 – 7.26 (m, 1H), 3.67 (dd, *J* = 13.5, 6.5 Hz, 0H), 1.32 – 1.12 (m, 1H).

¹³C NMR (75 MHz, CD₂Cl₂) δ C_q obscured, 134.61 (d, *J* = 16.6 Hz), 132.94 (d, *J* = 27.2 Hz), 130.76, 129.31 (d, *J* = 10.1 Hz), 44.91, 12.66.

³¹P NMR (121 MHz, CD₂Cl₂) δ 8.53.

IR (cm⁻¹): ν (CO) 2008, 1911, 1823.

[W(CO)₃(S₂CNEt₂)₂] (11b)

Method 1: THF (60 mL) was added to [W₂(CO)₇Br₄] (**9**) (1.021 g, 1.1 mmol, 1.0 equiv.) and Ag[S₂CNEt₂] (**2a**) (1.282 g, 5.0 mmol, 4.2 equiv.), whereat gas evolution was observed. The resulting slurry was stirred for 30 min at RT. The red solution was isolated

by cannula filtration and evaporated in vacuo to yield crude **11b** as orange-red solid. Yield: 1.031 g (1.8 mmol, 79%)

Method 2: THF (3 mL) was added to $[W(CO)_4Cl_2]$ (**8a**) (0.054 g, 0.15 mmol, 1 equiv.) and $Ag[S_2CNEt_2]$ (**2a**) (0.079 g, 0.31 mmol, 2.2 equiv.), whereat gas evolution was observed. The resulting dark brown slurry was stirred for 1 hr. at RT. Filtration and evaporation of the solvent in vacuo yielded crude **11b** as black solid. Yield: 0.033 g (0.06 mmol, 60%)

1H NMR (300 MHz, CD_2Cl_2) δ 3.69 (q, $J = 7.2$ Hz, 8H), 1.27 (t, $J = 7.2$ Hz, 12H).

^{13}C NMR (75 MHz, CD_2Cl_2) δ 234.12, 207.85, 44.92, 12.66.

IR (cm^{-1}): ν (CO) 2009, 1931, 1911, 1878, 1868

$[W(CO)_2(S_2CNEt_2)_2]$ (**11b'**)

THF (3 mL) was added to $[W(CO)_2(NCMe)_2Cl_2]$ (**8b**) (0.059 g, 0.15 mmol, 1 equiv.) and $Ag[S_2CNEt_2]$ (**2a**) (0.079 g, 0.31 mmol, 2.2 equiv.) The resulting dark brown slurry was stirred for 1 hr. at RT. Filtration and evaporation of the solvent in vacuo yielded crude **11b'** as black solid. Yield: 0.079 g (0.15 mmol, 98%)

1H NMR (300 MHz CD_2Cl_2) δ 3.70 (t, $J = 7.2$ Hz, 8H), 1.27 (t, $J = 7.1$ Hz, 12H).

^{13}C NMR (75 MHz, CD_2Cl_2) δ 233.57, 207.27, 44.39, 12.12.

IR (cm^{-1}): ν (CO) 2007, 1976, 1910, 1892, 1879

$[W(CO)_3(S_2CNC_4H_8)_2]$ (**11c**)

THF (70 mL) was added to $[W_2(CO)_7Br_4]$ (**9**) (1.508 g, 1.7 mmol, 1.0 equiv.) and $NH_4[S_2CNC_4H_8]$ (**2b**) (1.215 g, 7.4 mmol, 4.4 equiv.), whereat gas evolution was observed. The resulting slurry was stirred for 16 h at RT. The red solution was isolated by cannula filtration and the residue was washed with 50 mL pentane. The combined pentane and THF solutions were evaporated in vacuo to yield crude **11c** as orange-red solid. Yield: 1.493 g, (2.7 mmol, 78%)

1H NMR (300 MHz, CD_2Cl_2) δ 3.74 – 3.62 (m, 1H), 2.03 (td, $J = 6.9, 6.4, 3.4$ Hz, 1H).

^{13}C NMR (75 MHz, CD_2Cl_2) δ 234.27, 203.77, 50.04, 25.06.

IR (cm^{-1}): ν (CO) 2007, 1929, 1905, 1867

$[W(CO)_3(S_2COEt)_2]$ (**12a**)

THF (70 mL) was added to $[W_2(CO)_7Br_4]$ (**9**) (1.409 g, 1.7 mmol, 1.0 equiv.) and $K[S_2COEt]$ (**3a**) (1.193 g, 7.4 mmol, 4.4 equiv.), whereat gas evolution was observed. The resulting slurry was stirred for 16 h at RT. The dark green solution was isolated by Schlenk filtration over celite. The filtration residue was washed with 50 mL pentane. The combined pentane and THF solutions were evaporated in vacuo to yield crude **12a** as black, highly viscous oil. Yield: 1.214 g (2.4 mmol, 75%)

^1H NMR (300 MHz, CD_2Cl_2) δ 4.65 (qd, $J = 7.1$ Hz, 4H), 1.48 (t, $J = 7.1$ Hz, 6H).

^{13}C NMR (75 MHz, CD_2Cl_2) δ 230.15, 229.33, 69.23, 14.10, 14.06.

IR (cm^{-1}): ν (CO) 2023, 1929, 1909

[W(CO)₃(S₂CO*n*-Bu)₂] (12b)

THF (70 mL) was added to $[\text{W}_2(\text{CO})_7\text{Br}_4]$ (**9**) (1.513 g, 1.7 mmol, 1.0 equiv.) and $\text{K}[\text{S}_2\text{C}(\text{O}n\text{-Bu})]$ (**3c**) (1.140 g, 6.1 mmol, 3.6 equiv.), whereat gas evolution was observed. The resulting slurry was stirred for 16 h at RT. The red solution was isolated by cannula filtration and the residue was washed with 50 mL pentane. The combined pentane and THF solutions were evaporated in vacuo to yield crude (**12b**) as black highly viscous oil.

Yield: 1.448 g (2.5 mmol, 74%)

^1H NMR (300 MHz, CD_2Cl_2) δ 4.59 (td, $J = 6.5, 4.6$ Hz, 4H), 1.90 – 1.73 (m, 4H), 1.51 – 1.38 (m, 4H), 0.96 (td, $J = 7.7, 2.2$ Hz, 6H).

^{13}C NMR (75 MHz, CD_2Cl_2) δ 230.17, 229.41, 72.96, 30.55, 19.46, 13.89.

IR (cm^{-1}): ν (CO) 2022, 1933, 1910

[W(CO)₃(S₂C*S*t-Bu)₂] (13)

THF (70 mL) was added to $[\text{W}_2(\text{CO})_7\text{Br}_4]$ (**9**) (1.493 g, 1.7 mmol, 1.0 equiv.) and $\text{K}[\text{S}_2\text{C}(\text{S}t\text{-Bu})]$ (**4a**) (1.453 g, 7.1 mmol, 4.2 equiv.), whereat gas evolution was observed. The resulting slurry was stirred for 2 h at RT. The dark red solution was isolated by cannula filtration and the residue was washed with 50 mL pentane. The combined pentane and THF solutions were evaporated in vacuo to yield crude **13** as black solid. Yield: 1.433 g (2.5 mmol, 71%)

^1H NMR (300 MHz, CD_2Cl_2) δ 1.70 (s, 18H).

^{13}C NMR (75 MHz, CD_2Cl_2) δ 246.78, 231.01, 56.13, 30.45.

IR (cm^{-1}): ν (CO) 2023, 1930, 1900

W(CO)₂(S,N-oxa)₂ (14)

Method 1: At -78°C (dry ice/acetone) a solution of S,N-oxa (**5**) (0.99 g, 0.5 mmol, 2.0 equiv.) in CH_2Cl_2 was added to $[\text{W}(\text{CO})_3(\text{PPh}_3)_2\text{Cl}_2]$ (**7**) (0.200 g, 0.2 mmol, 1.0 equiv.) dissolved in CH_2Cl_2 . The stirred reaction mixture was allowed to slowly warm to RT overnight. The orange solution was evaporated to dryness to yield crude **14** as orange solid. Recrystallization from toluene at -25°C yielded white crystals. The supernatant liquid was isolated, concentrated to dryness to yield **14** as orange solid. Crystals suitable for structure determination by X-ray crystallography were obtained from toluene at -35°C . Yield: 0.046 g (0.07 mmol, 35%)

Method 2: THF (60 mL) was added to $W_2(CO)_7Br_4$ **9** (1.079, 1.2 mmol, 1.0 equiv.) and the S,N-oxa **5** (0.956 g, 5.0 mmol, 4.1 equiv.), whereat gas evolution was observed. The resulting slurry was stirred for 2 h at RT. The orange-red solution was evaporated to dryness. Extraction of the residue with toluene and evaporation in vacuo yielded crude **14** as red solid. Trituration with THF-heptane and isolation of the precipitate yielded **14** as yellow-orange solid. Yield: 0.181 g (0.3 mmol, 12%)

1H NMR (300 MHz, CD_2Cl_2) δ 7.89 (d, $J = 7.7$ Hz, 1H), 7.84 (d, $J = 8.0$ Hz, 1H), 7.56 – 7.48 (m, 1H), 7.35 (t, $J = 7.3$ Hz, 1H), 3.91 (d, $J = 8.2$ Hz, 1H), 2.80 (d, $J = 8.3$ Hz, 1H), 0.83 (s, 3H), 0.52 (s, 3H).

^{13}C NMR (75 MHz, CD_2Cl_2) δ C_q obscured, 167.28, 165.46, 132.00, 130.92, 130.50, 125.85, 125.65, 77.64, 74.19, 28.78, 23.05.

IR (cm^{-1}): ν (CO) 1917, 1807

Carbonyl-Acetylene- Compounds

$[W(C_2H_2)(CO)(S_2CNEt_2)_2]$ (**15a**)

Method 1: $[W(CO)_2(PPh_3)(S_2CNEt_2)_2]$ (**11**) (0.400 g, 0.50 mmol, 1 equiv.) was dissolved in 25 mL CH_2Cl_2 and acetylene was bubbled through for 30 min. Whereat the solution's color progressively changed from deep red to deep green. Removal of the solvent in vacuo, trituration with ether and filtration yielded crude **15a** as green solid. $Ph_3P=S$, $PPh_3=O$ and starting material were identified as impurities. Yield: 0.244 g (0.46 mmol, 73%)

Method 2: $[W(CO)_3(S_2COEt)_2]$ (**12a**) (0.738 g, 1.4 mmol, 1 equiv.) was dissolved in 50 mL CH_2Cl_2 and acetylene was bubbled through for 15 min. Whereat the solution's color progressively changed from deep red to deep green. Removal of the solvent in vacuo and trituration with heptane yielded **15a** as green solid. Crystals suitable for structure determination by X-ray crystallography were obtained from a supersaturated heptane solution at $-35^\circ C$. Yield: 0.585 g (1.1 mmol, 80%).

Unit cell: mP, $a = 10.361(3)$ Å, $b = 15.165(5)$ Å, $c = 12.038(4)$ Å, $\beta = 90.459(9)^\circ$ ^[56]

1H NMR (300 MHz, CD_2Cl_2) δ 13.03 (s, 2H), 3.93 – 3.46 (m, 8H), 1.40 – 1.09 (m, 12H).

^{13}C NMR (75 MHz, CD_2Cl_2) δ 237.53, 213.07, 206.59 ($HC\equiv CH$), 200.54, 46.67, 45.13, 44.90, 44.76, 13.11, 12.69, 12.66, 12.50.

IR (cm^{-1}): ν (CO) 1904

$[W(C_2H_2)(CO)(S_2CNC_4H_8)_2]$ (**15b**)

Method 1: THF (25 mL) was added to $[W(CO)_4Cl_2]$ (**8a**) (0.370 g, 1.0 mmol, 1 equiv.) and $NH_4[S_2CNC_4H_8]$ (**2b**) (0.348 g, 2.1 mmol, 2.1 equiv.). The red, supernatant liquid was

isolated after stirring at RT for 16 h and acetylene 2.6 was bubbled through for 20 min. After reduction of the volume to a third a white solid precipitated, this was removed by filtration to yield crude **15b** as green foam. Trituration with heptane yielded **15b** as microcrystalline solid. Yield: 0.387 g (0.7 mmol, 73%)

Method 2: $[\text{W}(\text{CO})_3(\text{S}_2\text{CNEt}_2)_2]$ (**11b**) (1.493 g, 2.6 mmol, 1 equiv.) was dissolved in 25 mL CH_2Cl_2 and acetylene was bubbled through for 45 min. Whereat the solution's color progressively changed from deep red to deep green. Removal of the solvent in vacuo yielded **15b** as green solid. Yield: 1.270. g (2.4 mmol, 90%).

^1H NMR (300 MHz, CD_2Cl_2) δ 13.09 (s, 2H), 3.66 (dd, $J = 34.4, 29.4$ Hz, 8H), 1.98 (s, 8H).

^{13}C NMR (75 MHz, CD_2Cl_2) δ 208.62, 207.55 (HC \equiv CH), 197.29, 191.88, 51.47, 50.53, 50.18, 50.16, 25.49, 25.39, 25.33, 25.13.

IR (cm^{-1}): ν (CO) 1903

Oxo-Tungsten(IV)-Acetylene Complexes

$[\text{OW}(\text{C}_2\text{H}_2)(\text{S}_2\text{CNEt}_2)_2]$ (**16a**)

Method 1: $[\text{Mo}_2\text{O}_3(\text{S}_2\text{P}(\text{OEt})_2)_4]$ (**10**) (0.120 g, 0.12 mmol, 1.2 equiv.) dissolved in CH_2Cl_2 was added to $[\text{W}(\text{C}_2\text{H}_2)(\text{CO})(\text{S}_2\text{CNEt}_2)_2]$ (**15a**) (0.055g, 0.1 mmol, 1 equiv.) dissolved CH_2Cl_2 . After stirring at RT for 2hrs, the solution was evaporated to dryness to yield crude **16a** as purple solid.

Method 2: Pyridine *N*-oxide (0.0113 g, 0.12 mmol, 1.2 equiv.) dissolved in CH_2Cl_2 was added to $[\text{W}(\text{C}_2\text{H}_2)(\text{CO})(\text{S}_2\text{CNEt}_2)_2]$ (**15a**) (0.051 g, 0.10 mmol, 1.0 equiv.) dissolved CH_2Cl_2 . The solution was stirred overnight, whereat the dark green solution faded, evaporation to dryness to yield crude **16a** as pale yellow solid.

Method 3: Acetonitrile was added to a schlenk flask containing $[\text{W}(\text{C}_2\text{H}_2)(\text{CO})(\text{S}_2\text{CNEt}_2)_2]$ (**15a**) (0500 g, 0.94 mmol, 1.0 equiv.) and trimethylamine *N*-oxide (0.083 g, 1.1 mmol, 1.1 equiv.), whereat the dark green solution slowly faded to pale yellow. After stirring at RT for 3 h the solution was isolated by filtration and evaporated to dryness. Trituration with diethyl ether and filtration, and evaporation to dryness yielded **16a** as pale orange/brown solid. Yield: 0.324 g (0.62 mmol ,48%)

^1H NMR (300 MHz, CD_2Cl_2) δ 10.70 (s, 1H), 10.49 (s, 1H), 3.84 (q, $J = 7.6$ Hz, 8H), 1.35 (dt, $J = 12.1, 7.1$ Hz, 12H).

^{13}C NMR (75 MHz, CD_2Cl_2) δ 205.94, 200.15, 154.28, 147.01, 54.00, 46.53, 46.39, 46.26, 45.72, 13.00, 12.65, 12.42, 12.06.

IR (cm^{-1}): CH_2Cl_2 : ν (W=O) 937

[OW(C₂H₂)(S₂CNC₄H₈)₂] (16b)

Acetonitrile was added to a schlenk flask containing [W(C₂H₂)(CO)(S₂CNC₄H₈)₂] (**15b**) (0.500 g, 0.43 mmol, 1.0 equiv.) and trimethylamine *N*-oxide (0.078 g, 1.03 mmol, 1.1 equiv.), whereat the dark green solution slowly faded to pale yellow. After stirring at RT for 3 h the solution was isolated by filtration and evaporated to dryness. Trituration with diethyl ether, filtration and evaporation to dryness yielded **16b** as pale orange/brown solid. Yield: 0.302 g (0.58 mmol, 62%)

¹H NMR (300 MHz, CDCl₃) δ 10.78 (s, 1H), 10.59 (m, 1H), 3.86 (s, 4H), 2.06 (m, 4H).

¹³C NMR (75 MHz, CDCl₃) δ 196.96, 154.27, 148.06, 77.16, 51.03, 50.85, 24.91, 24.55.

IR (cm⁻¹): CH₂Cl₂: ν (W=O) 93

VI. REFERENCES

- [1] D. L. Nelson, A. L. Lehninger, M. M. Cox, *Lehninger principles of biochemistry*, W.H. Freeman, New York, **2008**.
- [2] O. Carugo, F. Eisenhaber (Eds.) *Enzyme Databases*, Humana Press, Totowa, NJ, **2010**.
- [3] Y.-F. Liu, R.-Z. Liao, W.-J. Ding, J.-G. Yu, R.-Z. Liu, *J. Biol. Inorg. Chem.* **2011**, *16*, 745–752.
- [4] S. J. Lippard, J. M. Berg, *Principles of bioinorganic chemistry*, University Science Books, Mill Valley, Calif, **1994**.
- [5] A. L. Gavrilova, B. Bosnich, *Chem. Rev.* **2004**, *104*, 349–384.
- [6] L. E. Bevers, P.-L. Hagedoorn, W. R. Hagen, *Coord. Chem. Rev.* **2009**, *253*, 269–290.
- [7] A. Majumdar, S. Sarkar, *Coord. Chem. Rev.* **2011**, *255*, 1039–1054.
- [8] R. H. Holm, E. I. Solomon, A. Majumdar, A. Tenderholt, *Coord. Chem. Rev.* **2011**, *255*, 993–1015.
- [9] R. Hille, *Trends Biochem. Sci.* **2002**, *27*, 360–367.
- [10] J. R. Andreesen, K. Makdessi, *Ann. N.Y. Acad. Sci.* **2008**, *1125*, 215–229.
- [11] M. K. Johnson, D. C. Rees, M. W. W. Adams, *Chem. Rev.* **1996**, *96*, 2817–2840.
- [12] K. Makdessi, *J. Biol. Chem.* **2001**, *276*, 24557–24564.
- [13] H. Sugimoto, H. Tsukube, *Chem. Soc. Rev.* **2008**, *37*, 2609–2619.
- [14] A. F. Holleman, E. Wiberg, N. Wiberg, *Lehrbuch der anorganischen Chemie*, de Gruyter, Berlin, New York, **2007**.
- [15] M. A. Vincent, I. H. Hillier, G. Periyasamy, N. A. Burton, *Dalton Trans.* **2010**, *39*, 3816–3822.
- [16] G. B. Seiffert, G. M. Ullmann, A. Messerschmidt, B. Schink, P. M. H. Kroneck, O. Einsle, *Proc. Natl. Acad. Sci. U. S. A.* **2007**, *104*, 3073–3077.
- [17] I. Bertini, *Biological inorganic chemistry. Structure and reactivity*, University Science Books, Sausalito, Calif, **2007**.
- [18] J.-P. Bellenger, T. Wichard, Y. Xu, A. M. L. Kraepiel, *Environ. Microbiol.* **2011**, *13*, 1395–1411.
- [19] A. Kletzin, M. W. Adams, *FEMS Microbiol. Rev.* **1996**, *18*, 5–63.
- [20] a) O. Einsle, *Science* **2002**, *297*, 1696–1700. b) K. M. Lancaster, M. Roemelt, P. Ettenhuber, Y. Hu, M. W. Ribbe, F. Neese, U. Bergmann, S. DeBeer, *Science* **2011**, *334*, 974–977.
- [21] "W_Tungsten.jpg (JPEG-Grafik, 400 × 400 Pixel)", can be found under http://periodicnetwork2011tag.pbworks.com/f/1321309659/W_Tungsten.jpg, **2011**.
- [22] a) U. Leonhardt, J. R. Andreesen, *Arch. Microbiol.* **1977**, *115*, 277–284. b) R. Wagner, J. R. Andreesen, *Arch. Microbiol.* **1987**, *147*, 295–299.
- [23] I. Yamamoto, T. Saiki, S. M. Liu, L. G. Ljungdahl, *J. Biol. Chem.* **1983**, *258*, 1826–1832.

- [24] B. M. Rosner, B. Schink, *J. Biol. Chem.* **1995**, *177*, 5767–5772.
- [25] R.-Z. Liao, J.-G. Yu, F. Himo, *Proc. Natl. Acad. Sci. U. S. A.* **2010**, *107*, 22523–22527.
- [26] a) J. H. Enemark, J. J. A. Cooney, J.-J. Wang, R. H. Holm, *Chem. Rev.* **2004**, *104*, 1175–1200. b) M. J. Romao, *Dalton Trans.* **2009**, 4053–4068.
- [27] A. Messerschmidt, *Handbook of metalloproteins*, Wiley, Chichester ; New York, **2001-c2011**.
- [28] G. Schwarz, R. R. Mendel, M. W. Ribbe, *Nature* **2009**, *460*, 839–847.
- [29] F. tenBrink, "Acetylene Hydratase from *Pelobacter acetylenicus* : functional Studies on a Gas-Processing Tungsten, Iron-Sulfur Enzyme by Site Directed Mutagenesis and Crystallography"; PhD- Thesis, can be found under <http://kops.uni-konstanz.de/handle/urn:nbn:de:bsz:352-opus-116405>, **2010**.
- [30] C. Schulzke, *Eur. J. Inorg. Chem.* **2011**, *2011*, 1189–1199.
- [31] P. P. Samuel, S. Horn, A. Döring, K. G. V. Havelius, S. Reschke, S. Leimkühler, M. Haumann, C. Schulzke, *Eur. J. Inorg. Chem.* **2011**, *2011*, 4387–4399.
- [32] H. Sugimoto, M. Harihara, M. Shiro, K. Sugimoto, K. Tanaka, H. Miyake, H. Tsukube, *Inorg. Chem* **2005**, *44*, 6386–6392.
- [33] B. Schink, *Arch. Microbiol.* **1985**, *142*, 295–301.
- [34] R.-Z. Liao, F. Himo, *ACS Catal.* **2011**, *1*, 937–944.
- [35] M. Boll, B. Schink, A. Messerschmidt, P. M. Kroneck, *Biol. Chem.* **2005**, *386*, 999–1006.
- [36] M. Brzezińska, P. Rafalski, T. Włodarczyk, P. Szarlip, K. Brzeziński, *J. Soils Sediments* **2011**, *11*, 1142–1154.
- [37] K. Didriche, M. Herman, *Chem. Phys. Lett.* **2010**, *496*, 1–7.
- [38] a) X. Liang, R. Paul Philp, E. C. Butler, *Chemosphere* **2009**, *75*, 63–69. b) M. Kanakidou, B. Bonsang, J. C. Le Roulley, G. Lambert, D. Martin, G. Sennequier, *Nature* **1988**, *333*, 51–52.
- [39] R. S. Oremland, M. A. Voytek, *Astrobiology* **2008**, *8*, 45–58.
- [40] a) X. Xu, K. Inubushi, *Soil Sci. Plant Nutr.* **2005**, *51*, 683–688. b) X. Xu, K. Inubushi, *Chin. Sci. Bull.* **2008**, *53*, 1087–1093.
- [41] D. Kanner, R. Bartha, *J. Bacteriol.* **1980**, *150*, 989–992.
- [42] J. A. M. Bont, M. W. Peck, *Arch. Microbiol.* **1980**, *127*, 99–104.
- [43] J. C. Germon, R. Knowles, *Can. J. Microbiol.* **1988**, *34*, 242–248.
- [44] T.-Y. Tam, C. I. Mayfield, W. E. Inniss, *Curr. Microbiol.* **1983**, *8*, 165–168.
- [45] M. R. Hyman, A. Daniel, *Anal. Biochem.* **1988**, *173*, 207–220.
- [46] A. Magalon, J. G. Fedor, A. Walburger, J. H. Weiner, *Coord. Chem. Rev.* **2011**, *255*, 1159–1178.
- [47] F. tenBrink, B. Schink, P. M. H. Kroneck, *J. Bacteriol.* **2011**, *193*, 1229–1236.
- [48] R.-Z. Liao, W. Thiel, *J. Chem. Theory Comput.* **2012**, ahead of print.
- [49] R. U. Meckenstock, R. Krieger, S. Ensign, P. M. H. Kroneck, B. Schink, *Eur. J. Biochem.* **1999**, *264*, 176–182.
- [50] S. Antony, C. A. Bayse, *Organometallics* **2009**, *28*, 4938–4944.
- [51] J. Yadav, S. K. Das, S. Sarkar, *J. Am. Chem. Soc.* **1997**, *119*, 4315–4316.
- [52] J. W. McDonald, J. L. Corbin, W. E. Newton, *J. Am. Chem. Soc.* **1975**, *97*, 1970–1971.
- [53] J. W. McDonald, W. E. Newton, C. T. C. Creedy, J. L. Corbin, *J. Organomet. Chem.* **1975**, *92*, C25.

- [54] E. A. Maatta, R. A. D. Wentworth, W. E. Newton, J. W. McDonald, G. D. Watt, *J. Am. Chem. Soc.* **1978**, *100*, 1320–1321.
- [55] E. A. Maatta, R. A. D. Wentworth, *Inorg. Chem.* **1979**, *18*, 524–526.
- [56] L. Ricard, R. Weiss, W. E. Newton, G. J. J. Chen, J. W. McDonald, *J. Am. Chem. Soc.* **1978**, *100*, 1318–1320.
- [57] B. C. Ward, J. L. Templeton, *J. Am. Chem. Soc.* **1980**, *102*, 1532–1538.
- [58] W. E. Newton, J. W. McDonald, J. L. Corbin, L. Ricard, R. Weiss, *Inorg. Chem.* **1980**, *19*, 1997–2006.
- [59] J. L. Templeton, B. C. Ward, G. J. J. Chen, J. W. McDonald, W. E. Newton, *Inorg. Chem.* **1981**, *20*, 1248–1253.
- [60] S. K. Das, D. Biswas, R. Maiti, S. Sarkar, *J. Am. Chem. Soc.* **1996**, *118*, 1387–1397.
- [61] Merck KGaA, "Acetaldehyde data sheet merck", can be found under http://www.merckmillipore.com/germany/chemicals/acetaldehyd/MDA_CHEM-800004/p_4WOb.s1LvhcAAEWg.EfVhTI?WFSimpleSearch_NameOrId=75-07-0&BackButtonText=search+results.
- [62] R. A. Sheldon, *Pure Appl. Chem.* **2000**, *72*, 1233–1246.
- [63] G. J.-J. Chen, R. O. Yelton, J. W. McDonald, *Inorg. Chim. Acta* **1977**, *22*, 249–252.
- [64] A. J. Burn, S. K. Dewan, I. Gosney, P. S. G. Tan, *J. Chem. Soc., Perkin Trans. 2* **1990**, 753–758.
- [65] H. Vrubel, V. H. Cardozo Verzenhassi, S. Nakagaki, F. S. Nunes, *Inorg. Chem. Comm.* **2008**, *11*, 1040–1043.
- [66] G. J. J. Chen, J. W. McDonald, W. E. Newton, *Inorg. Chem.* **1976**, *15*, 2612–2615.
- [67] a) H. Gotthardt, W. Pflaumbaum, *Chem. Ber.* **1987**, *120*, 411–420. b) K.-B. Shiu, S.-J. Yu, Y. Wang, G.-H. Lee, *J. Organomet. Chem.* **2002**, *650*, 37–42. c) E. Carmona, A. Galindo, C. Guille-Photin, R. Lai, A. Monge, C. Ruiz, L. Sanchez, *Inorg. Chem.* **1988**, *27*, 488–492. d) A. Dinsmore, J. H. Birks, C. David Garner, J. A. Joule, *J. Chem. Soc., Perkin Trans. 1* **1997**, 801–808.
- [68] A. Gürsoy, Ö. Ateş, N. Karali, N. Cesur, M. Kiraz, *Eur. J. Med. Chem.* **1996**, *31*, 643–646.
- [69] a) K. Rasheed, J. D. Warkentin, *J. Org. Chem.* **1980**, *45*, 4041–4044. b) N. F. Haley, M. W. Fichtner, *J. Org. Chem.* **1980**, *45*, 175–177. c) J. Shi, A. Linden, H. Heimgartner, *Helv. Chim. Acta* **1994**, *77*, 1903–1920.
- [70] R. J. Millican, M. Angelopoulos, A. Bose, B. Riegel, D. Robinson, C. K. Wagner, *J. Am. Chem. Soc.* **1983**, *105*, 3622–3630.
- [71] F. P. Hao, E. Silvester, G. D. Senior, *Anal. Chem.* **2000**, *72*, 4836–4845.
- [72] R. Sekirnik, N. R. Rose, A. Thalhammer, P. T. Seden, J. Mecinović, C. J. Schofield, *Chem. Commun.* **2009**, 6376.
- [73] F. Carta, M. Aggarwal, A. Maresca, A. Scozzafava, R. McKenna, E. Masini, C. T. Supuran, *J. Med. Chem.* **2012**, *55*, 1721–1730.
- [74] a) G. L. Hillhouse, G. V. Goeden, B. L. Haymore, *Inorg. Chem.* **1982**, *21*, 2064–2071. b) P. K. Baker, S. G. Fraser, *Inorg. Chim. Acta* **1986**, *116*, L1.
- [75] J. A. Bowden, R. Colton, *Aust. J. Chem.* **1968**, *21*, 2657–2661.
- [76] S. Lee, D. L. Staley, A. L. Rheingold, N. J. Cooper, *Inorg. Chem.* **1990**, *29*, 4391–4396.
- [77] P. J. Blower, J. R. Dilworth, J. Hutchinson, T. Nicholson, J. A. Zubieta, *J. Chem. Soc., Dalton Trans* **1985**, 2639–2645.
- [78] R. Colton, C. J. Rix, *Aust. J. Chem.* **1969**, *22*, 305–310.

- [79] A. K. Brisdon, E. G. Hope, W. Levason, J. S. Ogden, *J. Chem. Soc., Dalton Trans* **1989**, 313–316.
- [80] M. W. Anker, R. Colton, I. B. Tomkins, *Aust. J. Chem.* **1967**, *20*, 9.
- [81] R. L. Richards, C. Shortman, D. C. Povey, G. W. Smith, *Acta Crystallogr C Cryst Struct Commun* **1987**, *43*, 2309–2311.
- [82] a) E. Rentschler, K. Dehnicke, *Zeitschrift für Kristallographie* **1994**, *209*, 89. b) J. L. Dutton, R. Tabeshi, M. C. Jennings, A. J. Lough, P. J. Ragogna, *Inorg. Chem.* **2007**, *46*, 8594–8602.
- [83] a) R. R. Schrock, L. G. Sturgeoff, P. R. Sharp, *Inorg. Chem.* **1983**, *22*, 2801–2806. b) N. C. Gonnella, C. Busacca, S. Campbell, M. Eriksson, N. Grinberg, T. Bartholomeyzik, S. Ma, D. L. Norwood, *Magn. Reson. Chem.* **2009**, *47*, 461–464. c) J. Drabowicz, J. Luczak, M. Mikolajczyk, *J. Org. Chem.* **1998**, *63*, 9565–9568.
- [84] T. Szymańska-Buzar, T. Głowiak, I. Czeluśniak, *Polyhedron* **2002**, *21*, 1817–1823.
- [85] M. Al-Jahdali, P. K. Baker, *J. Organomet. Chem.* **2001**, *628*, 91–98.
- [86] M. Al-Jahdali, P. K. Baker, A. J. Lavery, M. M. Meehan, D. J. Muldoon, *J. Mol. Catal. A Chem.* **2000**, *159*, 51–62.
- [87] P. K. Baker, S. G. Fraser, E. M. Keys, *J. Organomet. Chem.* **1986**, *309*, 319–321.
- [88] F. A. Cotton, L. R. Falvello, J. H. Meadows, *Inorg. Chem.* **1985**, *24*, 514–517.
- [89] J. A. Broomhead, C. G. Young, *Aust. J. Chem.* **1982**, *35*, 277–285.
- [90] G. L. Hillhouse, B. L. Haymore, *J. Am. Chem. Soc.* **1982**, *104*, 1537–1548.
- [91] R. F. Lang, T. D. Ju, G. Kiss, C. D. Hoff, J. C. Bryan, G. J. Kubas, *Inorg. Chem.* **1994**, *33*, 3899–3907.
- [92] R. F. Lang, T. D. Ju, J. C. Bryan, G. J. Kubas, C. D. Hoff, *Inorg. Chim. Acta* **2003**, *348*, 157–164.
- [93] G. J.-J. Chen, J. W. McDonald, W. E. Newton, *Inorg. Nucl. Chem. Lett.* **1976**, *12*, 697–702.
- [94] C. Lorber, J. P. Donahue, C. A. Goddard, E. Nordlander, R. H. Holm, *J. Am. Chem. Soc.* **1998**, *120*, 8102–8112.
- [95] a) S. Thomas, E. R. T. Tiekink, C. G. Young, *Inorg. Chem.* **2005**, *45*, 352–361. b) A. A. Eagle, C. G. Young, E. R. T. Tiekink, *Aust. J. Chem.* **2004**, *57*, 269–271. c) S. Thomas, E. R. T. Tiekink, C. G. Young, *Organometallics* **1996**, *15*, 2428–2430.
- [96] C. Khosla, A. B. Jackson, P. S. White, J. L. Templeton, *Organometallics* **2012**, *31*, 987–994.
- [97] a) S. A. Cohen, E. I. Stiefel, *Inorg. Chem.* **1985**, *24*, 4657–4662. b) T. Ikada, S. Kuwata, Y. Mizobe, M. Hidai, *Inorg. Chem.* **1998**, *37*, 5793–5797.
- [98] M. G. B. Drew, R. J. Hobson, P. P. E. M. Mumba, D. A. Rice, N. Turp, *J. Chem. Soc., Dalton Trans.* **1987**, 1163.
- [99] G. M. Sheldrick, *Acta Crystallogr A Found Crystallogr* **2008**, *64*, 112–122.
- [100] B. K. Sarma, G. Mugesh, *J. Am. Chem. Soc.* **2005**, *127*, 11477–11485.

VII. APPENDIX

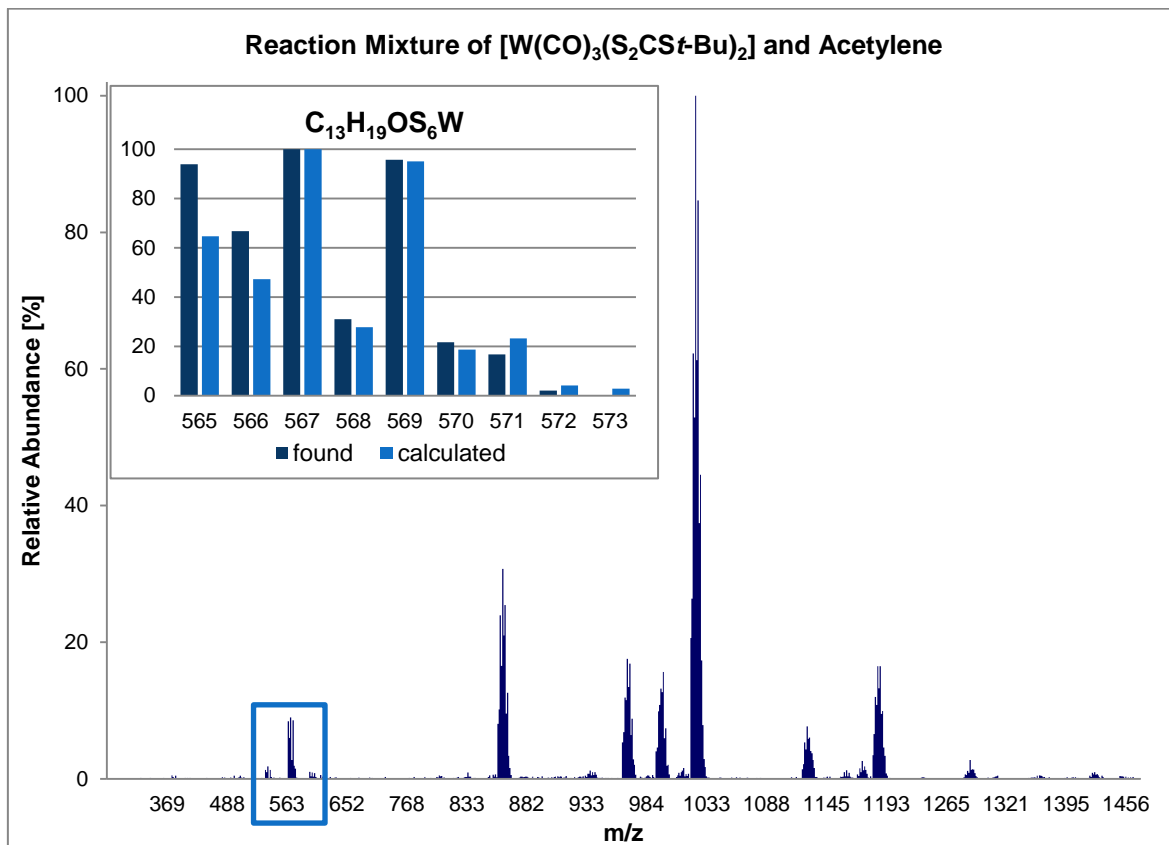


Figure 14: ESI chromatogram of the crude reaction mixture of $[\text{W}(\text{CO})_3(\text{S}_2\text{CS}\text{-}t\text{-Bu})_2]$ (**13**) and acetylene

CRYSTAL DATA REFINEMENT

Table 15: Crystal data and structure refinement for $[\text{PPh}_3\text{Cl}]_2[\text{WCl}_6]$ (**6**) and $\text{W}(\text{CO})_2(\text{PPh}_3)_2\text{Cl}_2$ (**7'**)

Crystal data		
Empirical formula	$\text{C}_{36}\text{H}_{30}\text{Cl}_3\text{P}_2\text{W}$	$\text{C}_{38}\text{H}_{30}\text{Cl}_2\text{O}_2\text{P}_2\text{W} \cdot 2\text{CH}_2\text{Cl}_2$
Formula weight	991.99	1005.16
Crystal description	block, orange	block, red
Crystal size	0.27 x 0.25 x 0.22mm	0.18 x 0.15 x 0.12mm
Crystal system, space group	trigonal, R -3	monoclinic, C 2/c
Unit cell dimensions:	a= 13.0514(5)Å c= 18.6382(8)Å	a= 15.357(2)Å b= 13.4971(18)Å c= 20.453(3)Å β = 107.869(2)°
Volume	2749.5(3)Å ³	4034.8(9)Å ³
Z	3	4

Calculated density	1.797Mg/m ³	1.655Mg/m ³
F(000)	1458	1984
Linear absorption coefficient μ	3.849mm ⁻¹	3.374mm ⁻¹
Absorption correction	semi-empirical from equivalents	semi-empirical from equivalents
Max. and min. transmission	0.4940 and 0.4148	0.7454 and 0.4989
Unit cell determination	2.83° < Θ < 31.19°	2.49° < Θ < 26.42°
	9995 reflections used at 100K	5856 reflections used at 100K
Data collection		
Scan type	Φ and ω scans	Φ and ω scans
Θ range for data collection	2.11 to 30.00°	2.05 to 26.00°
Index ranges	-18 ≤ h ≤ 18, -18 ≤ k ≤ 17, -23 ≤ l ≤ 26	-18 ≤ h ≤ 18, -13 ≤ k ≤ 16, -23 ≤ l ≤ 25
Reflections collected / unique	10871 / 1784	8147 / 3931
Significant reflections	1784 with I > 2 σ (I)	3617 with I > 2 σ (I)
R(int), R(sigma)	0.0220, 0.0119	0.0196, 0.0300
Completeness to $\Theta = 30.0^\circ$	100.0%	98.8%
Refinement		
Data / parameters / restraints	1784 / 73 / 0	3931 / 235 / 0
Goodness-of-fit on F ²	1.134	1.068
Final R indices [I > 2 σ (I)]	R1 = 0.0116, wR2 = 0.0318	R1 = 0.0196, wR2 = 0.0480
R indices (all data)	R1 = 0.0116, wR2 = 0.0318	R1 = 0.0239, wR2 = 0.0494
Extinction expression	none	none
Weighting scheme	w = 1/[$\sigma^2(F_o^2)$ +(aP) ² +bP] where P = (F _o ² +2F _c ²)/3	w = 1/[$\sigma^2(F_o^2)$ +(aP) ² +bP] where P = (F _o ² +2F _c ²)/3
Weighting scheme parameters a, b	0.0179, 2.7150	0.0262, 0.9933
Largest Δ/σ in last cycle	0.001	0.001
Largest difference peak and hole	0.569 and -0.517e/Å ³	1.053 and -0.681e/Å ³

Table 16: Crystal data and structure refinement for W₂(CO)₇Br₄ (**9**) and W(CO)₂(S,N-oxa)₂ (**14**)

Crystal data		
Empirical formula	C ₇ Br ₄ O ₇ W ₂	C ₂₄ H ₂₄ N ₂ O ₄ S ₂ W · C ₇ H ₈
Formula weight	883.41	744.56
Crystal description	needle, yellow	block, orange
Crystal size	0.21 x 0.08 x 0.04mm	0.28 x 0.24 x 0.21mm
Crystal system, space group	monoclinic, P 2 ₁ /n	monoclinic, C 2/c
Unit cell dimensions:	a= 15.2750(5)Å b= 6.5543(3)Å c= 15.5376(6)Å β = 104.853(2)°	a= 11.7208(4)Å b= 17.0974(6)Å c= 15.0871(6)Å β =101.8360(10)°
Volume	1503.60(10)Å ³	2959.10(19)Å ³
Z	4	4
Calculated density	3.902Mg/m ³	1.671Mg/m ³
F(000)	1544	1480
Linear absorption coefficient μ	25.940mm ⁻¹	4.084mm ⁻¹
Absorption correction	semi-empirical from equivalents	semi-empirical from equivalents
Max. and min. transmission	1.0000 and 0.4525	0.6479 and 0.5273
Unit cell determination	2.71° < Θ < 30.77°	2.34° < Θ < 30.93°
	5707 reflections used at 100K	9892 reflections used at 100K
Data collection		
Monochromator	graphite	graphite
Scan type	Φ and ω scans	Φ and ω scans

Θ range for data collection	2.71 to 30.00°	2.14 to 30.00°
Index ranges	-21 ≤ h ≤ 21, -8 ≤ k ≤ 9, -21 ≤ l ≤ 21	-16 ≤ h ≤ 16, -24 ≤ k ≤ 24, -21 ≤ l ≤ 19
Reflections collected / unique	12479 / 4376	16050 / 4317
Significant unique reflections	3626 with I > 2σ(I)	4224 with I > 2σ(I)
R(int), R(sigma)	0.0396, 0.0521	0.0196, 0.0164
Completeness to Θ = 30.0°	99.7%	100.0%
Refinement		
Data / parameters / restraints	4376 / 182 / 0	4317 / 209 / 0
Goodness-of-fit on F ²	1.122	1.054
Final R indices [I > 2σ(I)]	R1 = 0.0440, wR2 = 0.0940	R1 = 0.0138, wR2 = 0.0350
R indices (all data)	R1 = 0.0586, wR2 = 0.0987	R1 = 0.0144, wR2 = 0.0352
Extinction expression	none	none
Weighting scheme	w = 1/[σ ² (F _o ²)+(aP) ² +bP] where P = (F _o ² +2F _c ²)/3	w = 1/[σ ² (F _o ²)+(aP) ² +bP] where P = (F _o ² +2F _c ²)/3
Weighting scheme parameters a, b	0.0362, 25.257	0.0171, 3.7278
Largest Δ/σ in last cycle	0.001	0.002
Largest difference peak and hole	5.177 and -2.140e/Å ³	1.274 and -0.761e/Å ³

Table 17: Full list of bond lengths [Å] and angles [°] for [PPh₃Cl]₂[WCl₆] (**6**)

W(1)-Cl(1)	2.3824(3)	Cl(1) ⁱⁱ -W(1)-Cl(1) ⁱⁱⁱ	88.552(10)	C(5)-C(4)-C(3)	120.55(11)
W(1)-Cl(1) ⁱ	2.3824(3)	Cl(1)-W(1)-Cl(1) ⁱⁱⁱ	88.552(10)	C(5)-C(4)-H(4)	119.7
W(1)-Cl(1) ⁱⁱⁱ	2.3824(3)	Cl(1) ⁱ -W(1)-Cl(1) ⁱⁱⁱ	91.448(10)	C(3)-C(4)-H(4)	119.7
W(1)-Cl(1) ⁱⁱⁱⁱ	2.3824(3)	Cl(1) ⁱⁱ -W(1)-Cl(1) ⁱⁱⁱⁱ	91.448(10)	C(4)-C(5)-C(6)	119.99(11)
W(1)-Cl(1) ^v	2.3824(3)	Cl(1)-W(1)-Cl(1) ^v	91.448(10)	C(4)-C(5)-H(5)	120.0
W(1)-Cl(1) ^{vi}	2.3824(3)	Cl(1) ⁱⁱ -W(1)-Cl(1) ^{vi}	88.552(10)	C(6)-C(5)-H(5)	120.0
P(1)-Cl(2)	1.9993(7)	Cl(1) ⁱⁱⁱ -W(1)-Cl(1) ^{vi}	88.552(10)	C(5)-C(6)-C(1)	119.32(11)
P(1)-C(1)	1.7807(11)	Cl(1)-W(1)-Cl(1) ^v	88.552(10)	C(5)-C(6)-H(6)	120.3
P(1)-C(1) ⁱⁱⁱ	1.7807(11)	Cl(1) ⁱ -W(1)-Cl(1) ^v	91.448(10)	C(1)-C(6)-H(6)	120.3
P(1)-C(1) ^v	1.7807(11)	Cl(1) ⁱⁱⁱ -W(1)-Cl(1) ^v	88.552(10)		
C(1)-C(6)	1.3981(16)	Cl(1) ^v -W(1)-Cl(1) ^v	91.448(10)	C(1) ⁱⁱⁱ -P(1)-C(1)-C(6)	120.64(7)
C(1)-C(2)	1.4000(16)	C(1) ⁱⁱⁱ -P(1)-C(1) ^v	111.46(4)	C(1) ^v -P(1)-C(1)-C(6)	-4.59(13)
C(2)-C(3)	1.3852(16)	C(1) ⁱⁱⁱ -P(1)-C(1)	111.46(4)	Cl(2)-P(1)-C(1)-C(6)	-121.98(9)
C(2)-H(2)	0.95	C(1) ^v -P(1)-C(1)	111.46(4)	C(1) ⁱⁱⁱ -P(1)-C(1)-C(2)	-57.36(14)
C(3)-C(4)	1.3893(17)	C(1) ⁱⁱⁱ -P(1)-Cl(2)	107.40(4)	C(1) ^v -P(1)-C(1)-C(2)	177.40(8)
C(3)-H(3)	0.95	C(1) ^v -P(1)-Cl(2)	107.40(4)	Cl(2)-P(1)-C(1)-C(2)	60.02(10)
C(4)-C(5)	1.3884(17)	C(1)-P(1)-Cl(2)	107.40(4)	C(6)-C(1)-C(2)-C(3)	-2.15(18)
C(4)-H(4)	0.95	C(6)-C(1)-C(2)	120.52(11)	P(1)-C(1)-C(2)-C(3)	175.86(10)
C(5)-C(6)	1.3922(16)	C(6)-C(1)-P(1)	120.81(9)	C(1)-C(2)-C(3)-C(4)	1.32(19)
C(5)-H(5)	0.95	C(2)-C(1)-P(1)	118.65(9)	C(2)-C(3)-C(4)-C(5)	0.77(19)
C(6)-H(6)	0.95	C(3)-C(2)-C(1)	119.42(11)	C(3)-C(4)-C(5)-C(6)	-2.05(19)
		C(3)-C(2)-H(2)	120.3	C(4)-C(5)-C(6)-C(1)	1.21(18)
		C(1)-C(2)-H(2)	120.3	C(2)-C(1)-C(6)-C(5)	0.89(18)
		C(2)-C(3)-C(4)	120.15(11)	P(1)-C(1)-C(6)-C(5)	-177.08(9)
		C(2)-C(3)-H(3)	119.9		
		C(4)-C(3)-H(3)	119.9		

Symmetry transformations used to generate equivalent atoms: ⁱ -x, -y, 1-z ⁱⁱ x-y, x, 1-z ⁱⁱⁱ -y, x-y, z ^{iv} y, y-x, 1-z ^v y-x, -x, z

Table 18: Full list of bond lengths [Å] and angles [°] for W(CO)₂(PPh₃)₂Cl₂ (**7'**)

W(1)-C(1) [⊖]	1.962(2)	O(1)-C(1)-W(1)	176.3(2)	Cl(41)-C(4)-H(41)	109.2
W(1)-C(1)	1.962(2)	C(11)-P(1)-C(31)	105.68(12)	Cl(42)-C(4)-H(42)	109.2
W(1)-Cl(1) [⊖]	2.4140(6)	C(11)-P(1)-C(21)	102.04(11)	Cl(41)-C(4)-H(42)	109.2
W(1)-Cl(1)	2.4140(6)	C(31)-P(1)-C(21)	105.56(12)	H(41)-C(4)-H(42)	107.9
W(1)-P(1)	2.4816(7)	C(11)-P(1)-W(1)	114.88(8)		
W(1)-P(1) [⊖]	2.4816(7)	C(31)-P(1)-W(1)	106.01(9)	C(1) [⊖] -W(1)-P(1)-C(11)	85.81(12)
C(1)-O(1)	1.159(3)	C(21)-P(1)-W(1)	121.41(9)	C(1)-W(1)-P(1)-C(11)	-23.37(11)
P(1)-C(11)	1.826(3)	C(12)-C(11)-C(16)	119.6(2)	Cl(1) [⊖] -W(1)-P(1)-C(11)	-109.04(9)
P(1)-C(21)	1.837(2)	C(12)-C(11)-P(1)	121.5(2)	Cl(1)-W(1)-P(1)-C(11)	-175.55(9)
P(1)-C(31)	1.827(3)	C(16)-C(11)-P(1)	118.88(19)	P(1) [⊖] -W(1)-P(1)-C(11)	30.44(9)
C(11)-C(12)	1.394(4)	C(11)-C(12)-C(13)	119.6(3)	C(1) [⊖] -W(1)-P(1)-C(31)	-157.89(11)
C(11)-C(16)	1.398(4)	C(11)-C(12)-H(12)	120.2	C(1)-W(1)-P(1)-C(31)	92.92(11)
C(12)-C(13)	1.396(4)	C(13)-C(12)-H(12)	120.2	Cl(1) [⊖] -W(1)-P(1)-C(31)	7.26(9)
C(12)-H(12)	0.95	C(14)-C(13)-C(12)	120.5(3)	Cl(1)-W(1)-P(1)-C(31)	-59.25(8)
C(13)-C(14)	1.374(4)	C(14)-C(13)-H(13)	119.8	P(1) [⊖] -W(1)-P(1)-C(31)	146.74(9)
C(13)-H(13)	0.95	C(12)-C(13)-H(13)	119.8	C(1) [⊖] -W(1)-P(1)-C(21)	-37.74(12)
C(14)-C(15)	1.393(4)	C(13)-C(14)-C(15)	120.2(3)	C(1)-W(1)-P(1)-C(21)	-146.92(12)
C(14)-H(14)	0.95	C(13)-C(14)-H(14)	119.9	Cl(1) [⊖] -W(1)-P(1)-C(21)	127.41(10)
C(15)-C(16)	1.386(4)	C(15)-C(14)-H(14)	119.9	Cl(1)-W(1)-P(1)-C(21)	60.91(10)
C(15)-H(15)	0.95	C(16)-C(15)-C(14)	120.0(3)	P(1) [⊖] -W(1)-P(1)-C(21)	-93.11(10)
C(16)-H(16)	0.95	C(16)-C(15)-H(15)	120.0	C(31)-P(1)-C(11)-C(12)	-4.0(2)
C(21)-C(22)	1.391(4)	C(14)-C(15)-H(15)	120.0	C(21)-P(1)-C(11)-C(12)	-114.2(2)
C(21)-C(26)	1.399(4)	C(15)-C(16)-C(11)	120.1(3)	W(1)-P(1)-C(11)-C(12)	112.5(2)
C(22)-C(23)	1.396(4)	C(15)-C(16)-H(16)	120.0	C(31)-P(1)-C(11)-C(16)	176.8(2)
C(22)-H(22)	0.95	C(11)-C(16)-H(16)	120.0	C(21)-P(1)-C(11)-C(16)	66.6(2)
C(23)-C(24)	1.378(4)	C(22)-C(21)-C(26)	118.9(2)	W(1)-P(1)-C(11)-C(16)	-66.7(2)
C(23)-H(23)	0.95	C(22)-C(21)-P(1)	119.77(19)	C(16)-C(11)-C(12)-C(13)	0.9(4)
C(24)-C(25)	1.377(4)	C(26)-C(21)-P(1)	121.3(2)	P(1)-C(11)-C(12)-C(13)	-178.3(2)
C(24)-H(24)	0.95	C(21)-C(22)-C(23)	120.3(2)	C(11)-C(12)-C(13)-C(14)	-0.4(4)
C(25)-C(26)	1.391(4)	C(21)-C(22)-H(22)	119.8	C(12)-C(13)-C(14)-C(15)	-0.1(4)
C(25)-H(25)	0.95	C(23)-C(22)-H(22)	119.8	C(13)-C(14)-C(15)-C(16)	0.2(4)
C(26)-H(26)	0.95	C(24)-C(23)-C(22)	120.3(3)	C(14)-C(15)-C(16)-C(11)	0.4(4)
C(31)-C(36)	1.398(4)	C(24)-C(23)-H(23)	119.8	C(12)-C(11)-C(16)-C(15)	-0.9(4)
C(31)-C(32)	1.402(4)	C(22)-C(23)-H(23)	119.8	P(1)-C(11)-C(16)-C(15)	178.3(2)
C(32)-C(33)	1.385(4)	C(25)-C(24)-C(23)	119.7(2)	C(11)-P(1)-C(21)-C(22)	17.8(2)
C(32)-H(32)	0.95	C(25)-C(24)-H(24)	120.1	C(31)-P(1)-C(21)-C(22)	-92.4(2)
C(33)-C(34)	1.389(4)	C(23)-C(24)-H(24)	120.1	W(1)-P(1)-C(21)-C(22)	147.20(18)
C(33)-H(33)	0.95	C(24)-C(25)-C(26)	120.8(3)	C(11)-P(1)-C(21)-C(26)	-162.5(2)
C(34)-C(35)	1.384(4)	C(24)-C(25)-H(25)	119.6	C(31)-P(1)-C(21)-C(26)	87.3(2)
C(34)-H(34)	0.95	C(26)-C(25)-H(25)	119.6	W(1)-P(1)-C(21)-C(26)	-33.1(3)
C(35)-C(36)	1.394(4)	C(25)-C(26)-C(21)	120.0(3)	C(26)-C(21)-C(22)-C(23)	0.1(4)
C(35)-H(35)	0.95	C(25)-C(26)-H(26)	120.0	P(1)-C(21)-C(22)-C(23)	179.8(2)
C(36)-H(36)	0.95	C(21)-C(26)-H(26)	120.0	C(21)-C(22)-C(23)-C(24)	-0.9(4)
C(4)-Cl(42)	1.767(3)	C(36)-C(31)-C(32)	118.9(2)	C(22)-C(23)-C(24)-C(25)	1.0(4)
C(4)-Cl(41)	1.769(3)	C(36)-C(31)-P(1)	122.1(2)	C(23)-C(24)-C(25)-C(26)	-0.4(4)
C(4)-H(41)	0.99	C(32)-C(31)-P(1)	119.0(2)	C(24)-C(25)-C(26)-C(21)	-0.5(4)
C(4)-H(42)	0.99	C(33)-C(32)-C(31)	120.8(3)	C(22)-C(21)-C(26)-C(25)	0.6(4)
		C(33)-C(32)-H(32)	119.6	P(1)-C(21)-C(26)-C(25)	-179.1(2)
C(1)-W(1)-Cl(1)	146.23(7)	C(31)-C(32)-H(32)	119.6	C(11)-P(1)-C(31)-C(36)	-104.9(2)
Cl(1)-W(1)-P(1) [⊖]	138.01(2)	C(32)-C(33)-C(34)	119.8(3)	C(21)-P(1)-C(31)-C(36)	2.7(2)
P(1)-W(1)-P(1) [⊖]	132.36(3)	C(32)-C(33)-H(33)	120.1	W(1)-P(1)-C(31)-C(36)	132.7(2)
C(1)-W(1)-C(1) [⊖]	104.36(14)	C(34)-C(33)-H(33)	120.1	C(11)-P(1)-C(31)-C(32)	77.4(2)
C(1) [⊖] -W(1)-Cl(1) [⊖]	146.23(7)	C(35)-C(34)-C(33)	120.1(3)	C(21)-P(1)-C(31)-C(32)	-174.9(2)
C(1)-W(1)-Cl(1) [⊖]	96.17(7)	C(35)-C(34)-H(34)	120.0	W(1)-P(1)-C(31)-C(32)	-44.9(2)
C(1) [⊖] -W(1)-Cl(1)	96.17(7)	C(33)-C(34)-H(34)	120.0	C(36)-C(31)-C(32)-C(33)	0.8(4)
Cl(1) [⊖] -W(1)-Cl(1)	80.11(3)	C(34)-C(35)-C(36)	120.4(3)	P(1)-C(31)-C(32)-C(33)	178.5(2)
C(1) [⊖] -W(1)-P(1)	73.48(7)	C(34)-C(35)-H(35)	119.8	C(31)-C(32)-C(33)-C(34)	-1.6(4)
C(1)-W(1)-P(1)	77.82(7)	C(36)-C(35)-H(35)	119.8	C(32)-C(33)-C(34)-C(35)	1.5(4)
Cl(1)-W(1)-P(1)	82.82(2)	C(35)-C(36)-C(31)	120.0(2)	C(33)-C(34)-C(35)-C(36)	-0.5(4)
C(1) [⊖] -W(1)-P(1) [⊖]	77.82(7)	C(35)-C(36)-H(36)	120.0	C(34)-C(35)-C(36)-C(31)	-0.4(4)
C(1)-W(1)-P(1) [⊖]	73.48(7)	C(31)-C(36)-H(36)	120.0	C(32)-C(31)-C(36)-C(35)	0.2(4)
Cl(1) [⊖] -W(1)-P(1) [⊖]	82.82(2)	Cl(42)-C(4)-Cl(41)	111.92(16)	P(1)-C(31)-C(36)-C(35)	-177.4(2)
Cl(1) [⊖] -W(1)-P(1)	138.01(2)	Cl(42)-C(4)-H(41)	109.2		

Symmetry transformations used to generate equivalent atoms: [⊖] 1-x, y, 3/2-z

Table 19: Full list of bond lengths [Å] and angles [°] for $W_2(CO)_7Br_4$ (9)

W(1)-C(6)	1.972(11)	C(6)-W(1)-Br(4)	131.8(3)	C(1)-W(2)-Br(2)-W(1)	-103.7(4)
W(1)-C(5)	1.990(11)	C(5)-W(1)-Br(4)	85.9(3)	C(4)-W(2)-Br(2)-W(1)	-156.6(3)
W(1)-C(7)	2.006(10)	C(7)-W(1)-Br(4)	155.5(3)	C(3)-W(2)-Br(2)-W(1)	129.9(3)
W(1)-Br(1)	2.6234(10)	Br(1)-W(1)-Br(4)	88.13(3)	C(2)-W(2)-Br(2)-W(1)	60.6(8)
W(1)-Br(3)	2.6715(10)	Br(3)-W(1)-Br(4)	76.29(3)	Br(4)-W(2)-Br(2)-W(1)	38.52(3)
W(1)-Br(2)	2.6905(11)	Br(2)-W(1)-Br(4)	78.23(3)	Br(3)-W(2)-Br(2)-W(1)	-40.71(3)
W(1)-Br(4)	2.6961(10)	C(1)-W(2)-C(4)	71.0(4)	C(6)-W(1)-Br(2)-W(2)	96.9(4)
W(2)-C(1)	2.009(11)	C(1)-W(2)-C(3)	114.0(4)	C(5)-W(1)-Br(2)-W(2)	-80.2(8)
W(2)-C(4)	2.016(11)	C(4)-W(2)-C(3)	75.7(4)	C(7)-W(1)-Br(2)-W(2)	158.8(3)
W(2)-C(3)	2.043(9)	C(1)-W(2)-C(2)	73.3(4)	Br(1)-W(1)-Br(2)-W(2)	-126.37(3)
W(2)-C(2)	2.046(9)	C(4)-W(2)-C(2)	119.8(4)	Br(3)-W(1)-Br(2)-W(2)	40.69(3)
W(2)-Br(4)	2.6392(10)	C(3)-W(2)-C(2)	76.9(4)	Br(4)-W(1)-Br(2)-W(2)	-37.82(3)
W(2)-Br(2)	2.6489(10)	C(1)-W(2)-Br(4)	136.8(3)	C(1)-W(2)-Br(3)-W(1)	173.8(3)
W(2)-Br(3)	2.6606(10)	C(4)-W(2)-Br(4)	151.7(3)	C(4)-W(2)-Br(3)-W(1)	110.4(3)
C(1)-O(1)	1.134(13)	C(3)-W(2)-Br(4)	92.5(3)	C(3)-W(2)-Br(3)-W(1)	-16.3(13)
C(2)-O(2)	1.120(12)	C(2)-W(2)-Br(4)	81.0(3)	C(2)-W(2)-Br(3)-W(1)	-118.1(3)
C(3)-O(3)	1.133(12)	C(1)-W(2)-Br(2)	126.6(3)	Br(4)-W(2)-Br(3)-W(1)	-41.29(3)
C(4)-O(4)	1.136(13)	C(4)-W(2)-Br(2)	76.0(3)	Br(2)-W(2)-Br(3)-W(1)	41.06(3)
C(5)-O(5)	1.132(13)	C(3)-W(2)-Br(2)	96.4(3)	C(6)-W(1)-Br(3)-W(2)	-177.7(3)
C(6)-O(6)	1.151(13)	C(2)-W(2)-Br(2)	159.5(3)	C(5)-W(1)-Br(3)-W(2)	119.7(3)
C(7)-O(7)	1.135(12)	Br(4)-W(2)-Br(2)	79.98(3)	C(7)-W(1)-Br(3)-W(2)	-116.7(3)
C(6)-W(1)-C(5)	72.8(4)	C(1)-W(2)-Br(3)	76.9(3)	Br(1)-W(1)-Br(3)-W(2)	-0.07(10)
C(6)-W(1)-C(7)	72.6(4)	C(4)-W(2)-Br(3)	111.1(3)	Br(2)-W(1)-Br(3)-W(2)	-40.46(3)
C(5)-W(1)-C(7)	106.7(4)	C(3)-W(2)-Br(3)	168.9(3)	Br(4)-W(1)-Br(3)-W(2)	40.47(3)
C(6)-W(1)-Br(1)	126.4(3)	C(2)-W(2)-Br(3)	105.7(3)	C(1)-W(2)-Br(4)-W(1)	95.6(4)
C(5)-W(1)-Br(1)	77.6(3)	Br(4)-W(2)-Br(3)	77.44(3)	C(4)-W(2)-Br(4)-W(1)	-70.6(6)
C(7)-W(1)-Br(1)	74.7(3)	Br(2)-W(2)-Br(3)	77.47(3)	C(3)-W(2)-Br(4)-W(1)	-134.5(3)
C(6)-W(1)-Br(3)	73.8(3)	W(2)-Br(2)-W(1)	87.13(3)	C(2)-W(2)-Br(4)-W(1)	149.2(3)
C(5)-W(1)-Br(3)	113.4(3)	W(2)-Br(3)-W(1)	87.28(3)	Br(2)-W(2)-Br(4)-W(1)	-38.42(3)
C(7)-W(1)-Br(3)	115.5(3)	W(2)-Br(4)-W(1)	87.21(3)	Br(3)-W(2)-Br(4)-W(1)	40.84(3)
Br(1)-W(1)-Br(3)	159.79(4)	O(1)-C(1)-W(2)	179.4(9)	C(6)-W(1)-Br(4)-W(2)	-93.7(4)
C(6)-W(1)-Br(2)	128.4(3)	O(2)-C(2)-W(2)	179.2(9)	C(5)-W(1)-Br(4)-W(2)	-156.2(3)
C(5)-W(1)-Br(2)	158.7(3)	O(3)-C(3)-W(2)	177.0(8)	C(7)-W(1)-Br(4)-W(2)	81.3(7)
C(7)-W(1)-Br(2)	83.7(3)	O(4)-C(4)-W(2)	178.9(8)	Br(1)-W(1)-Br(4)-W(2)	126.15(3)
Br(1)-W(1)-Br(2)	87.83(3)	O(5)-C(5)-W(1)	179.3(10)	Br(3)-W(1)-Br(4)-W(2)	-40.87(3)
Br(3)-W(1)-Br(2)	76.57(3)	O(6)-C(6)-W(1)	176.1(10)	Br(2)-W(1)-Br(4)-W(2)	37.98(3)
		O(7)-C(7)-W(1)	178.6(9)		

Table 20: Full list of bond lengths [Å] and angles [°] for W(CO)₂(S,N-oxa)₂ (14)

W(1)-C(1) ^{ij}	1.9718(15)	N(13)-W(1)-S(1) ^{ij}	90.61(3)	C(35)-C(34)-H(34)	120.0
W(1)-C(1)	1.9718(15)	N(13) ^{ij} -W(1)-S(1)	90.61(3)	C(33)-C(34)-H(34)	120.0
W(1)-N(13)	2.2190(12)	O(1)-C(1)-W(1)	175.76(13)	C(34)-C(35)-C(36)	120.0
W(1)-N(13) ^{ij}	2.2190(12)	C(12)-O(11)-C(15)	105.06(11)	C(34)-C(35)-H(35)	120.0
W(1)-S(1)	2.3636(4)	N(13)-C(12)-O(11)	116.85(13)	C(36)-C(35)-H(35)	120.0
W(1)-S(1) ^{ij}	2.3636(4)	N(13)-C(12)-C(22)	128.77(13)	C(35)-C(36)-C(31)	120.0
C(1)-O(1)	1.1589(19)	O(11)-C(12)-C(22)	113.93(12)	C(35)-C(36)-H(36)	120.0
O(11)-C(12)	1.3496(17)	C(12)-N(13)-C(14)	105.21(11)	C(31)-C(36)-H(36)	120.0
C(12)-N(13)	1.2893(18)	C(12)-N(13)-W(1)	124.18(10)		
N(13)-C(14)	1.5197(18)	C(14)-N(13)-W(1)	129.80(9)	C(15)-O(11)-C(12)-N(13)	6.74(17)
C(14)-C(15)	1.524(2)	C(16)-C(14)-N(13)	115.80(11)	C(15)-O(11)-C(12)-C(22)	179.77(13)
O(11)-C(15)	1.4531(19)	C(16)-C(14)-C(15)	112.37(13)	O(11)-C(12)-N(13)-C(14)	13.77(16)
C(12)-C(22)	1.4589(19)	N(13)-C(14)-C(15)	99.82(11)	C(22)-C(12)-N(13)-C(14)	-158.05(14)
C(14)-C(16)	1.513(2)	C(16)-C(14)-C(17)	110.53(12)	O(11)-C(12)-N(13)-W(1)	-175.66(9)
C(14)-C(17)	1.529(2)	N(13)-C(14)-C(17)	106.41(11)	C(22)-C(12)-N(13)-W(1)	12.5(2)
C(15)-H(151)	0.99	C(15)-C(14)-C(17)	111.38(13)	C(1)-W(1)-N(13)-C(12)	-141.62(12)
C(15)-H(152)	0.99	O(11)-C(15)-C(14)	103.28(12)	N(13) ^{ij} -W(1)-N(13)-C(12)	43.13(10)
C(16)-H(161)	0.98	O(11)-C(15)-H(151)	111.1	S(1)-W(1)-N(13)-C(12)	-47.64(11)
C(16)-H(162)	0.98	C(14)-C(15)-H(151)	111.1	S(1) ^{ij} -W(1)-N(13)-C(12)	125.81(11)
C(16)-H(163)	0.98	O(11)-C(15)-H(152)	111.1	C(1)-W(1)-N(13)-C(14)	26.51(12)
C(17)-H(171)	0.98	C(14)-C(15)-H(152)	111.1	N(13) ^{ij} -W(1)-N(13)-C(14)	-148.73(13)
C(17)-H(172)	0.98	H(151)-C(15)-H(152)	109.1	S(1)-W(1)-N(13)-C(14)	120.49(11)
C(17)-H(173)	0.98	C(14)-C(16)-H(161)	109.5	S(1) ^{ij} -W(1)-N(13)-C(14)	-66.06(11)
S(1)-C(21)	1.7658(14)	C(14)-C(16)-H(162)	109.5	C(12)-N(13)-C(14)-C(16)	-147.63(13)
C(21)-C(26)	1.404(2)	H(161)-C(16)-H(162)	109.5	W(1)-N(13)-C(14)-C(16)	42.53(17)
C(21)-C(22)	1.410(2)	C(14)-C(16)-H(163)	109.5	C(12)-N(13)-C(14)-C(15)	-26.78(14)
C(22)-C(23)	1.3992(19)	H(161)-C(16)-H(163)	109.5	W(1)-N(13)-C(14)-C(15)	163.37(10)
C(23)-C(24)	1.384(2)	H(162)-C(16)-H(163)	109.5	C(12)-N(13)-C(14)-C(17)	89.10(14)
C(23)-H(23)	0.95	C(14)-C(17)-H(171)	109.5	W(1)-N(13)-C(14)-C(17)	-80.74(14)
C(24)-C(25)	1.390(3)	C(14)-C(17)-H(172)	109.5	C(12)-O(11)-C(15)-C(14)	-23.82(16)
C(24)-H(24)	0.95	H(171)-C(17)-H(172)	109.5	C(16)-C(14)-C(15)-O(11)	153.34(12)
C(25)-C(26)	1.383(2)	C(14)-C(17)-H(173)	109.5	N(13)-C(14)-C(15)-O(11)	30.05(14)
C(25)-H(25)	0.95	H(171)-C(17)-H(173)	109.5	C(17)-C(14)-C(15)-O(11)	-82.02(15)
C(26)-H(26)	0.95	H(172)-C(17)-H(173)	109.5	C(1) ^{ij} -W(1)-S(1)-C(21)	-137.99(7)
C(31)-C(32)	1.39	C(21)-S(1)-W(1)	106.38(5)	C(1)-W(1)-S(1)-C(21)	144.39(7)
C(31)-C(36)	1.39	C(26)-C(21)-C(22)	117.73(13)	N(13)-W(1)-S(1)-C(21)	47.81(6)
C(31)-C(37)	1.500(8)	C(26)-C(21)-S(1)	117.19(12)	N(13) ^{ij} -W(1)-S(1)-C(21)	-40.83(6)
C(32)-C(33)	1.39	C(22)-C(21)-S(1)	125.04(11)	W(1)-S(1)-C(21)-C(26)	147.03(10)
C(32)-H(32)	0.95	C(23)-C(22)-C(21)	120.27(13)	W(1)-S(1)-C(21)-C(22)	-30.77(13)
C(33)-C(34)	1.39	C(23)-C(22)-C(12)	118.08(13)	C(26)-C(21)-C(22)-C(23)	-4.1(2)
C(33)-H(33)	0.95	C(21)-C(22)-C(12)	120.84(12)	S(1)-C(21)-C(22)-C(23)	173.73(11)
C(34)-C(35)	1.39	C(24)-C(23)-C(22)	120.78(15)	C(26)-C(21)-C(22)-C(12)	165.47(13)
C(34)-H(34)	0.95	C(24)-C(23)-H(23)	119.6	S(1)-C(21)-C(22)-C(12)	-16.75(19)
C(35)-C(36)	1.39	C(22)-C(23)-H(23)	119.6	N(13)-C(12)-C(22)-C(23)	-157.61(15)
C(35)-H(35)	0.95	C(23)-C(24)-C(25)	119.21(14)	O(11)-C(12)-C(22)-C(23)	30.38(19)
C(36)-H(36)	0.95	C(23)-C(24)-H(24)	120.4	N(13)-C(12)-C(22)-C(21)	32.6(2)
C(37)-H(371)	0.98	C(25)-C(24)-H(24)	120.4	O(11)-C(12)-C(22)-C(21)	-139.37(13)
C(37)-H(372)	0.98	C(26)-C(25)-C(24)	120.56(14)	C(21)-C(22)-C(23)-C(24)	0.2(2)
C(37)-H(373)	0.98	C(26)-C(25)-H(25)	119.7	C(12)-C(22)-C(23)-C(24)	-169.56(14)
		C(24)-C(25)-H(25)	119.7	C(22)-C(23)-C(24)-C(25)	3.2(2)
		C(25)-C(26)-C(21)	121.22(15)	C(23)-C(24)-C(25)-C(26)	-2.8(2)
		C(25)-C(26)-H(26)	119.4	C(24)-C(25)-C(26)-C(21)	-1.1(2)
		C(21)-C(26)-H(26)	119.4	C(22)-C(21)-C(26)-C(25)	4.5(2)
		C(32)-C(31)-C(36)	120.0	S(1)-C(21)-C(26)-C(25)	-173.45(12)
		C(32)-C(31)-C(37)	120.5(5)	C(36)-C(31)-C(32)-C(33)	0.0
		C(36)-C(31)-C(37)	119.5(5)	C(37)-C(31)-C(32)-C(33)	-179.9(5)
		C(33)-C(32)-C(31)	120.0	C(31)-C(32)-C(33)-C(34)	0.0
		C(33)-C(32)-H(32)	120.0	C(32)-C(33)-C(34)-C(35)	0.0
		C(31)-C(32)-H(32)	120.0	C(33)-C(34)-C(35)-C(36)	0.0
		C(32)-C(33)-C(34)	120.0	C(34)-C(35)-C(36)-C(31)	0.0
		C(32)-C(33)-H(33)	120.0	C(32)-C(31)-C(36)-C(35)	0.0
		C(34)-C(33)-H(33)	120.0	C(37)-C(31)-C(36)-C(35)	179.9(5)
		C(35)-C(34)-C(33)	120.0		
C(1)-W(1)-N(13) ^{ij}	172.47(5)				
C(1) ^{ij} -W(1)-N(13)	172.47(5)				
S(1)-W(1)-S(1) ^{ij}	170.645(17)				
C(1) ^{ij} -W(1)-C(1)	77.46(8)				
C(1)-W(1)-N(13)	97.12(5)				
C(1) ^{ij} -W(1)-N(13) ^{ij}	97.12(5)				
N(13)-W(1)-N(13) ^{ij}	88.73(6)				
C(1)-W(1)-S(1) ^{ij}	92.48(4)				
C(1) ^{ij} -W(1)-S(1)	92.48(4)				
C(1)-W(1)-S(1)	94.82(4)				
C(1) ^{ij} -W(1)-S(1) ^{ij}	94.82(4)				
N(13)-W(1)-S(1)	82.69(3)				
N(13) ^{ij} -W(1)-S(1) ^{ij}	82.69(3)				

Symmetry transformations used to generate equivalent atoms: ^{ij} 1-x, y, 3/2-z

CURRICULUM VITAE

Persönliche Daten

Lydia Maria Christina Peschel
Adresse: Ghegagasse 13/34
8020 Graz
Geburtstag: 05. 12. 1987
Familienstand: Ledig
Staatsangehörigkeit: Österreich

Akademischer Werdegang

Seit 12. Feb. 2011 Masterstudium Chemie im Rahmen von NAWI Graz
11. Feb. 2011 Abschluss des Bachelorstudiums
Juni 2005- Dez. 2005 Austauschstudentin in Brisbane/ Australien
Queensland University of Technology,
2 George Street, Brisbane QLD 4000
Okt. 2007- Feb. 2011 Bachelorstudium Chemie im Rahmen von NAWI Graz
Sept. 2006- Mai 2007 Low Budget Backpacking Trip durch Thailand, Malaysia, Singapur,
Indonesien, Australien, Neuseeland, Chile, Argentinien und Brasilien
20.Juni 2006 Abschluss des Realgymnasiums, Matura mit ausgezeichnetem Erfolg
Feb. 2005- Aug. 2005 Austauschschülerin in Brisbane/ Australien
Indooroopilly State High School,
Ward Street, Indooroopilly QLD 4068
1999-2006 Besuch des Realgymnasiums mit wirtschafts- und sozialpraktischem
Schwerpunkt
Schulverein der Kreuzschwestern,
4020 Linz, Stockhofstraße 10
1994-1999 Besuch der Volksschule
3532 Rastenfeld, Rastenfeld 88

Beschluss der Curricula-Kommission für Bachelor-, Master- und Diplomstudien vom 10.11.2008
Genehmigung des Senates am 1.12.2008

EIDESSTATTLICHE ERKLÄRUNG

Ich erkläre an Eides statt, dass ich die vorliegende Arbeit selbstständig verfasst, andere als die angegebenen Quellen/Hilfsmittel nicht benutzt, und die den benutzten Quellen wörtlich und inhaltlich entnommene Stellen als solche kenntlich gemacht habe.

Graz, _____

Datum

Unterschrift